Eye-opening and the control of visual synapse development in the mouse superior colliculus

by

Marnie A. Phillips

B.S. Biology and Anthropology-Zoology
University of Michigan, 1998

SUBMITTED TO THE DEPARTMENT OF BRAIN AND COGNITIVE SCIENCES IN
PARTIAL FULLFILLMENT OF THE REQUIREMENTS FOR THE DEGREE OF

DOCTOR OF PHILOSOPHY IN NEUROSCIENCE
AT THE
MASSACHUSETTS INSTITUTE OF TECHNOLOGY
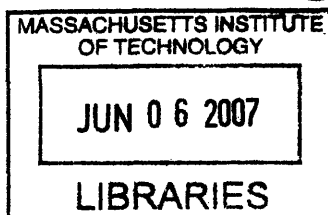
JUNE 2007

Signature of Author:_____
Department of Brain and Cognitive Sciences
May 25, 2007

Certified by: _____
Martha Constantine-Paton
Professor of Biology
Thesis Supervisor

Accepted by: _____
Matthew Wilson
Professor of Neurobiology
Chair, Graduate Committee

1

Eye-opening and the control of visual synapse development in the mouse superior colliculus

by

Marnie A. Phillips

ABSTRACT

The mammalian superior colliculus (SC) coordinates visual, somatosensory, and auditory stimuli to guide animal behavior. The superficial layers (sSC) receive visual information via two major afferent projections: 1) A direct retinal projection and 2) an indirect projection from Layer V visual cortex. The retinal projection reaches the rat sSC by embryonic day 16, is topographic, and refines to form a high resolution map of visual space early in development, before eye-opening in rodents (~P12-P14). The cortical projection is delayed by about eight days, just reaching the sSC around P4, and does not complete its topographic refinement until around the time of eye-opening. These afferents compete for synaptic space during a time when patterns of spontaneous and evoked activity are rapidly changing. I have used the mouse sSC as a model system to test the role of new activity patterns due to the initial onset of visual experience after eye-opening in visual synaptic development. I have described the organization of retinal and cortical afferents and the laminar organization of the mouse sSC in Chapter 3. Previous work demonstrated eye-opening (EO) induces the appearance of dendritic PSD-95 and LTP in the sSC within 2-4 hours. I provide evidence that EO-induced PSD-95 trafficking is required for the stabilization of new synapses *in vivo* as a result of patterned visual experience after eye-opening. mEPSC frequency recorded in a vertical neuronal subtype of the mid-SGS increases at least three-fold after eye-opening, indicating a rapid synaptogenesis that does not occur in PSD95KO mice, or in age-matched littermates deprived of initial visual experience. A structural analysis of these neurons revealed caliber-specific patterns of spine and filopodia development that depend on EO and the projection from visual cortex. Between P11 and P13, dendrites post-synaptic to cortical axons undergo an EO-independent tripling of filopodial density and an EO-dependent maintenance of dendritic spine density. These data suggest that rapid vision-induced trafficking of PSD-95 enables long-term potentiation and stabilization of newly formed cortico-collicular synapses in response to patterned visual stimuli. Furthermore, these data suggest that cortical inputs are sensitive to pattern vision deprivation between P12 and P13, but retinal inputs are not.

THESIS SUPERVISOR: Martha Constantine-Paton
TITLE: Professor of Biology

2

TABLE OF CONTENTS

CHAPTER FOUR: GENERAL DISCUSSION

CHAPTER ONE: INTRODUCTION

The development of visual pathways between the retina and the brain is a gradual process largely incomplete at birth (Maurer et al. 2005), progressing through a series of developmental epochs that consolidate and refine initially imprecise afferents. These epochs are in part defined by changes in the quality and quantity of neuronal activity. Large, spontaneous waves of activity sweep across the retina at birth, but diminish with age (Wong 1999), transitioning to more clustered bursts of spontaneous spiking in retinal ganglion cells (Wong et al. 1993, Firth et al. 2005), followed by a progressive increase in light-evoked responses to diffuse visual stimuli (Krug et al. 2001) and finally to high frequency cortical responses to pattern stimuli after eye-opening (Nase et al. 2003). In general these transitions are gradual, but eye-opening is a transition point at which afferent activity could change extremely rapidly. Accompanying these activity transitions are changes in protein expression (Corriveau 1999, Nedivi 1999), synaptic protein composition (Aamodt and Constantine-Paton 1999), and neurotransmitter receptor function (Hestrin 1992, Townsend et al. 2004). These changes are thought to affect the mechanisms by which synapses in visual pathways are stabilized and eliminated (Constantine-Paton and Cline 1998, Law et al. 1994).

The superior colliculus (SC), is the primary destination of retinal axons in the rodent brain (Drager and Hofbauer 1985), and is an accessible structure for assays of developmental changes at contacts between sensory afferents and post-synaptic targets.

I have used the mouse SC as a model system to assay the development of synaptic structure and function over the eye-opening transition period. In Chapter 2, I define the organization of neurons and visual afferents in the visual layers of the mouse SC. In Chapter 3, I show that cells in the SC rapidly gain

5

functional synaptic contacts after eye-opening, and the structural correlate of this gain is a complex dance of spine and filipodial turnover under new cortical terminals. I then examine a post-synaptic determinate of these functional changes--the synaptic up-regulation of PSD-95--and the dependence of these structural changes on eye-opening and the presence of visual cortical afferents, which differentially innervate distinct regions of the dendritic arbor. I conclude with a model for the organization and postnatal development of synaptic connectivity in the mouse SC.

Eye-opening: A critical transition in visual pathway development

Long-range afferents initially use molecular cues to guide axonal outgrowth and targeting during a time when there are few synapses (McLaughlin and O'Leary 2005; Verhage et al. 2000). Spontaneous activity dominates the embryonic and early postnatal brain, in the form of low frequency, giant depolarizing potentials that sweep across horizontal and vertical cellular strata during their development (Garaschuk et al. 2000, Leinekugel et al., 2002; Wong et al, 1993). Synaptic transmission is unreliable at this age, but does improve, especially with heightened synaptogenesis and the development of myelination around the second postnatal week in rodents (Shi et al. 1997). Neurons use this spontaneous activity to aid in the formation of appropriate axonal topography (Cang et al. 2005, McLaughlin et al. 2003).

As neurons continue to differentiate and mature, and the connectivity of neuronal circuits improves, neurons become responsive to sensory stimuli. In the rat retina, this occurs at least four days before eye-opening (Molotchnikoff and Itaya 1993). Light through the closed eyelids is capable of inducing retinal ganglion cells to spike, and this signal is transmitted across at least two synapses to induce responses in visual cortex (Krug et al. 2001). During this period, spontaneous activity is still present, but the quality of this activity has

changed. In the retina spontaneous RGC spiking transitions from a cholinergic-driven circuit to a glutamate-driven one, and becomes intermixed with light-evoked activity (Demas et al. 2003).

Eye-opening in rodents typically occurs over a period of days, but when experimentally synchronized it drives a rapid series of changes in neuronal activity (Lu and Constantine-Paton 2004), protein trafficking (Yoshii et al. 2003), and synaptic plasticity in the SC (Zhao and Constantine-Paton 2006) between two and 24 hours after eye-opening. Given the ability of light exposure in dark-adapted animals to induce plasticity-related transcription factor (NGF1-A) expression in the SC within 10-30 minutes (Giraldi-Guimaraes et al. 2005), and to induce the expression of downstream structural effector proteins within four hours (eg, CPG15) (Nedivi et al. 1996), this rapid timecourse of events is not unfeasible. NMDA receptor activity and function also switches over this period (Shi et al. 1997, Townsend et al. 2004), causing synaptic depression and elimination before eye-opening, and balanced elimination, depression, potentiation, and stabilization afterward (Colonnese et al. 2005, Colonnese and Constantine-Paton 2006, Zhao and Constantine-Paton 2006).

A sudden, rapid switch in the intensity and frequency of afferent visual activity patterns is hypothesized to occur at eye-opening, and a similarly rapid onset of sensory experience and activity may occur for other sensory modalities as well; for example audition (Harris and Dallos 1984), and somatosensation at the onset of whisking (Landers et al. 2006). Thus, the mechanisms by which eye-opening induces the onset of a new developmental epoch in the SC may be conserved in other brain regions which are similarly awakened to sensory experience during development. The SC is especially well suited to these studies, because it receives visual information from two sources, the retina and visual cortex, and does not make feedback projections to either of these

7

structures (Harting et al. 1991, 1980). These afferents can compete for synaptic space in the neuropil (Lund 1978), and thus make the SC a useful model for competitive rearrangements inherent in the development of all sensory pathways.

Visual experience after eye-opening and the postnatal development of visual function

Human visual acuity improves at least five-fold in the first six months after birth (Maurer and Lewis 2001). Post-natal changes in visual ability appear to result from anatomical and functional development at all levels of the sensory afferent pathway from retina to cortex (Kiorpes and Kiper 1996, Chen and Regehr, 2000, Movshon et al. 2005, Kourtzi et al. 2006). The anatomical and functional development of visual axonal afferents to target structures like the visual cortex requires normal visual experience in early development. When animals are monocularly deprived, normal afferent patterns to visual cortex in the form of eye-specific ocular dominance columns, for example, are disrupted (Wiesel and Hubel 1965, LeVay et al. 1980). Children born with cataracts who experience luminance cues, but not high contrast pattern vision, face the possibility of permanent blindness if the lens is not corrected before the end of an early critical period (around 7-9 years of age, reviewed in Maurer et al. 2005), although recent reports suggest a functional, though imperfect, vision can develop after correction as late as 12 years of age (Ostrovsky et al. 2006), and a limited degree of recovery is possible even in adults. Even with extended periods of recovery in adulthood, however, early deprivation grossly impairs spatial acuity, contrast sensitivity, complex form and pattern recognition (Fine et al. 2003), as well as direction sensitivity to stimuli in motion (Ellemberg 2002).

In owls, manipulation of early visual experience is also known to alter the

8

topographic alignment of visual and auditory afferent maps necessary for normal localization and targeting of prey using visual and auditory cues (Hyde and Knudsen 2002). The midbrain optic tectum (superior colliculus in mammals) controls this plasticity, and receives direct inputs from the retina in birds and mammals and is critical in both Classes for integration of visual, auditory, and somatosensory cues to direct behavior.

Thus post-natal visual experience is critical to development of normal vision and visually-guided behavior, but the mechanisms and loci of these experience-dependent changes are just beginning to be understood. Post-natal visual deprivation affects visual circuit development in the ascending retinothalamo-cortical pathway at every level: the retina (Tian and Copenhagen 2003, Feller 2003), LGN (Levitt et al. 2001, Hooks and Chen 2006), and visual cortex (LeVay et al. 1980). And in mammals, long-term deprivation in the form of eye-occlusion or dark rearing does not simply reflect loss-of-function, but rather induces active degradation of existing function. In a human case in which vision was lost at three years of age, adult acuity was actually 25 times _lower_ than that expected at age three (Fine et al. 2003). And while many of these visual functions in humans, such as acuity, are known to take months to years to develop to mature levels, the initial appearances of visually evoked responses in target structures have been observed to develop in mammals such as cats even before the eyes open (reviewed in Stein 1984).

Many studies have documented rapid developmental changes and effects of visual deprivation on synaptic structure or cellular function in visual cortex, which are correlated with the eye-opening period, without necessarily controlling or measuring the timing of eye-opening (Mataga et al. 2004, Maffei et al. 2004, Smith and Trachtenberg 2007). Recent evidence from the mammalian superior colliculus in which the timing of eye-opening is controlled, suggest that this initial post eye-opening experience causally sets in motion

rapid, dramatic changes in synaptic and cellular function in visual afferents and their post-synaptic targets (Lu and Constantine-Paton 2004, Yoshii et al. 2003). Specifically, after eye-opening in rats a rapid sequence of post-synatpic events unfolds, as measured by whole-cell voltage clamp electrophysiology. Within two hours the PDZ-domain containing protein PSD-95 is enriched at synaptic sites, followed at as early as six hours by the appearance of slow, NR2B-mediated spontaneous NMDAR currents and an increase in the proportion of silent synapses. This is followed by an increase in of AMPAR current frequency and a small enhancement in amplitude within 12 hours, and modifications in electrophysiological assays of refinement (number of contacts per axon and number of inputs per cell) within 24 hours. There is no change of pre-synaptic release probability over this period. The rapid time-course of these events emphasizes the importance of precise experimental control of the timing of eye-opening for their detection.

What is not yet clear, however, is to what degree modifications of synaptic connectivity, especially structural changes, play in this re-wiring of connectivities as assayed by electrophysiology. Without control of eye-opening and examination of the periods before and after eye-opening, it is additionally difficult to understand whether these differences are due to changes induced by eye-opening, or changes induced by visual deprivation (Gandhi et al. 2005). It is also becoming clear that visual "deprivations" in the form of complete action-potential blockade with TTX, dark rearing, or eye occlusion, involve different mechanisms and create vastly different outcomes (eg, Hooks and Chen 2006). Because the retina is spontaneously active at birth, and visually-evoked potentials in visual cortex can readily be evoked through closed eyelids well before the eyes open, neuronal silencing or dark rearing are insufficient to test the role of visual experience after eye-opening. Rather, simply keeping the eyes closed permits light-evoked activity to pass through the closed eyelid and on to the brain, while eliminating patterns of RGC activity that encode pattern

10

and shape information.

In the SC several questions regarding visual experience-driven modifications remain. These include 1) Whether the rapid changes in miniature event frequency reflect the creation of new spine-like structures, 2) Where these synapses are located, 3) What the mechanism of any structural modifications might be, and 4) Whether after eye-opening any of these induced modifications are maintained.

Control of eye-opening combined with a parallel examination of the structural and electrophysiological changes over the entire post-natal period can help dissociate age-dependent from vision- vs deprivation-induced effects, and reveal the importance of underlying structural mechanisms. A combined approach may be critical to our understanding of what, exactly, early vision does to our brains to permit high resolution vision in later life.

The Superior Colliculus as a Model for Sensory Experience-Dependent Development in the CNS

While the primate superior colliculus (SC) is a relatively small and inaccessible structure located deep in the brain, the rodent superior colliculus is comparably enormous, and forms a laminar structure on the large dorsal roof of the midbrain, entirely exposed to external observation and manipulation except for the overlying posterior portions of the cortical hemispheres. In mice it is the major target of retinal axons from the optic nerve (Drager and Hofbauer 1985), which sprout collaterals into the dLGN of the thalamus and pretectal nucleii on their way to their final terminations in the superficial laminae of the SC (sSC). The other major afferents to the sSC are axons from layer V pyramids in visual cortex, and in this way it is both a direct target of retinal axons, and an indirect target via afferents from visual cortex. It thus receives information about basic

11

stimulus properties from retina, as well as transformed information about color, pattern, motion, and shape, from occipital cortex. The fact that it is a target of visual afferents means that afferent activity can be easily and reversibly manipulated, and the fact that it is a superficial structure means that pharmacological manipulation is possible in vivo. Moreover, its laminar organization allows for reproducible identification and targeting of specific cell types characterized by laminar position. These features make it an excellent model CNS structure for sensory experience-dependent development.

A. Anatomical organization and development of the rodent sSC

Connections of Superficial Layers. The rodent SC receives input from visual afferents in the dorsal superficial lamina (sSC, consisting of the following layers in dorsal to ventral order, identified on the basis of Nissl staining and myelination patterns in adult animals: stratum zonale, SZ, stratum griseum superficiale, SGS, and stratum opticum, SO). The two dominant afferent projections are from the contralateral retinal and the ipsilateral visual cortex, and there are minor projections from the ipsilateral retina, the ventral lateral geniculate nucleus (vLGN), the pre-tectal nucleus of the optic tract, the parabigeminal nucleus, and the *locus coeruleus*. Axons of cells in the superficial layers arborize either locally, or project efferent axons. In hamster, ~40% of neurons in the sSC send at least one axon collateral to the deeper layers of the SC (Mooney et al. 1988). Efferent axons are also found projecting to vision-related nucleii in ascending uncrossed pathways to the pre-tectum or thalamus (dLGN, vLGN, lateral posterior-pulvinar complex) and descending pathways to the parabigeminal nucleus.

Connections of Intermediate and Deep Layers. Intermediate layers (stratum griseum intermediale, SGI), receive afferents from a broad spectrum of sensory and motor afferents, and send efferents to brainstem and motor pathways from

the SGI and its deepest layers (stratum griseum profundum, SGP). Thus there is a certain degree of segregation of function in the SC, with superficial layers receiving purely sensory input, and intermediate and deep layers receiving multimodal sensory and motor input. However, there must also be extensive overlap, because the dendrites of neurons in SGI extend dorsally throughout the depth of the sSC, and neurons of the SGS send axons ventrally to the SGI. SGI is considered to be critical for multimodal sensory integration and coordination of behavior driven by multiple sensory modalities (eg, direction of gaze towards an auditory cue). (Vanegas 1984).

Cell Types. Cellular morphology and organization has been described in the rat sSC using Golgi-Rapid and Golgi-Kopsch approaches. Based on anatomical criteria, a minimum of 11 potential cell types have been identified, in approximate dorso-ventral order of their somata: Marginal, Horizontal, Stellate, Piriform, Narrow field vertical (superficial, intermediate, and deep vertical fusiform), Pyramidal, Type II ganglion, Type III ganglion, and Wide field vertical (Langer and Lund 1974). Except for three cell types,1) Marginal cells, which sit just under the pial membrane and have a small, restricted ventrally-projecting dendritic arbor, 2) Horizontal cells, which have laterally projecting dendrites often spanning the entire colliculus and make inhibitory dendro-dendritic contacts, and 3) Stellate cells, which have multipolar non-oriented dendrites and predominantly locally arborizing axons, the other cell types described are vertically oriented with large dorsal dendritic arbors and axons which project either locally or ventrally into the deeper layers of the SC. A revised classification method was proposed by Tokunaga and Otani (1976), based almost exclusively on dendritic arborization patterns of large numbers of reconstructed cells. This revised classification identified 12 major cell types, with discrepancies mostly for the vertically oriented neurons. Tokunaga and Otani did not find evidence for separation of narrow-field vertical from piriform from pyramidal, *per se*, rather, classed all neurons with narrow, cylindrically

shaped dendritic arbors as "cylindrical narrow-field verticals", with distinctions made depending on whether the cell had a predominantly dorsal dendritic arbor (Type 5) or a predominant dorsal arbor with some ventral dendrites also apparent (Type 3).

Organization of Afferents. Golgi reconstructions, and anterograde labeling of contralateral and ipsilateral retinal afferents, and ipsilateral visual cortical afferents, have all been assayed in adult rodents with independent studies in separate animals. Early qualitative evidence suggested that the SZ and SGS contain retinal axons and occasionally visual cortical axons, that the deep SGS contains axons from both retina and visual cortex and occasionally vLGN, and that the SO contains axons from visual and other cortical and subcortical regions. One study in which restricted injections of HRP were made into visual cortex of C57BL mice found labeled axons only in the deep portion of SGS/SO, and confirmed that these axons originate exclusively from pyramidal neurons in the bottom half of Layer V (Rhoades et al. 1985). Later evidence, however, using degeneration studies after retinal and cortical lesion experiments, suggested a major presence of cortical terminals in the zone of horizontal neurons in the superficial SGS (Mize 1983). Additionally, qualitative anterograde DiI labeling studies from visual cortex concluded that cortical axons arborize specifically in the most superficial layers of SGS (Inoue et al. 1992). Much of the ambiguity may stem from the lack of dual or triple labeling approaches which label complete afferent projections in single animals, in which the location of each afferent and cell type can be determined in relation to one another, as well as a lack of quantitative approaches and confirmation of the labeled area in visual cortex. This, as well as the paucity of information about the organization of cell types and afferents to the mouse sSC, necessitated a basic investigation of mouse sSC anatomy.

Development of Retinal Afferents. In mice and rats the development of the

14

retinal and, to a lesser degree, the cortical afferents to the sSC has been studied. Axons from the contralateral retina have reached the sSC by E16 through the rostral margin of the superior colliculus, and have reached the caudal margins of the SC by E18 (Lund and Bunt 1976), followed a few days later by axons from the ipsilateral retina (Godement et al. 1984). At this time collicular neurogenesis is complete (Mustari et al. 1979) and the first synapses can be observed ultrastructurally (Lund and Bunt 1976). By two days after birth axonal branching into both topographically appropriate and inappropriate locations has begun (Edwards et al. 1986, Sachs et al. 1986). By three to four days after birth there is greater axonal elaboration into topographically appropriate locales, but the elimination of all topographically inappropriate branches is not complete until P12, two to three days before eye-opening in rats (Simon and O'Leary 1992). Well-myelinated axonal tracts in the stratum opticum are not easily visible until sometime between P15 and P30 (Wharton and Jones 1985). Refined axonal arbors display precise point-to-point topography, with rostral SC receiving input from temporal retina, caudal SC receiving input from nasal retina, and the dorso-ventral retinal axis represented latero-medially in the SC.

Development of Cortical Afferents. The development of cortical afferents is significantly delayed with respect to retinal axons in the SC. Cortico-tectal cells can be retrogradely labeled from the rat SC as early as P3 (Dreher et al. 1985), and cortical axon arbors are detected in the SGS by P7. In mice in which small groups of cortical axons have been labeled at high resolution with the tracer DiI, collateral axonal branches have been observed to form a bright, focused terminal zone in the mouse SGS by as early as P11, which shrinks over the next two postnatal weeks (Inoue et al. 1992), achieving mature topography by P17-19 through a similar pattern of branch elaboration and elimination as the retinal projection (Lopez-Medina et al. 1989). In mice which congenitally lack retinal inputs to the sSC, the cortico-collicular projection forms globally normal

topography, although it occupies the upper laminae of the SGS (Rhoades et al. 1985), This suggests that intrinsic collicular cues mediate the topographic ingrowth and refinement of cortical afferents, but that the normal dorso-ventral organization of cells and afferents in the sSC requires the early presence of retinal afferents.

Development of Dendrites. Development of rat collicular neurons has been investigated with qualitative Golgi procedures (Wharton and Jones 1986). Growth of all major cell types occurs over the 2-3 week postnatal period, with spines first detected by the end of the first or second postnatal week. However, morphological and positional criteria for the determination of cell types have not been established for developing animals. Vertically-oriented neurons in the deep SGS, in particular, are identified on the basis of the location and extent of dendritic arbors (predominantly dorsal arbors, or equally large dorsal+ventral arbors), and in young animals as old as P9 or P15 images of Golgi-stained neurons in the SGS appear to contain rudimentary apical dendritic shafts that do not appear to extend to the surface of the SGS, and largely bare of side branches or ventral or somatic dendrites. These properties make it difficult to identify the cell type of these randomly and possibly incompletely stained cells to begin with, and thus a method of reproducibly labeling a neuronal subset would greatly improve our understanding of the postnatal development of individual cell types.

Synaptogenesis. Very few synaptic contacts have been detected in the newborn rat SC (Lund and Lund 1972). When synapses are counted with quantitative two-dimensional EM assays and sampled at unspecified depths of the sSC at P7, P14, P21, and P28 (with natural eye-opening in rats occurring sometime around P14), however, the proportions of somatic, dendritic, and spinous synapses can be estimated. Very few somatic synapses are detected at any age. 60-70% of synapses in the neuropil are found on dendrites, with the rest on

spines, and significant differences in the distribution were not detected at any of these time-points (Bakkum et al. 1991). However, the population of GABAergic horizontal neurons that make up a large proportion of the SGS are known to form dendro-dendritic contacts with neighboring cells almost exclusively, and could represent the bulk of the dendrites sampled. Synapses become more numerous as maturation proceds, with the largest increases detected sometime between the time of eye-opening (around P14 in rats) and P21 (Wharton and McCart 1984, Bakkum et al. 1991). Between P21 and adulthood total synaptic density appears to level off. While informative, and indicative of a growing and dynamic post-synaptic neuropil, these EM studies are limited in their ability to sample consistently from known cell types and populations of contacts. The few Golgi studies which have examined spine development on single neurons suggested that spines appear on neurons in the SGS sometime between P9 and P15 (Wharton and Jones 1985), however a time-course of chronological development is made difficult by the uncontrollable nature of the Golgi label, and the inability to confirm that similar cell types are labeled at different ages.

B. Functional contribution of the retino- and cortico-tectal inputs to the sSC

SC response properties. Mature sSC cells will respond to stationary flashed light, but preferentially respond to moving stimuli at relatively low velocities, and prefer stimuli moved in specific directions across the receptive field (ie, are direction selective). Receptive field size increases as electrodes are moved into deeper layers, with cells of the SZ having the smallest recorded receptive field sizes in the SC (Kao et al. 1994, Stein 1984). This appears reasonable from an anatomical standpoint, given that cells in the superficial SGS have small dendritic arbors, the larger cells in the deep SGS have dorsally elongated, conical arbors, wide-field vertical neurons in the SO span the largest rostro-

caudal extent, and cells of the deeper layers receive multiple sensory inputs from the superficial layers and elsewhere. Both the retinal and cortical afferents are excitatory glutamatergic projections. The effect of cortex on SC response properties is described below.

Development of response properties. These neuronal response properties in the SC and the acute and/or developmental role of visual afferents in those properties has been best studied in cats, highly visual mammals who also open their eyes post-natally and show a progressive acquisition of visual capabilities and visually-evoked behavior after eye-opening. Visual functions in cats begins to develop in the first few postnatal weeks, with initial eye opening occurring around the end of the first postnatal week (Norton 1974, Sireteanu and Maurer 1982). Development of response properties has been studied over the eye-opening period without control or measurement of the timing of eye-opening, so precise time-courses locked to eye-opening are difficult to assess. By P6-P8, the first visually-evoked responses can be measured in the SZ and sSGS, and by P9-P10, approximately after eye-opening, virtually all cells in the sSC are visually responsive, including SZ, sSGS, dSGS, and SO, with no increase in responsiveness detected at P12-P13. Around the time of eye-opening, and for a few days afterward, cells prefer stationary flashed light (over moving stimuli), are sensitive to moving stimuli of even lower velocity than adult cells, and lack direction selectivity. Cells also have have broad ON/OFF type responses only to large stimuli (Stein et al. 1973a, b), which are likely due to lack of retinal segregation of ON/OFF properties. Young SC cells also have long response latencies and fire inconsistently, properties which have been attributed to a lack of myelination of optic afferents (Moore et al. 1976), immaturity of retinal ganglion cell responses (Hamasaki and Flynn 1977), as well as the poor optical quality of the kitten eye (Thorn et al. 1976, Bonds and Freeman 1978).

Role of the Cortico-collicular Projection. The rapid development of direction

selectivity over eye-opening led to investigations of the role of the cat cortico-collicular afferents in the development of these properties. Pyramids of cat visual cortex are known to be highly direction selective, and develop mature response properties before visual experience onset (Hubel and Wiesel 1963), much earlier than collicular neurons. Lesion of visual cortex in neonates prevents the development of direction selectivity (Flandrin et al. 1977, Mize and Murphy 1976, Stein and Magalhaes-Castro 1975) and decortication in adults similarly abolishes direction selectivity of SC cells (Berman and Cynader 1976, Wickelgren and Sterling 1969). However, it is not clear whether anatomical ingrowth of cortical afferents can account for the appearance of these properties in cats (Anker 1977, Stein and Edwards 1979). Complete serial reconstruction of individual axons reveals highly complex and branched terminal axons in the superficial SGS by one week of age. Labeling of small regions of visual cortex reveal in cats that terminal zones are appropriately topographically confined by one week after birth, however, they are not qualitatively adult-like until 12 weeks of age (Plummer and Behan 1992). In cats the terminal arbors of individual cortical axons appear to extend over an area as large as 30-40% of the total medio-lateral extent of the SC, which potentially reflects the greater role of the visual cortex in SC-mediated vision in highly visual mammals, compared to rodents. Acute cortical inactivation by cooling can reversibly change the number of discharges from SC neurons evoked by presentation of a visual stimulus. At the end of the first postnatal week (P8-12), few SC cells are affected by visual cortical cooling (<10%). However, by P13-14 this proportion has changed dramatically (>40%) and remains approximately constant to adulthood, with a similar developmental time-course for the development of direction selectivity (Stein and Gallagher 1981).

The rapid development of response properties in the sSC over the eye-opening period, which are dependent on visual cortical activity, suggests a parallel functional and/or anatomical change in the number, strength, or distribution of

19

cortical contacts onto neurons of the SGS. However, this has not been tested, and the dependence of these changes on visual experience is also unknown.

Spines and filopodia as dynamic structural sites of synaptogenesis and synaptic plasticity

Spines and filopodia as indicators of excitatory synaptic sites. The CA1 region of the hippocampus has provided the best information regarding synaptic localization on spines to date. Spines are abundant on mature CA1 pyramidal neurons, and excitatory synapses in the adult are located almost exclusively on spines, in vitro or in vivo. Analyses of the structural geometry of spines with serial EM in P15 vs Adult rats reveals significant correlations with the occurrence and size of PSDs and spine apparatuses within them (Harris et al. 1992). When spine geometry is classed according to thresholded length vs width relationships, significant differences are detected in the likelihood and size of functional synaptic structures within them.   Filopodia (defined as a dendritic protrusion with a length much greater than its width, (Harris et al. 1992)), are detected on CA1 dendrites in developing neuropil in the first two postnatal weeks. In CA1, about 25% of developing synapses are present on filopodia as early as P12 (Fiala et al. 1998), but do not typically contain synapses anywhere along their length by P15 (Harris et al. 1992), Synapses can, however, appear on filopodia at later ages when activity levels are pharmacologically reduced (Petrak et al. 2005), One hypothesis is that spines are necessary for bridging the gap between dendrites and nearby axons (Swindale 1981) and that long filopodial extensions in particular are necessary in developing neuropil (or after deafferentation) where the extracellular distance required for dendrites to traverse in order to come into contact with pre-synaptic axons is large (Saito et al. 1992, Cooper and Smith 1992). Thin spines, defined as a dendritic protrusion whose length is greater than its width, stubby spines, defined as neck diameter equal to its length, and mushroom

20

spines, defined as neck diameter that is much shorter than the head diameter (Harris et al. 1992), are all more likely to contain synapses than filopodia. At P15 0% of filopodia contain synapses, at P15-Adult 99-100% of thin spines identified by the geometric width/length ratios described above contain thick non-perforated PSDs (Hariris et al. 1992), 50% of all spines contain smooth ER, and 80% of mushroom spines identified based on structural geometry contain a well-laminated, mature spine apparatus (Harris 1999).

Thus while it is impossible to know with certainty whether any given spine structure identified geometrically is apposed to a pre-synaptic release site and contains a functional post-synaptic density, it is reasonable to assume that a "spine", identified by a large width:length ratio, indicates a high likelihood of a synapse, and any given "filopodia", identified by its small width:length ratio, is less likely to contain a synapse. In addition, all synapses are not created equal. Thinner spines have smaller PSDs than stubby and mature spines at both P15 and adult.

Structural correlates of synaptogenesis. Filopodia are more prevalent in developing neuropil during periods of high synaptogenesis (Ramoa et al. 1987, Saito et al. 1992, Zuo et al. 2005), and synapses can be detected on filopodia even early in development in certain cell types (Saito et al. 1992). In vitro, filopodia can be observed to contact nearby axons, and the disappearance of filopodia is correlated with the appearance of persistent spines opposite functional release sites (Ziv and Smith 1996). Although filipodial and spine dynamics change with development, at 1month of age filopodia (classified geometrically as length > 3 x width) on the apical dendrites of Layer V pyramids are highly dynamic and turn over more rapidly than spines. Approximately 15% of these filopodia are converted to stable, spine shaped structures (with length < 3 x width) over four hours of *in vivo* imaging, and ~40% of these converted filopodia are maintained 24 hours later (Zuo et al.

2005). So there is good evidence that filopodia can form the structural basis for synaptic contacts, that filopodia can become dendritic spines, and that the presence of filopodia is indicative of a period of dynamic synaptogenesis and spinogenesis (both elaborative and eliminative). As animals mature, filopodia involved in spinogenesis are lost, total fewer filopodia are observed (CA1: Harris 1999), and mature, stable, spines are present, which appear to persist through adulthood (Zuo et al. 2005). In CA1, in the first week after birth, 70% of synapses are detected on shafts. In the second week, filopodia are present and the majority of synapses shift to stubby and mushroom shaped spines (Harris 1999). Thus synaptogenesis during development appears to involve a generalized timecourse involving a shift from synapses on dendritic shafts to synapses on spines, with a transitory, dynamic period of synaptogenesis in between that is mediated in large part by dendritic filopodia.

Structural correlates of synapse function. Spines are specialized structures whose specialized geometry do serve a purpose in signal transmission and plasticity and have important implications for function. The ability of a spine to restrict depolarization and subsequent calcium influx to the individual spine or adjacent spines is thought to be important for providing input specificity for a given synapse and preventing spread to distant dendritic shafts and soma. Spine head geometry and volume are correlated with the number of functional postsynaptic receptors and the calcium flux through them (Noguchi et al. 2005, Nusser et al. 1998), and to the number of docked vesicles at the apposed pre-synaptic release site (Schikorski and Stevens 1999). Calcium diffusion kinetics into the spine and spread to the shaft can also be determined by the shape of the spine head and length of the spine neck (Majewska et al. 2000, Yuste et al. 2000, Noguchi et al. 2005). Furthermore, the spatial location of the spine on the dendrite is also important: The dendritic location and diameter of the parent dendrite from which a spine protrudes contributes to control of calcium dynamics within spines, such that slower, double exponential calcium decay

kinetics are detected in spines on thicker dendrites (Holthoff et al. 2002).

Structural correlates of synaptic plasticity. Artificial LTP induction paradigms using tetanic stimuli delivered to afferent layers to induce potentiation at post-synaptic sites have been used in parallel with serial EM and fluorescent spine reconstructions to assay changes in spine number or morphology after LTP induction. Results are highly variable (see Yuste and Bonhoeffer 2001 for review), potentially in part due to anomalous sprouting and/or suppression of spine structures after living slices are cut (Kirov et al. 1999), or after time in culture in the case of organotypic slices (DeSimoni et al. 2003), and so I will discuss only *in vivo* results here.

As assayed with quantitative analysis of ultrathin 2D EM sections, high frequency tetanus delivered *in vivo* that induced LTP resulted in 33–50% more synapses on dendritic shafts in CA1, with no apparent change in the number of synapses on spines or morphological parameters of PSDs, or spines, or the number of spines containing synapses (Lee et al. 1979b). In the absence of serial reconstruction of dendrites, however, it is impossible to know whether these represented contacts on excitatory pyramids or inhibitory aspiny neurons. However, in the dentate gyrus, serial EM reconstruction revealed an increase in spine number by ~50% after in vivo LTP induction (Andersen et al. 1987a,b, Trommald et al. 1990). Part of the difficulty in detecting changes in spine or synapse morphology with EM after afferent pathway stimulation is due to an inability to know *which* synapses are being potentiated, and hence, where to look for changes. Filling individual cells with fluorescent dyes combined with confocal reconstruction can allow one to sample spine populations across the arbor of individual neurons, as well as follow individual spines over time, and thus can increase the power of the random sample statistical approach. This would require, ideally, in vivo LTP induction and fluorescent imaging in the intact animal. In the absence of such data, however, the consistent phenotype

obtained with current in vivo induction methods and in vivo perfused EM methods is a net gain of synaptic sites following LTP induction.

Modifications of synaptic strength by LTP/LTD and synapse stabilization/elimination.

Adjustment of Synaptic Strength . Correlated activity through NMDA receptors is believed to modify synaptic strength through mechanisms such as long-term potentiation and depression (LTP and LTD) (Collingridge et al. 1983, Harris et al. 1984, Mulkey and Malenka 1992). These are powerful models of NMDA receptor function in the developing nervous system because nascent synapses are thought to be weak synapses that are stabilized or eliminated by the repeated induction of LTP or LTD (Durand et al. 1996, Isaac et al. 1997, Mulkey and Malenka 1992). LTP, particularly using spike-timing dependent protocols , can modify sensory response strengths (Dan and Poo, 2006), and may therefore represent the natural mechanism by which long-lasting synaptic changes are induced via NMDAR activation. However, NMDA receptors are not the only mechanism by which correlated pre- and post-synaptic activity can be coupled to post-synaptic calcium influx, although it is the most direct. Voltage-gated calcium channels and metabotropic glutamate receptors (Kemp and Bashir 1999, Bortolotto and Collingridge 1993, Oliet et al. 1997) can indirectly couple detection of pre-synaptic release via post-synaptic depolarization (due to glutamate receptor activation) or direct detection of glutamate release coupled to signal transduction pathways which release calcium from intracellular stores. All of these receptors may work in concert to detect pre- and post-synaptic activity and induce divergent yet overlapping signal transduction pathways to modify synaptic strength and structure.

24

Calcium-driven synaptic modifications are bidirectional. For example, either long-term potentiation (LTP) or long-term depression (LTD) of synaptic strength are induced by different patterns and levels of calcium entry triggered by NMDA receptor activation (Nishiyama et al. 2000, Yang et al. 1999). Current data supports a hypothesis by which consistent and repetitive induction of synaptic plasticity eventually leads to the elimination or maturation of particular synapses during development. There is a tendency for LTD to predominate in the young brain, with a switch to LTP as the brain matures (Feldman et al. 1998, Sawtell et al. 2003). One might expect then, that many synapses in early development are weak synapses, which mature as the ability to potentiate synapses in response to correlated activity develops (Constantine-Paton and Cline, 1998). This switch from LTD to LTP correlates with many developmental changes, including a developmental progression of NMDA receptor subunit expression, as well as proteins associated with the NMDAR in a post-synaptic NMDA receptor complex (van Zundert et al. 2004).

Data from the visual and somatosensory systems supports the concept of the NMDAR as a major causal link between changes in synaptic strength and structural rearrangements during development of afferent pathways (Hahm et al. 1991, Cline and Constantine-Paton 1989, Roberts et al. 1998, Daw et al. 1999, Iwasoto et al. 1997). In the superior colliculus, this process is used to refine and limit axonal connections during formation of the retinotopic map (Simon et al., 1992).

Activity-dependent competition based on maintaining convergence of similarly active inputs has also been extensively studied in visual cortex. Axons of LGN neurons projecting to cortex segregate into eye-specific domains early in the development of binocular animals, but remain plastic and sensitive to monocular deprivation by lid suture during a critical period (for review see Daw 1995). As a result, most cortical cells become responsive to the non-deprived

eye, and responsiveness to the deprived eye is lost. This competition is prevented when correlations between pre- and post-synaptic activity are disrupted by suppression of post-synaptic activation (Bear et al. 1990). Recent work suggests that selective elimination of the deprived eye by NMDA receptor-dependent plasticity is the driving force for this plasticity (Frenkel and Bear, 2004).

Visual Experience and Synapse Development

Insights from the visual cortex: EM and Golgi The role of experience in the development of spines and synapses has been best studied by in vivo sampled and longitudinal studies of pyramidal neurons of the visual cortex. Enriched environments affect not only synapse density but the appearance of mature sub-synaptic structures such as polyribosomes thought to be important for dendritic protein translation and long-term plasticity, as assayed with EM (Greenough et al. 1985, Jones et al. 1997). Optic nerve deafferentation and visual experience deprivation have long been known to disrupt spines on the apical dendrite of cortical pyramidal neurons in the mouse as well (Valverde 1967).

Insights from the visual cortex: Fluorescent microscopy. The basic pyramidal neuronal and basal and dendritic arbor structure is quite stereotyped, and in particular the long, straight, apical dendrite makes for reproducible sampling of spines on determined portions of the main dendrite at fixed intervals along the shaft from the soma. The apical dendrite is actually the least spiny dendrite of pyramid cells, however, with the majority of spines formed on the more complexly branched basal dendrites or apical tuft. Side branches off the apical dendrite are also highly spiny. The apical dendrite of Layer V pyramids becomes progressively spinier with age. Monocular deprivation for four days is disruptive to spine density when given either at P24-P31 or P57-P66, and these

26

disruptions do not occur in the absence of a normal balance of excitation and inhibition in the neuropil (Mataga et al. 2004). Pyramids of Layer III are also sensitive to manipulations of visual experience, and long term maintenance of animals in the dark affects both spine density and shape, at least on basal dendrites (Wallace and Bear 2004). These deprivations appear to induce somewhat permanent and non-recoverable damage, because normal spine densities are not recovered even after 10 days of normal visual experience.

Effects of Dark Rearing in the sSC. Effects of dark rearing from birth on synaptogenesis in the SC have been tested using quantitative EM approaches, and have produced variable results. When analysed as mean number of synapses per unit area of neuropil, dark reared rats from birth had fewer SGS synapses than normally reared animals, and this difference reached statistical significance by P56, but was not significant at P30 (Bakkum et al. 1991). Dark-rearing to P39 was also observed to cause a substantial deficit in the synapse-to-neuron ratio with similar methods (Mackay and Bedi 1987), When measured either as a synapse density per unit area, or as a synapse-to-neuron ratio using the newly created dissector method, however, no significant differences were observed in rats dark-reared to _either_ P30 or P65 (Fukui and Bedi 1991). No longitudinal or fluorescent morphological assays have been conducted on specific neuronal cell types or synapses in the mammalian sSC, however.

Thus visual deprivation by lid suture or dark-rearing can affect both spine number and the structural correlates of spine maturation in either the positive or negative directions in at least some visual cell types in the CNS. It is still unclear how rapidly these changes can occur.

Regulation of NMDARs, PSD-95, and synaptic plasticity by vision onset

Regulation of NMDARs and LTP. The ability to control the activity of retinal afferents to the brain has made the visual system a valuable model for NMDAR regulation by sensory experience. NMDAR current and subunit composition at the synapse is tightly regulated by vision in target neurons of the superior colliculus (reviewed in van Zundert et al. 2004). In the first postnatal week in the superior colliculus, both synaptic and extra-synaptic responses are solely mediated by NR2B receptors. Just before the eyes open, the first NR2A subunits begin to be incorporated into NMDARs. As photoreceptors begin to respond to light through the closed eyelids, glutamatergic retinal activity induces a rapid downregulation (shortening) of the NMDAR calcium current that is mediated by the phosphatase calcineurin (Townsend et al. 2004). The enzyme is held at NMDARs through its interaction with AKAPs via PSD-95. It de-phosphorylates receptors containing new NR2A subunits that have just begun to be expressed in the superior colliculus. Visual experience soon after the eyes open drives an increased accumulation of PSD-95 at synapses (Yoshii et al. 2003), which bind increasing amounts of NR2A-containing receptors. During this time, the primary synaptic NMDARs become those containing NR2A. It is within four hours of this initial eye-opening that tetanus-induced LTP can first be induced in collicular neurons by stimulation of the stratum opticum (Zhao and Constantine-Paton, SFN abstract). LTP cannot be induced in littermates whose eyes have been prevented from opening. There is some evidence that the ability to generate NMDAR-dependent LTP may be conferred by the presence of the NR2A subunit (Liu et al. 2004, JP Zhao personal communication), and genetic deletion of the NR2A subunit results in a progressive loss of synaptic NMDAR currents (miniature NMDAR-EPSCs) in parallel with the normal upregulation of NR2A. Early synaptic and later extrasynaptic responses mediated by NR2B are preserved. LTD can be induced by 1Hz stimulation either before or after eye-opening (Zhao et al. 2006 and personal communication)

Regulation of synaptic receptor composition. Visual experience not only regulates receptor composition, it also drives changes in the composition of synapses within hours after the eyes have opened. Six hours of visual experience is sufficient to detect new, miniature NMDAR currents containing NR2B-receptors and representing presumptively new, immature, "silent" synapses. AMPA receptors appear within 12 hours and by 24 hours most NMDARs have fast current decays characteristic of NR2A-containing NMDARs (Lu and Constantine-Paton 2004).

MAGUKs defined. MAGUKs are intracellular proteins that contain multiple protein-protein interaction domains and bind to both NMDARs and many of the signaling molecules through which the NMDAR effects cytoskeletal rearrangements and other calcium-dependent processes (Kennedy et al. 2005, Kim and Sheng 2004). They may prove to be critically important in linking calcium influx through NMDARs to specific signaling pathways by tethering the necessary molecules close to the channel pore. Two MAGUKs, SAP102 and PSD-95, are differentially expressed during development of the sSC, and they now appear to have some specificity for NMDAR complexes containing NR2B, or NR2A, respectively (Townsend et al. 2003). In the superior colliculus, hippocampus, and visual cortex, developmental expression of the MAGUKs are associated with similar changes in NMDAR expression. Of the three MAGUKs that scaffold NMDARs, only SAP102 is expressed at the early age when NR2B-containing receptors predominate (reviewed in van Zundert et al. 2004). Like NR2B, SAP102 expression does not disappear, but continues to be expressed in the adult. Also like NR2B, SAP102 localizes to extrasynaptic sites after the first two postnatal weeks, and both NR2B and SAP102 are preferentially associated with SynGAP (synaptic GTPase activating protein), suggesting that all three might consitute an extrasynaptic signaling complex.

Regulation of PSD-95. PSD-95 appears at the synapse in parallel with NR2A

29

subunits, and preferentially associates with NMDARs containing NR2A. This entire complex is anchored to the lipid raft at the PSD by the palmitoylation site on PSD-95. PSD-95 has recently been shown to produce synapse potentiation by anchoring stargazin/AMPAR complexes in the PSD (Bats et al. 2007, Ehrlich and Malinow 2004), and activation of NMDARs containing NR2A have been reported to promote insertion of AMPARs containing GluR1 (Kim et al. 2005). Two hours of visual experience is sufficient to induce increases in the amount of PSD-95 detected in collicular synaptoneurosomes (Yoshii et al. 2003). Thus initial visual experience drives a near simultaneous increase in PSD-95, and ability to induce LTP, in collicular neurons. The structural or functional implications of these events is unknown. However, these results do suggest that the subunit-specific interaction of NMDARs and their associated protein complex may direct changes in synaptic strength that underly developmental refinement of neuronal connectivity and structure.

PSD-95 in synaptogenesis

PSD-95 and synaptogenesis. The appearance of non-mobile neuroligin-containing clusters is correlated with the development of new excitatory synaptic sites on hippocampal neurons in vitro. These clusters are distinguishable from more mobile clusters which contain PSD-95, suggesting that PSD-95 is not involved in new excitatory synapse formation per se (Gerrow et al. 2006). Indeed, NMDAR recruitment to new sites of axo-dendritic contact is not necessarily accompanied by PSD-95 or AMPARs, whose recruitment to new synaptic sites occurs on a slower time scale than NMDARs in vitro (Washbourne et al. 2002). The largest evidence to date for PSD-95 function are in vitro studies that implicate the protein in the synaptic clustering of molecules at existing synaptic sites (Rao et al. 1998, Chetkovich et al. 2002), and AMPAR trafficking (El-Husseini et al. 2002, Nakagawa et al. 2004, Bats et al. 2007). Overexpression of PSD-95 enhances the number of AMPAR at synapses in vitro

(Schnell et al. 2002, Ehrlich and Malinow, 2004). However, knockdown of PSD-95 in postnatal animals of unspecified ages reduces the frequency of miniature events in acute slices with no detectable effect on amplitude (Elias et al. 2006). The divergence in these results may have something to do in part with the overexpression approach, which may disrupt AMPAR homeostasis and drive more AMPARs than usual into existing synapses. It is also not clear whether this reduced frequency represents silencing of synapses, or a reduction in the number of synapses on the dendritic arbor. It is furthermore not understood why PSD-95 elimination appears to affect only certain synapses, and not others. It is interesting to note that NR2AKO mice, which have reduced NR-EPSCs and LTP (Sakimura et al. 1995) show a similar synapse-specificity to their deficit, which has been attributed to differential expression of the subunit at the commisural/associational-CA3 synapse versus the Fimbrial-CA3 synapses (Ito et al. 1997).

GFP-tagged PSD-95 clusters followed in vivo over time in visual cortex confirm that PSD-95 is dynamic, and that the retention of PSD-95 clusters in spines increases with developmental age. Furthermore, spine head size was correlated with the accumulation of PSD-95, as well as with the maintenance of PSD-95 clusters (Gray et al. 2006). Thus, maintainance of PSD-95 accumulation may be critical to the more mature spines that form later in development. Indeed, genetic deletion of PSD-95 disrupts the development of normal adult spine density on Golgi-impregnated dendrites in both the striatum and hippocampus (Vickers et a. 2006).

PSD-95 and synaptic plasticity. In vivo studies have provided the most reproducible results in the study of the role of PSD-95 in the ability to induce LTP in slices with tetanic stimuli. They appear to support a modulatory rather than essential function for PSD-95 in LTP induction, in either of the two regions that have been assayed, CA1 and the striatum. CA1 tetanus-induced field LTP

is preserved, and actually enhanced, in a PSD-95 truncation mutant which arrests protein translation in the second PDZ domain (Migaud et al. 1998). In this line of mice, it was concluded that the truncated protein was present in whole lysates, albeit not at synapses, and thus potentially was not a true knockout in the hippocampus. However, detection of the presence of the truncated protein was rendered difficult due to the lack of a specific antibody. In an independent line of knockout mice, truncation of the more distal C-terminal GK domain of PSD-95 resulted in the complete disappearance of the protein from both whole lysates and synaptoneurosomes, confirmed with an N-terminal specific antibody (Yao et al. 2004). The enhanced LTP observed in the hippocampus of the mice assayed in Migaud et al. could be explained by the upregulation of SAP102 protein in the adult that has been shown to occur in these mice (Cuthbert et al. 2007)), especially at the older ages at which field LTP studies are conducted.

Acute dissociation of the PSD-95-NMDAR interaction with disrupting peptides delivered by whole-cell patch clamp and accompanied by electrophysiological assays of whole-cell synaptic properties and LTP induction did not detect an acute effect on basal synaptic transmission or induction of LTP in CA1. However, pre-incubation of dissociated hippocampal neurons in vitro with membrane-permeable peptides did result in fewer dendritic clusters of PSD-95 and NR1 (Lim et al. 2003).

Overexpression of PSD-95 in organotypic slice cultures occludes LTP (Ehrlich and Malinow 2004). However, the same group, using siRNA mediated knockdown of PSD-95 in organotypic slice cultures have also found no effect on LTP (Ehrlich et al. 2007). Slices which are cultured ex vivo display enormous anomalous sprouting of dendrites, spines, and enhanced AMPAR currents (DeSimoni et al. 2003), and neurons and synapses in organotypic slice cultures are in general thought to have reduced plasticity. Nevertheless, the combined

results of these in vivo and in vitro studies are supportive of a modulatory or priming role for PSD-95 in the generation of LTP, and show that tetanus-induced LTP can be generated in the absence of PSD-95.

What are the implications of a disrupted ability to induce normal LTP to postnatal development? LTP-induction is enhanced in PSD95 mutant mice, who have a full ocular dominance plasticity in visual cortex. But this is in contrast to the impaired ocular dominance plasticity observed in NR2AKO mice which also have a greatly reduced ability to generate LTP (Fagiolini et al. 2003, Ito et al. 1996). It is not clear whether specific deficits in synapse formation, maintenance, or elimination underlie these deficits.

Literature Cited

Aamodt SM, Constantine-Paton M. 1999. The role of neural activity in synaptic development and its implications for adult brain function. Adv Neurol. 79:133-44.

Andersen P, Blackstad T, Hulleberg G, Trommald M, Vaaland JL. 1987. Dimensions of dendritic spines of rat dentate granule cells during long-term potentiation. J Physiol 390: P264.

Anker R. 1977. The prenatal development of some of the visual pathways of the cat. J Comp Neurol 173: 185-204.

Bakkum BW, Benevento LA, Cohen RS. 1991. Effects of light/dark- and dark-rearing on synaptic morphology in the superior colliculus and visual cortex of the postnatal and adult rat. J Neurosci Res. 28(1):65-80.

Bats C, Groc L, Choquet D. 2007. The interaction between Stargazin and PSD-95 regulates AMPA receptor surface trafficking. Neuron. Mar 1;53(5):719-34.

Berman N, Cynader M. 1976. Early versus late visual cortex lesions: Effects on receptive fields in cat superior colliculus. Exp Brain Res 25: 131-37.

Bonds AB, Freeman RD. 1978. Development of optical quality in the kitten eye. Vision Res 18: 391-98.

Brainard MS and Knudsen EI. 1998. Images in neuroscience. Brain development, V: Experience affects brain development. Am J Psychiatry. Aug;155(8):1000.

Cang J, Renteria RC, Kaneko M, Liu X, Copenhagen DR, Stryker MP. 2005. Development of precise maps in visual cortex requires patterned spontaneous activity in the retina. Neuron 48(5):797-809.

Chen C, Regehr WG. 2000. Developmental remodeling of the retinogeniculate synapse. Neuron 28(3):955-66.

Chetkovich DM, Chen L, Stocker TJ, Nicoll RA, Bredt DS. 2002. Phosphorylation of the postsynaptic density-95 (PSD-95)/discs large/zona occludens-1 binding site of stargazin regulates binding to PSD-95 and synaptic targeting of AMPA receptors. J Neurosci. 22(14):5791-6.

Collingridge GL, Kehl SJ, McLennan 1983. Excitatory amino acids in synaptic transmission in the Schaffer collateral-commissural pathway of the rat hippocampus. J Physiol. 334:33-46.

Colonnese MT, Constantine-Paton M. 2006. Developmental period for N-methyl-D-aspartate (NMDA) receptor-dependent synapse elimination correlated with visuotopic map refinement.
J Comp Neurol. 494(5):738-51.

Colonnese MT, Zhao JP, Constantine-Paton M. 2005. NMDA receptor currents suppress synapse formation on sprouting axons in vivo. J Neurosci. 25(5):1291-303.

Constantine-Paton M, Cline HT. 1998. LTP and activity-dependent synaptogenesis: the more alike they are, the more different they become. Curr Opin Neurobiol. 8(1):139-48

Corriveau RA. 1999. Electrical activity and gene expression in the development of vertebrate neural circuits. J Neurobiol. 41(1):148-57.

Cuthbert PC, Stanford LE, Coba MP, Ainge JA, Fink AE, Opazo P, Delgado JY, Komiyama NH, O'Dell TJ, Grant SG. 2007. Synapse-associated protein 102/dlgh3 couples the NMDA receptor to specific plasticity pathways and learning strategies. J Neurosci. 27(10):2673-82.

Demas J, Eglen SJ, Wong RO. 2003. Developmental loss of synchronous spontaneous activity in the mouse retina is independent of visual experience. J Neurosci. 23(7):2851-60.

DeSimoni AD, Griesinger CB, Edwards FA. 2003. Development of rat CA1 neurones in acute versus organotypic slices: role of experience in synaptic morphology and activity. J Physiol 550.1: 135-147.

Drager UC, Hofbauer A. 1985. Depth segregation of retinal ganglion cells projecting to mouse superior colliculus. JCN 234: 465-74.

Dreher B, Shameem N, Thong IG, McCall MJ. 1985. Development of cortical afferents and cortico-tectal efferents of the mammalian (rat) primary visual cortex. Australian and New Zealand Journal of Ophtalmology 13: 251-261.

Edwards MA, Schneider GE, Caviness VS, Jr. 1986. Development of the crossed retinocollicular projection in the mouse. J Comp Neurol 248: 410-421.

Ehrlich I, Klein M, Rumpel S, Malinow R. 2007. PSD-95 is required for activity-driven synapse stabilization. Proc Natl Acad Sci U S A. 104(10):4176-81.

Ehrlich I, Malinow R. 2004. Postsynaptic density 95 controls AMPA receptor incorporation during long-term potentiation and experience-driven synaptic plasticity. J Neurosci. 24(4):916-27.

Elias GM, Funke L, Stein V, Grant SG, Bredt DS, Nicoll RA. 2006. Synapse-specific and developmentally regulated targeting of AMPA receptors by a family of MAGUK scaffolding proteins. Neuron. Oct 19;52(2):307-20.

Ellemberg Lewis TL, Maurer D, Brar S, Brent HP. 2002. Better perception of global motion after monocular than after binocular deprivation, Vision Res. 42: 169-179.

Frenkel MY, Bear MF. 2004. How monocular deprivation shifts ocular dominance in visual cortex of young mice. Neuron 44(6):917-23.

Fagiolini M, Katagiri H, Miyamoto H, Mori H, Grant SG, Mishina M, Hensch TK. 2003. Separable features of visual cortical plasticity revealed by N-methyl-D-aspartate receptor 2A signaling. Proc Natl Acad Sci U S A100(5):2854-9.

Feller MB.   2003. Visual system plasticity begins in the retina. Neuron. Jul 3;39(1):3-4.

Fine, I., Wade, A.R., Brewer, A.A., May, M.G., Goodman, D.F., Boynton, G.M., Wandell, B.A., &
MacLeod, D.I. (2003). Long-term deprivation affects visual perception and cortex. Nature Neuroscience, 6, 915-916.

Firth SI, Wang CT, Feller MB. 2005. Retinal waves: mechanisms and function in visual system development. Cell Calcium. 2005 May;37(5):425-32.

Flandrin JM, Jeannerod M. 1977. Lack of recovery in collicular neurons from the effects of early deprivation or neonatal cortical lesion in the kitten. Brain Res 120: 362-66.

Fukui Y, Bedi KS. 1991. Quantitative study of the development of neurons and synapses in rats reared in the dark during early postnatal life. 1. Superior colliculus. J Anat. 1991 174:49-60.

Gandhi SP, Cang J, Stryker MP. 2005. An eye-opening experience. Nat Neurosci. Jan;8(1):9-10.

Garaschuk O, Linn J, Eilers J, Konnerth A. 2000. Large-scale oscillatory calcium waves in the immature cortex. Nat Neurosci. 3(5):452-9.

Gerrow K, Romorini S, Nabi SM, Colicos MA, Sala C, El-Husseini A. 2006. A preformed complex of postsynaptic proteins is involved in excitatory synapse development. Neuron 49: 547-62.

Godement P, Salaun J, Imbert M.   1984.   Prenatal and postnatal development of retinogeniculate and retinocollicular projections in the mouse. J Comp Neurol 230: 552-75.

Gray NW, Weimer RM, Bureau I, Svoboda K. 2006.   Rapid redistribution of synaptic PSD-95 in the neocortex in vivo. PLoS Biol. 4(11):e370.

Greenough WT, Hwang HM, Gorman C. 1985. Evidence for active synapse formation or altered postsynaptic metabolism in visual cortex of rats reared in complex environments. Proc Natl Acad Sci U S A. 82(13):4549-52.

Giraldi-Guimaraes A, Mendez-Otero R.   2005. Visually-induced NGFI-A protein expression in the calbindin-, parvalbumin- and nitric oxide synthase-neuronal populations of the rat superior colliculus. J Chem Neuroanat. 2005 May;29(3):209-16.

Hamasaki KI, Flynn JT. 1977. Physiological properties of retinal ganglion cells of 3-week-old kittens. Vision Res 17: 275-84.

Harris DM, Dallos P. 1984. Ontogenetic changes in frequency mapping of a mammalian ear.
Science 225(4663):741-3.

Harris EW, Ganong AH, Cotman CW. Long-term potentiation in the hippocampus involves activation of N-methyl-D-aspartate receptors. Brain Res. 323(1):132-7.

Harris KM, Jensen FE, Tsao B. 1992. Three-dimensional structure of dendritic spines and synapses in rat hippocampus (CA1) at postnatal day 15 and adult ages: Implications for the maturation of synaptic physiology and long-term potentiation. J Neurosci 12: 2685-2705.

Harris KM. 1999. Structure, development, and plasticity of dendritic spines. Curr Opin Neurobiol 9: 343-348.

Harting JK, Huerta MF, Hashikawa T, van Lieshout DP. 1991. Projection of the mammalian superior colliculus upon the dorsal lateral geniculate nucleus: organization of tectogeniculate pathways in nineteen species. J Comp Neurol. 304(2):275-306.

Harting JK, Huerta MF, Frankfurter AJ, Strominger NL, Royce GJ. 1980. Ascending pathways from the monkey superior colliculus: an autoradiographic analysis. J Comp Neurol. 192(4):853-82.

Hestrin S. 1992. Developmental regulation of NMDA receptor-mediated synaptic currents at a central synapse. Nature 357(6380):686-9.

Holthoff K, Tsay D, Yuste R. 2002. Calcium dynamics of spines depend on their dendritic location. Neuron 33: 425-437.

Hooks BM, Chen C. 2006. Distinct roles for spontaneous and visual activity in remodeling of the retinogeniculate synapse. Neuron. 52(2):281-91.

Hubel DH, Weisel TN. 1963. Receptive fields of cells in striate cortex of very young, visually inexperienced kittens. J Neurophysiol 26: 994-1002.

Hyde PS and Knudsen EI. 2002. The optic tectum controls visually guided adaptive plasticity in the owl's auditory space map. Nature. Jan 3;415(6867):73-6.

Inoue K, Terashima T, Inoue Y. 1992. Postnatal development of the corticotectal projection from the visual cortex of the mouse. Okajimas Folia Anatomica Japonica 68: 319-332.

Ito I, Futai K, Katagiri H, Watanabe M, Sakimura K, Mishina M, Sugiyama H. 1997. Synapse-selective impairment of NMDA receptor functions in mice lacking NMDA receptor epsilon 1 or epsilon 2 subunit. J Physiol. 500 (Pt 2):401-8.

Ito I, Sakimura K, Mishina M, Sugiyama H. 1996. Age-dependent reduction of hippocampal LTP in mice lacking N-methyl-D-aspartate receptor epsilon 1 subunit. Neurosci Lett 203(1):69-71.

Jones TA, Klintsova AY, Kilman VL, Sirevaag AM, Greenough WT. 1997. Induction of multiple synapses by experience in the visual cortex of adult rats. Neurobiol Learn Mem. 68(1):13-20.

Kao C-Q, McHaffie JG, Meredith MA, Stein BE. 1994. Functional development of a central visual map in cat. J Neurophys 72: 266-272.

Katz LC, Shatz CJ. 1996. Synaptic activity and the construction of cortical circuits. Science 274(5290):1133-8.

Kennedy MB, Beale HC, Carlisle HJ, Washburn LR. 2005. Integration of biochemical signalling in spines. Nat Rev Neurosci. 6(6):423-34.

Kim E, Sheng M. 2004. PDZ domain proteins of synapses. Nat Rev Neurosci. 5(10):771-81.

Kim MJ, Dunah AW, Wang YT, Sheng M. 2005. Differential roles of NR2A- and NR2B-containing NMDA receptors in Ras-ERK signaling and AMPA receptor trafficking. Neuron 46(5):745-60.

Kiorpes L, Kiper DC. 1996. Development of contrast sensitivity across the visual field in macaque monkeys (Macaca nemestrina). Vision Res. Jan;36(2):239-47.

Kirov SA, Sorra KE, Harris KM. 1999. Slices have more synapses than perfusion-fixed hippocampus from both young and mature rats. J Neurosci 19: 2876-86.

Kourtzi Z, Augath M, Logothetis NK, Movshon JA, Kiorpes L. 2006. Development of visually evoked cortical activity in infant macaque monkeys studied longitudinally with fMRI. Magn Reson Imaging. May;24(4):359-66.

Krug K, Akerman CJ, Thompson ID. 2001. Responses of neurons in neonatal cortex and thalamus to patterned visual stimulation through the naturally closed lids. J Neurophysiol. 85(4):1436-43.

Law CC, Bear MF, Cooper LN. 1994. Role of the visual environment in the formation of receptive fields according to the BCM theory. Prog Brain Res. 102:287-301.

Landers M, Philip Zeigler H. 2006. Development of rodent whisking: trigeminal input and central pattern generation. Somatosens Mot Res. 23(1-2):1-10.

Langer TP and Lund RD. 1974. The upper layers of the superior colliculus of the rat: A golgi study. J Comp Neur 158: 405-436.

Lee KS, Schottler F, Oliver M, Lynch G. 1979. Synaptic change associated with the induction of long-term potentiation. Anat. Rec. 193: 601-2.

Leinekugel X, Khazipov R, Cannon R, Hirase H, Ben-Ari Y, Buzsaki G. 2002. Correlated bursts of activity in the neonatal hippocampus in vivo. Science 296(5575):2049-52.

LeVay, S., Wiesel, T.N., & Hubel, D.H. (1980). The development of ocular dominance columns in normal and visually deprived monkeys. The Journal of Comparative Neurology, 191, 1-53.

Levitt JB, Schumer RA, Sherman SM, Spear PD, Movshon JA. 2001. Visual response properties of neurons in the LGN of normally reared and visually deprived macaque monkeys. J Neurophysiol. May;85(5):2111-29.

Lim IA, Merrill MA, Chen Y, Hell JW. 2003. Disruption of the NMDA receptor-PSD-95 interaction in hippocampal neurons with no obvious physiological short-term effect. Neuropharmacology. 45(6):738-54.

Lopez-Medina A, Bueno-Lopez JL, Reblet C. 1989. Postnatal development of the occipito-tectal pathway in the rat. Int J Dev Biol. 33(2):277-86.

Lu W, Constantine-Paton M. Eye opening rapidly induces synaptic potentiation and refinement.
Neuron. 2004 Jul 22;43(2):237-49.

Lund RD. 1978. *Development and plasticity of the brain.* New York: Oxford University Press.

Lund RD, Bunt AH. 1976. Prenatal development of central optic pathways in albino rats. J Comp Neurol 165: 247-64.

Maffei A, Nelson SB, Turrigiano GG. 2004. Selective reconfiguration of layer 4 visual cortical circuitry by visual deprivation. Nat Neurosci. Dec;7(12):1353-9

Majewska A, Tashiro A, Yuste R. 2000. Regulation of spine calcium dynamics by rapid spine motility. J Neurosci 20: 8262-68.

Mataga N, Mizuguchi Y, Hensch TK. 2004. Experience-dependent pruning of dendritic spines in visual cortex by tissue plasminogen activator. Neuron. Dec 16;44(6):1031-41.

Maurer D and Lewis TL, Visual acuity: the role of visual input in inducing postnatal change, Clin. Neurosci. Res. 1 (2001), pp. 239-247

Maurer, D., Lewis, T.L., & Mondloch, C.J. (2005). Missing sights: Consequences for visual cognitive development. Trends in Cognitive Sciences, 9, 144-151.
Medline, ISI

McLaughlin T, Torborg CL, Feller MB, O'Leary DD. 2003. Retinotopic map refinement requires spontaneous retinal waves during a brief critical period of development. Neuron 40(6):1147-60.

McLaughlin T, O'Leary DD. 2005. Molecular gradients and development of retinotopic maps.
Annu Rev Neurosci. 2005;28:327-55.

Mize RR. 1983. Patterns of convergence and divergence of retinal and cortical synaptic terminals in the cat superior colliculus. Exp Brain Res 51: 88-96.

Mize RR, Murphy EH. 1976. Alterations in receptive field properties of superior colliculus cells produced by visual cortex ablation in infant and adult cats. J Comp Neurol 168: 393-424.

Molotchnikoff S, Itaya SK. 1993. Functional development of the neonatal rat retinotectal pathway.
Brain Res Dev Brain Res. 72(2):300-4.

Mooney RD, Nikoletseas MM, Hess PR, Allen Z, Lewin AC, Rhoades RW. 1988. The projection from the superficial to the deep layers of the superior colliculus: An intracellular horseradish peroxidase injection study in the hamster. J Neurosci 8: 1384-1399.

Moore CL, Kalil R, Richards W. 1976. Development of myelination in optic tract of the cat. J Comp Neurol 165: 125-136.

Movshon JA, Kiorpes L, Hawken MJ, Cavanaugh JR. 2005. Functional maturation of the macaque's lateral geniculate nucleus. J Neurosci. 25(10):2712-22.

Mulkey RM, Malenka RC. 1992. Mechanisms underlying induction of homosynaptic long-term depression in area CA1 of the hippocampus. Neuron 9(5):967-75.

Mustari MJ, Lund RD, Graubard K. 1979. Histogenesis of the superior colliculus of the albino rat: a tritiated thymidine study. Brain Res 164: 39-52.

Nakagawa T, Futai K, Lashuel HA, Lo I, Okamoto K, Walz T, Hayashi Y, Sheng M. 2004.Quaternary structure, protein dynamics, and synaptic function of SAP97 controlled by L27 domain interactions. Neuron. 44(3):453-67.

Nase G, Singer W, Monyer H, Engel AK. 2003. Features of neuronal synchrony in mouse visual cortex. J Neurophysiol. (2):1115-23.

Nedivi E, Fieldust S, Theill LE, Hevron D. 1996.   A set of genes expressed in response to light in the adult cerebral cortex and regulated during development. Proc Natl Acad Sci 93(5):2048-53.

Nedivi E. 1999. Molecular analysis of developmental plasticity in neocortex. J Neurobiol 41(1):135-47.

Noguchi J, Matsuzaki M, Ellis-Davies GC, Kasai H. 2005. Spine-neck geometry determines NMDA receptor-dependent Ca++ signaling in dendrites. Neuron 46: 609-22.

40

Norton TT. 1974. Receptive-field properties of superior colliculus cells and development of visual behavior in kittens. J Neurophysiol. 37: 674-90.

Nusser Z, Lujan R, Laube G, Roberts JDB, Molnar E, Somogyi P. 1998. Cell type and pathway dependence of synaptic AMPA receptor number and variability in the hippocampus. Neuron 21: 545-59.

Ostrovsky Y, Andalman A, Sinha P. 2006. Vision following extended congenital blindness. Psychol Sci. 2006 Dec;17(12):1009-14.

Petrak LJ, Harris KM, Kirov SA. 2005. Synaptogenesis on mature hippocampal dendrites occurs via filopodia and immature spines during blocked synaptic transmission. J Comp Neurol. 484(2):183-90.

Plummer KL, Behan M. 1992. Postnatal development of the corticotectal projection in cats. J Comp Neurol 315: 178-199.

Rao A, Kim E, Sheng M, Craig AM. 1998. Heterogeneity in the molecular composition of excitatory postsynaptic sites during development of hippocampal neurons in culture. J Neurosci. 18(4):1217-29.

Rhoades RW, Mooney RD, Fish SE. 1985. Subcortical projections of area 17 in the anopthalmic mouse. Dev Brain Res 17: 171-181.

Sachs GM, Jacobson M, Caviness VS Jr. 1986. Postnatal changes in arborization patterns of murine retinocollicular axons. J Comp Neurol 246: 395-408.

Saito Y, Murakami F, Song WJ, Okawa K, Shimono K, Katsumaru H. 1992. Developing corticorubral axons of the cat form synapses on filopodial dendritic protrusions. Neurosci Lett. 147(1):81-4.

Sakimura K, Kutsuwada T, Ito I, Manabe T, Takayama C, Kushiya E, Yagi T, Aizawa S, Inoue Y, Sugiyama H, et al. 1995. Reduced hippocampal LTP and spatial learning in mice lacking NMDA receptor epsilon 1 subunit. Nature. 373(6510):151-5.

Schikorski T, Stevens C. 1999. Quantitative fine-structural analysis of olfactory cortical synapses. PNAS 96: 4107-12.

Shi J, Aamodt SM, Constantine-Paton M. 1997. Temporal correlations between functional and molecular changes in NMDA receptors and GABA neurotransmission in the superior colliculus.
J Neurosci. 17(16):6264-76.

Simon DK, O'Leary DD. 1992. Development of topographic order in the mammalian retinocollicular projection. J Neurosci. 12(4):1212-32.

Sireteanu R and Maurer D. 1982. The development of the kitten's visual field. Vision Res 22: 1105-11.

Smith SL, Trachtenberg JT. 2007. Experience-dependent binocular competition in the visual cortex begins at eye opening. Nat Neurosci. Mar;10(3):370-5.

Stein BE, Edwards SB. 1979. Cortico-tectal and other corticofugal projections in neonatal cat. Brain Res 161: 399-409.

Stein BE, Gallagher H. 1981. Maturation of cortical control over superior colliculus cells in cat. Brain Res 223: 429-35.

Stein BE, Labos E, Kruger L. 1973b. Determinants of response latency in neurons of superior colliculus in kittens. J Neurophysiol 36: 680-89.

Stein BE, Labos E, Kruger L. 1973a. Sequence of changes in properties of neurons of superior colliculus of the kitten during maturation. J Neurophysiol 36: 667-79.

Stein BE, Magalhaes-Castro B. 1975. Effects of neonatal cortical lesions upon the cat superior colliculus. Brain Res 83: 480-85.

Stein BE. 1984. Development of the superior colliculus. Ann Rev Neurosci 7: 95-125.

Stein V, House DR, Bredt DS, Nicoll RA. 2003. Postsynaptic density-95 mimics and occludes hippocampal long-term potentiation and enhances long-term depression. J Neurosci. 23(13):5503-6.

Swindale NV. 1981. Dendritic spines only connect. TINS 4: 240-241.

Thorn F, Gollender M, Erickson P. 1976. The development of the kitten's visual optics. Vision Res 16: 1145-50.

Tian N, Copenhagen DR. 2003. Visual stimulation is required for refinement of ON and OFF pathways in postnatal retina. Neuron. Jul 3;39(1):85-96.

Townsend M, Liu Y, Constantine-Paton M. 2004. Retina-driven dephosphorylation of the NR2A subunit correlates with faster NMDA receptor kinetics at developing retinocollicular synapses.
J Neurosci. 24(49):11098-107.

Trommald M, Hulleberg G, Andersen P. 1996. Long-term potentiation is associated with new excitatory spine synapses on rat dentate granule cells. Learn Mem 3: 218-228.

Valverde F. 1967. Apical dendritic spines of the visual cortex and light deprivation in the mouse. Exp Brain Res. 3(4):337-52.

Vanegas H 1984. Comaparative Neurology of the Optic Tectum.

Verhage M, Maia AS, Plomp JJ, Brussaard AB, Heeroma JH, Vermeer H, Toonen RF, Hammer RE, van den Berg TK, Missler M, Geuze HJ, Sudhof TC. 2000. Synaptic assembly of the brain in the absence of neurotransmitter secretion. Science 287(5454):864-9.

Vickers CA, Stephens B, Bowen J, Arbuthnott GW, Grant SG, Ingham CA. 2006. Neurone specific regulation of dendritic spines in vivo by post synaptic density 95 protein (PSD-95). Brain Res. 1090(1):89-98.

Wallace W, Bear MF. 2004. A morphological correlate of synaptic scaling in visual cortex. J Neurosci. 2004 Aug 4;24(31):6928-38.

Warton SS, Jones DG. 1985. Postnatal development of the superficial layers in the rat superior colliculus: a study with Golgi-Cox and Kluver-Barrera techniques. Exp Brain Res. 58(3):490-502.

Warton SS, McCart R. 1989. Synaptogenesis in the stratum griseum superficiale of the rat superior colliculus. Synapse 3(2):136-48.

Washbourne P, Bennett JE, McAllister AK. 2002. Rapid recruitment of NMDA receptor transport packets to nascent synapses. Nat Neurosci 5: 751-759.

Wickelgren BG, Sterling P. 1969. Influence of visual cortex on receptive fields in the superior colliculus of the cat. J Neurophysiol 32: 16-23.

Wiesel, T.N., & Hubel, D.H. (1965). Comparison of the effects of unilateral and bilateral eye closure on cortical unit responses in kittens. Journal of Neurophysiology, 28, 1029-1040.

Witten IB and Knudsen EI. 2005. Why seeing is believing: merging auditory and visual worlds. Neuron. Nov 3;48(3):489-96.

Wong RO, Meister M, Shatz CJ. 1993. Transient period of correlated bursting activity during development of the mammalian retina. Neuron 11(5):923-38.

Wong RO. 1999. Retinal waves and visual system development. Annu Rev Neurosci. 22:29-47.

Yao WD, Gainetdinov RR, Arbuckle MI, Sotnikova TD, Cyr M, Beaulieu JM, Torres GE, Grant SG, Caron MG. 2004. Identification of PSD-95 as a regulator of dopamine-mediated synaptic and behavioral plasticity. Neuron 41(4):625-38.

Yoshii A, Sheng MH, Constantine-Paton M. Eye opening induces a rapid dendritic localization of PSD-95 in central visual neurons. Proc Natl Acad Sci U S A. 2003 Feb 4;100(3):1334-9. Epub 2003 Jan 27.

Yuste R, Majewska A, Holthoff K. 2000. From form to function: calcium compartmentalization in dendritic spines. Nat Neurosci 3: 653-59.

Zhao JP, Phillips MA, Constantine-Paton M. 2006. Long-term potentiation in the juvenile superior colliculus requires simultaneous activation of NMDA receptors and L-type Ca2+ channels and reflects addition of newly functional synapses. J Neurosci. 26(49):12647-55.

Zhao J, Constantine-Paton M. 2006. Roles of L-type calcium channel and the NR2A NMDAR subunit in superior colliculus and hippocampal CA1 LTP, Program No. 786.7. Neuroscience Meeting Planner. Atlanta, GA: Society for Neuroscience. Online.

Zuo Y, Lin A, Chang P, Gan WB. 2005. Development of long-term dendritic spine stability in diverse regions of cerebral cortex. Neuron. 46(2):181-9.

CHAPTER TWO

Initial visual experience stabilizes new synapses via PSD-95

SUMMARY

Eye-opening (EO) induces the appearance of dendritic PSD-95 and LTP in the visual superior colliculus (sSC) within 2-4 hours. Here, we provide evidence that EO-induced PSD-95 trafficking is required for the stabilization of new synapses *in vivo* as a result of patterned visual experience. mEPSC frequency recorded in a vertical neuronal subtype of the mid-SGS in the sSC increases at least three-fold after eye-opening, indicating a rapid synaptogenesis that does not occur in PSD95KO mice, or in age-matched littermates deprived of initial visual experience. A structural analysis of these neurons revealed caliber-specific patterns of spine and filopodia development that depend on EO and a projection from visual cortex. Between P11 and P13, dendrites post-synaptic to cortical axons undergo an EO-independent tripling of filopodial density and an EO-dependent maintenance of dendritic spine density. These data suggest that rapid vision-induced trafficking of PSD-95 enables long-term potentiation and stabilization of newly formed cortico-collicular release sites and maintainence of spine density in response to patterned visual stimuli.

INTRODUCTION

The maturation and fine-tuning of mammalian visual neuronal responses after eye-opening is a gradual process typically reaching adult levels over a period of weeks to months (Schmidt et al. 1999). At eye-opening, animals are exposed to patterned visual stimuli for the first time, and consolidation and refinement of synaptic connections begins to fine-tune neural responses. This further refinement of receptive fields and improved fidelity of neuronal responses is easily disrupted by manipulations preventing eye-opening (Lu and Constantine-Paton 2004, King and Carlile 1993, Schmidt et al. 1999, Smith and Trachtenberg 2007).

45

We have previously shown that eye-opening triggers synaptic and functional modifications on the order of hours to days in neurons of the visual layers of the superior colliculus (sSC) (Yoshii et al. 2003, Lu and Constantine-Paton 2004). Perhaps most dramatically, as little as four to six hours of visual experience is sufficient to trigger an increase in silent synapses (Lu and Constantine-Paton 2004) and a switch in synaptic plasticity, enabling tetanus-induced long-term potentiation of synapses which were previously insensitive to such stimuli (Zhao and Constantine-Paton, 2006). Whether it is stimulus amplitude or frequency that drives these changes, the most immediate outcome of the visual activation of target neurons after eye-opening is a rapid onset of plasticity involving increased delivery of the glutamate receptor scaffold PSD-95, to synapses, followed by an increased synaptic delivery of AMPA receptors.

Considerable evidence links PSD-95 to the synaptic localization of AMPARs (Elias et al. 2006, Beique et al. 2006, Ehrlich and Malinow 2004, Beique and Andrade 2003, Schnell et al. 2002, El-Husseini et al. 2000). Deletion of PSD-95 *in vivo* has been shown to result in fewer spines on cells of the striatum and hippocampus (Vickers et al. 2006), and a reduced number of spines containing GluR1 in hippocampal neurons *in vitro* (Elias et al. 2006). However, not all synapses which normally contain PSD-95 are affected by these manipulations, and the involvement of PSD-95 in synaptogenesis *per se* remains unclear. Initial synapse formation does not necessarily require synaptic transmission (Verhage et al. 2000), or PSD-95 (Gerrow et al. 2006). However, the activity-dependent stabilization and elimination of synapses can be exquisitely sensitive to specific patterns of afferent activity (McLaughlin et al. 2003, Zhou et al. 2003, Constantine-Paton and Cline 1998, Law et al. 1994, Constantine-Paton et al. 1990) and might require PSD-95 *in vivo* (Fagiolini et al. 2003). These processes are difficult, however, to assay with *in vitro* culture paradigms.

In this study, we ask whether the rapid changes in PSD-95 and LTP triggered by eye-opening are associated with *in vivo* functional and structural modification of specific visual collicular neurons that receive both retinal and visual cortical inputs. Such modifications might underlie the later ability of synapses to undergo further experience-dependent consolidation and refinement. Given the demonstrated role of visual experience in many regions of the brain in the regulation of PSD-95 (Yoshii et al. 2003), NMDARs (Lu and Constantine-Paton 2004, Philpot et al. 2001), and LTP (Zhao and Constantine-Paton 2006, Philpot et al. 2007, Kirkwood et al. 1995), we hypothesized that initial experience with patterned visual stimuli might drive a rapid remodeling of dendritic structure in the SC through the formation and/or stabilization of specific synapses, and that PSD-95 could be crucial to these processes.

Using a controlled eye-opening paradigm (Yoshii et al. 2003) to synchronize the onset of pattern visual experience, we have studied the development and distribution of spines and filopodia on dendritic arbors of a class of visual neurons in the sSC, before and after eye-opening at P12, or in littermates whose eyes are kept closed over the same period. We assayed in parallel the development of miniature excitatory post-synaptic currents (mEPSCs) in these cells, as an estimate of the number of functional glutamatergic release sites on each neuron, and tested the dependence of this functional developmental change on vision-induced increases in dendritic PSD-95.

METHODS

Animals All procedures followed MIT IACUC-approved protocols. Wild-type C57BL/6 mice were purchased (Jackson Laboratories), or bred in-house from purchased stock. PSD-95 mutant mice (Migaud et al. 1998) were bred in-house by matings of homozygous males (age 4-10 weeks) to heterozygous females. Pup survival required cross-fostering to Balb/c mice at birth, but once fostered normal Mendelian ratios were obtained. Apart from occasional runting, no

gross morphological differences were observed between mutants and heterozygous littermates at any age. However, significant post-natal lethality from undetermined causes was observed in homozygous mutants at ~2.5-3 months of age [Incidence of post-weaning spontaneous morbidity or illness-induced euthanasia: PSD95Mutant: 16/46, PSD95Het: 2/37, WT: 0/26]. Heterozygous C57BL/6 transgenic mice expressing eGFP under control of the Thy-1 promoter (Feng et al. 2000) were genotyped by epifluorescent detection of GFP-fluorescence in ear punches at weaning, and bred to homozygosity as confirmed by test matings to wild-type mice. Birthdating was done by observation of late pregnant mothers twice per day, enabling determination of birth dates within +/- 12 hours. The day pups were first observed was labeled "P0". On the morning of P11, each litter was closely investigated for signs of eye-opening (rare at this age), and any pups with even minor openings in the eyelid seam excluded. A thin layer of tissue bonding glue (VetBond, 3M) was applied to the eyelid seams of the remaining pups with a microapplicator. Pups were checked twice a day for the next two days, and small amounts of glue re-applied if necessary. Any pups with premature eye-openings were removed from the study. On P12, one-half of the litter was randomly selected for eye-opening, the glue overlying the eyelid seam was removed, and the eyelids popped open with mild tension. Nesting material was removed, and the cage exposed to 24 hours of continuous illumination within an environmental isolation unit.

Histology. Mice at P11, P13, P16, or Adult (4-8 weeks) were anesthetized with vaporized isofluorane (Samuel Perkins, MA), given a heparin flush through the left ventricle, and rapidly gravity perfused with 0.2um filtered PBS pH 7.4 followed by 4% paraformaldehyde/PBS pH 7.4 prepared fresh (EMS, 1ml per gram animal). Brains were dissected, trimmed if necessary to fully expose the midbrain, and post-fixed at 4C for 4-12 hours. Sequential, para-sagittal 200um vibratome sections of the entire superior colliculus from each brain

were collected floating into PBS, and mounted in aqueous antifade media (Fluoromount G, EMS).

Confocal Microscopy. Within 24 hours of mounting, serial sections from every animal were scanned under low magnification epifluorescence (20X/0.75NA) for the presence of well-labeled vertically oriented neurons, identified by their depth in the mid-deep SGS and vertical shape and orientation of the soma. These cells have dorsally-weighted dendritic arbors, and few ventral dendrites. These criteria are sufficient to exclude narrow-field vertical neurons located in the deep extent of the dSGS with arbors more evenly distributed dorsally and ventrally (Langer and Lund 1974, Tokunaga and Otani 1976). Once a well-labeled neuron of this type was identified, it was first confirmed that the majority (>80-90%) of its dendritic arbor was well labeled and present in a single slice. Every cell that fulfilled these criteria was selected for further analysis. Beginning at the soma, confocal z-series of portions of the dendritic arbor were then collected at high magnification with a 60X/1.4 NA oil-immersion objective and 2X digital zoom at 0.5um intervals on a Nikon PCM2000 (MVI) with SimplePCI acquisiton software (Compix), for a final pixel resolution of x y. Multiple image series were required to cover the entire dendritic arbor of each cell, and typically 100-200 images in each series required to cover the depth of the arbor. Four consecutive images of each optical slice were collected and averaged online during collection. This greatly enhanced the signal-to-noise ratio, and allowed analysis of spines relatively deep in the slice (60-100um). However, it also increased photobleaching, thus laser intensity was reduced to 10% (0.4mW). The acquisition gain was determined independently for each cell to be below the maximum threshold which caused saturation of pixels in spines. Finally, a low-magnification image of each cell was collected for later reconstruction of the location of each dendrite on the cell's arbor.

Structural Analysis. Z-series were exported in Tiff format, samples from all control and experimental groups at different ages were randomly intercalated, and the files coded by an independent investigator. Coded files were exported to a 3D image analysis program (Softworx for SGI, DeltaVision) allowing greater magnification, contrast enhancement, and three-dimensional measurement of dendritic branch lengths. Beginning at the soma, the total length of each dendrite from origination to next branching point was measured, along with the number of spines or filopodia along that length. We also recorded the subjective branch classification as "primary", "secondary", or "tertiary". Dynamic online contrast enhancement was used to normalize the diminished intensity among dendrites and spines located deeper in the slice, so that spine and filopodial densities from deeper branches were not underestimated. Only dendrites in which labeling was of sufficient resolution to determine spine vs filopodial identity were analysed. Branch diameter was calculated as the average of three measurements along the segment (proximal, middle, and distal) and were chosen to be representative.

Anterograde afferent labeling. Retinal and cortical afferents to the SGS were labeled by direct injection of a 0.5% solution of Alexa 488, 555, or 647-conjugated Cholera Toxin B subunits (Invitrogen) dissolved in 2% DMSO/sterile PBS pH 7.4. Intravitreal: Under vaporized isofluorane anesthesia, dye solution is injected through a small hole in the ciliary margin, using a blunt custom Hamilton syringe (5ul volume, 32G tip) to completely fill the vitreous with dye solution. Complete fill is confirmed by observation of the dye through the cornea. Cortical: Microinjection tips were prepared from glass capillaries (Drummond #1-000-0300) and broken using a sterile forceps to the following tip dimensions: 0.8 cm L x 36 um ID, 45 degree bevel. 1-3ul of dye solution was injected through a small burr hole in medio-posterior cortex (Using Paxinos' coordinates from Lambda: 3mm in adult mice, scaled for other ages) using a positive displacement injection system (CellTram Vario, Eppendorf).

Successful labeling only occurred when injections were performed slowly (over ~30-40 minutes), and wound did not leak during injection or after needle retraction. After 1-3 days animals were perfused, and confirmation of complete fills and localization and extent of cortical injection confirmed under stereoscopic examination of optic nerves, cortices, and collicular lobes with combination brightfield and epifluorescence microscopy using the appropriate filters.

Axon Colocalization Analysis. Confocal image stacks were examined for co-localization between eGFP-labeled neurons and anterogradely labeled retinal and cortical axons using ImageJ (NIH), for a total of three cells each from two separate labeling experiments. Only pixels exceeding a fixed intensity threshold were used to identify co-localization. This threshold was empirically determined by evaluation of the threshold required to discriminate in-focus from out-of-focus fluorescence, and was set at 5.5 standard deviations above the mean pixel intensity. Confocal z-series encompassing the neuron were batch processed for co-localized pixels using an automated algorithm (ImageJ; NIH). The density and localization of the overlapped pixels on dendritic branches of individual neurons was then measured in Softworx (SGI), using the original neuronal image stack overlapped with a binary image stack of the co-localized pixels.

Starting from the cell soma and progressing outward, 10um lengths of dendrite were measured. Three optical slices encompassing the dendritic segment were collapsed, and the number of overlapped pixels along the 10um lengths counted. Branch diameter was measured by taking the average of three measurements made at the start, middle, and end of the segment. Because images were collected at a minimum pixel resolution of 0.3um x 0.3um x ?um (xyz), single pixel overlap represents a large enough area to encompass both a CTB-enriched pre-synaptic terminal (CTB label) and a post-synaptic site (eGFP

label). Mean overlapped pixel densities per um of dendrite were plotted as a function of normalized branch thickness as described.

Control for non-specific overlap. Multiple contiguous overlapped pixels could represent locally elaborated axonal branches, which make several synaptic contacts onto a portion of a dendritic segment, or they could simply reflect *en passant* axons traveling along a dendritic shaft. To reveal the degree of overlap we might expect from chance, overlap analysis were first conducted on images in which the axon label was rotated with respect to the eGFP labeled neuron. We then conducted an analysis of the distribution of overlapped pixel cluster sizes in the non-rotated vs rotated images. Due to the opposing vertical gradients of cortical and retinal label, 180 degree rotation placed a high density of the cortical label into the region of the dendritic arbor. The same rotation placed the retinal label out of the zone of the dendritic arbor, and resulted in 0 overlapped pixels. Therefore, the retinal label images were rotated 90 degrees. The rotation angle and direction was chosen to maximize the potential for overlap between the axon label and the eGFP dendrite, and thus should overestimate the degree of random overlap in the original images.

Optical sections encompassing the labeled neuron were isolated, and a rectangular bounding box drawn to encompass the entire dorsal dendritic arbor (excluding the cell soma). Overlapped contiguous pixel clusters of 1-100 pixels in area within this region were counted with an automated particle counter (ImageJ) in all control and rotated optical z-series. Pixel cluster values were pooled, and the resulting distributions analysed. Cluster size distribution was significantly different in rotated vs control images for both the cortical and retinal overlaps (Mann-Whitney for CTP and RTP $p < 0.02$). The large contiguous overlapped pixel clusters in the original, non-rotated images were not present in rotated images. 95% confidence intervals for overlap pixel cluster sizes were

generated for rotated data for each label and used to set minimum acceptable cluster sizes for overlap counting in original images.

Cortical lesions. Cortical lesions were made in the posterior occipital lobe of eGFP-S transgenic pups on P9 - P10. In one half of each litter, a rectangular bone flap was generated covering the approximate coordinates of adult visual cortex, but proportionally adjusted for the smaller size of the brain of P10 animals, at an angle parallel to the posterior margin of the cortical lobe. The underlying cortex was micro-aspirated with weak suction and a sterile micropipette tip, taking care not to damage the underlying white matter. The wound was then packed with GelFoam, the skull flap replaced, and the skin sutured with fine sutures (6-0 Silk, Amicon) and sealed with Vetbond. The second half of each litter (Sham) was treated similarly, except the skull flap was replaced without making a lesion. All pups were returned to the mother and observed carefully until perfused at P13, 24 hours after eye-opening. Lesion locations and extent were confirmed at the time of perfusion, and in no case was there evidence of infection, or degeneration external to the lesion site.

Immunohistochemistry. 60um coronal sections were prepared from 4%para/PBS perfused and post-fixed brains directly by vibratome, or by cryostat after overnight immersion in 30% sucrose/PBS. All sections were processed floating, blocked with 10% goat serum, permeabilized with 0.3% TX100, followed by incubation with polyclonal sheep antibody against the N-terminus of PSD95 (Zymed), in 1% goat serum/0.1% TX100 solution overnight at 4C, followed by goat or donkey secondary antibodies conjugated to Alexa dyes (1-2 hours at room temp, 1% goat serum/0.1% TX100) (Invitrogen, 1:700). Single image planes from the mid rostro-caudal SGS were collected by confocal microscopy from mounted sections from PSD95 mutant or wild-type mice with the investigator blind to genotype, with a 20x/0.75NA objective.

Synaptoneurosomes. Techniques for dissection and isolation of tissue and for preparation and quantitation of protein for western blot analyses are as previously described (Yoshii et al. 2003). Tissue is obtained from the 'crown' of the superior colliculus, containing the stratum opticum, stratum griseum centrale and the stratum zonale. Synaptoneurosome preparation is from Hollingsworth et al. (1985). Aliquots of synaptoneurosomes are stored in Laemmli buffer for immunoblotting, and 5ug is probed on PVDF membrane with an affinity-purified polyclonal antibody generated against the N-terminal domain of PSD-95 (Synaptic Systems).

Electrophysiology. Whole-cell recordings were from neurons of the SGS of C57BL/6 mouse superior colliculus in acute para-saggital slices. Recordings from PSD-95 mutant mouse pups were conducted blind to genotype, with tail tips collected on the day of recording. Recorded neurons were imaged with infrared differential interference contrast and selected based on their position in the intermediate portion of the SGS (upper portion of the deep SGS), with vertically-oriented or pear-shaped somas and dorsal-originating proximal dendrites. These criteria exclude non-vertical cell types (eg, marginal, stellate, or horizontal), as well as other vertically-oriented neuronal types (wide-field verticals, narrow-field verticals, and TypeII ganglion, located in the stratum opticum, and smaller, superficial reverse conicals, located in the superficial SGS (Langer and Lund 1974, Tokunaga and Otani 1976). 350um vibratome slices were equilibrated in carboxygenated ACSF (117 mM NaCl, 4 mM $MgCl_2$, 4 mM KCl, 1.2 mM $NaHPO_4$, 26 mM $NaHCO_3$, 4 mM $CaCl_2$ _ $2H_2O$, 15 mM glucose, and 2 _M glycine) for at least 1 hr prior to recording. Recording pipettes (6-9 mΩ) were filled with 122.5 mM Cs-gluconate, 17.5 mM CsCl, 8 mM $CaCl_2$, 10 mM HEPES (CsOH), 0.2 mM Na-EGTA, 2 mM Mg-ATP, and 0.3 mM Na-GTP at pH 7.2-7.4. All neurons maintained seal resistances of above 5 GΩ. Series resistances were <40 MΩ, and input resistances were 800-900 MΩ. Recordings were collected with an Axopatch 220B amplifier, a Digidata 1322A interface,

and PClamp 8.1 for Windows (Axon Instruments) on a PC. Currents were sampled at 10 kHz and filtered at 5 kHZ. Miniature glutamatergic synaptic events (mEPSCs) were isolated at a holding potential of -70mV with 1uM TTX, 10uM BMI in the absence of Mg++ to enhance detection of NMDAR currents.

RESULTS
Visual experience is required for synaptic increases after eye-opening

Our goal in this study was to investigate synaptogenesis between visual axons and their post-synaptic partners during the initial onset of visual experience. We used mice because of the availability of a genetically manipulated strain in which eGFP is expressed in defined neuronal subsets, allowing reproducible sampling of similar neuronal types (Feng et al., 2000), and a strain in which PSD-95 expression is disrupted (Migaud et al. 1998). The superficial layers of the SC (sSC) are the major target of retinal ganglion cell axons in the mouse (Drager and Hofbauer 1985), and also receive visual information indirectly via a projection from Layer V pyramids in visual cortex (Rhoades et al. 1985). We focused our analysis on vertical neurons with dorsally-weighted dendrites (DWV neurons) in the deep SGS (Tokunaga and Otani, 1976), as these express eGFP at high levels in eGFP transgenic mice, they express high levels of PSD-95 in wild-type mice (see Figure 9B), their descending axon suggests they belong to an excitatory class of projection neuron, and their consistent somatic location and orientation enable targeting under DIC for patch-clamp recording.

Previous recordings in both the dLGN and the sSC have reported no change in the probability of synaptic release over the eye-opening interval (Chen and Regehr 2000, Lu and Constantine-Paton 2004), and thus mEPSC frequency should reflect the number of functional glutamatergic release sites as previously reported (Chen and Regehr 2000, Lu and Constantine-Paton 2004). We therefore assayed the frequency, amplitude, rise, and decay time of

miniature synaptic events from DWV neurons of the deep SGS in mice before and after eye-opening, and in animals whose eyes were never opened (Figure 1A). There was a 300% increase in mEPSC frequency after eye-opening, with no detectable change in amplitude (Figure 1B), rise or decay time (not shown). In the absence of eye-opening, no increase in mEPSCs occurs over this period (Figure 1B), suggesting that new synapses either did not form or were not maintained during this interval. No other property of the mEPSC is affected in eye-closed animals (data not shown).

Innervation of GFP-labeled neurons of the mouse sSC by retina and visual cortex

The two major inputs to the sSC arise from the retina and visual cortex, but the organization of visual afferents and their post-synaptic partners in the mouse sSC has not been well characterized. EO could induce synaptic change at retinal and/or cortical terminals, or at synapses downstream of these inputs. We therefore examined the dendritic innervation patterns of these afferents in order to understand 1) Whether DWV neurons are contacted by retinal and/or cortical axons and 2) What the spatial organization of these contacts might be. We examined this with a dual tract tracing study in eGFP transgenic mice.

We used Alexa fluorophore-conjugated Cholera Toxin B subunit to anterogradely label the retinal and cortical afferent pathways to the sSC. We simultaneously used differential anterograde labeling to trace axons from the contralateral retina and ipsilateral visual cortex to the sSC of eGFP transgenic mice (Figure 2A). After confirmation of complete labeling with brightfield and epifluorescence microscopy in the optic nerve (not shown) and occipital cortex (Figure 2B), sequential coronal sections were collected through the midbrain. Axons from ipsilateral visual cortex are dense in the deep layers of the sSC (stratum opticum, SO, and deep SGS) (Figure 2C-2D), while retinal axons

preferentially occupy a more superficial position. DWV neurons are located in the transition zone between the two projections (Figure 2E).

The density of eGFP-labeled DWV neurons is low (typically 3-4 cells per animal), facilitating visualization and reconstruction of the entire dendritic arbor with serial sectioning of fixed tissue and confocal microscopy.

To determine the locus of contact of retinal and cortical axons onto these neurons, we conducted a co-localization analysis of each afferent label and the eGFP-labeled dendritic arbor (Retina, Figure 2F; Cortex, Figure 2G). Colocalization analyses were conducted on individual binary thresholded optical sections of confocal z-series containing the entire dendritic arbor of three GFP-labeled neurons from two independent labeling experiments. After identification of overlapped pixels in the original z-series (Figure 2F-2G, in white), the number of overlapped pixels from each afferent was counted along fixed eGFP-labeled dendritic lengths and expressed as an overlapped pixel density (pixels per micron dendrite). We then asked whether afferent overlap patterns were differentially distributed across the dendritic arbor of these neurons.

Both retinal and cortical axons appeared to contact the dendrites of DWV neurons. However, the density of labeled axons in the neuropil is quite high, and we would expect a significant degree of non-specific overlap with this method due to *en passant* axons that did not make contact with the dendrite, but passed near enough to cause false positive overlap. The degree of non-specific overlap was estimated by rotation of the images containing afferent label with respect to those containing the GFP label for each afferent (Retina: Figure 2H, Cortex: Figure 2I). Non-specific overlap did occur, but overlapped pixel clusters in rotated images were significantly smaller than control images for both the retinal and cortical overlap, no more than 7-14 pixels in diameter,

compared to 25-50 pixels in diameter for the original images. This is especially apparent in Figure 2H, where a labeled retinal axon is observed to course alongside a length of eGFP dendrite, and probably accounts for the large overlapped cluster sizes observed in the original, non-rotated z-series. 95% confidence intervals for overlap pixel cluster sizes were generated for the rotated data for each label and used to set minimum acceptable sizes for overlap counting in control images (cortex: > 3.4 pixels, retina: > 2.8 pixels).

Examination of the original overlapped z-series revealed that cortical axons predominantly contact proximal branches of an intermediate thickness, and retinal axons predominantly contact distal, thinner dendrites. Initially, dendrites were categorized by "primary", "secondary", and "tertiary" designations. However, there are large variations in dendritic form within these categories, and the category designation itself is somewhat subjective. Multiple "Primary" dendrites originate from the cell soma, and while there is always one large apical trunk, additional, thinner, branches may originate either laterally or ventrally from the soma. In addition, thin dendrites can originate from larger dendrites at any point, yielding "Secondary" dendrites that are thinner than "Tertiary" dendrites. There is, additionally, some variability in dendrite thickness across cells, even of the primary dendrites, which made categorization by absolute caliber less than ideal.

In order to be able to reproducibly identify the dendrites of eGFP-labeled DWV neurons receiving retinal vs cortical input, we thus expressed the width of each dendritic segment as a proportion of the width of the thickest apical primary trunk. Thus "Caliber1" represents the thickest dendrites, that are 81-100% as thick as the widest primary trunk originating from the soma. "Caliber2" contains dendrites that are 61-80% as thick as the primary trunk, "Caliber3" includes dendrites that are 41-60% as thick as the primary trunk, and "Caliber4" includes dendrites that are 21-40% as thick as the primary trunk. "Caliber5" dendrites

that are 1-20% as thick as the primary trunk were not observed in all cells and so were excluded from analysis due to low representation. This method controlled for slight variability in dendrite thicknesses between cells, potentially because it incorporates a factor related to the *relative* order or position of the dendrite in relation to the cell soma or apical trunk. A three-dimensional Neurolucida reconstruction of the labeled neuron in Figure 2J illustrates the distribution of dendrites in each category (Figure 3A).

After correction for non-specific overlap, normalized caliber is a significant factor affecting the distribution of overlapped pixels for both retinal and cortical axons (Figure 3B). Overlapped pixel distributions are skewed towards thin Caliber4 dendrites for retinal axons, and intermediate Caliber3 dendrites for cortical axons.

Distribution of spines and filopodia on DWV dendrites

We examined DWV neurons for evidence of changes in the density or distribution of spine and filopodial structures on their dendritic arbors. Caliber is highly correlated with the distribution of retinal and cortical contacts on these dendrites and therefore we analysed the density of spine and filopodia structures along dendrites categorized using the same criteria. Dendritic protrusion geometries are not inherently binary, however. We simply defined "Spine" and "Filopodia" structures as those protrusions having Length vs width relationships more likely than chance to reflect the presence or absence of a synapse, as described below.

Based on serial reconstruction EM (Harris et al. 1992, Spacek and Harris 1998, Harris 1999), in vivo 2-photon microscopy (Zuo et al. 2005), and assays of synapse structure/function (Noguchi et al. 2005, Okabe et al. 2001, Nusser et al. 1998, Schikorski and Stevens 1999, Majewska et al. 2000, Yuste et al. 2000),

the threshold we have set to define "Spine" vs "Filopodia" structures should enrich for the presence of stable, asymmetric glutamatergic synapses in "Spine" structures, and the absence of stable synapses (or presence of dynamic, immature synapses) in "Filopodia" structures. We set a minimum dendritic protrusion length at 0.6um and drew from the above references (especially Harris et al. 1992 and Zuo et al. 2005, where the geometrical thresholds were clearly delineated), to classify all protrusions as "Spine" structures if $L \leq 3w$ or "Filopodia" structures if $3w < L \leq 6w$, where L = three-dimensional length from the base of the protrusion to the tip and w = greatest width of the protrusion, measured either at the neck or head, if present (Figure 4E). This threshold should place previously defined "Mushroom", "Stubby" and some "Thin" spines into the "Spine" category, and all filopodia and some "Thin" spines into the "Filopodia" category, as well as those with large heads on long drawn out necks, although these were fairly rare.

A representative DWV neuron at P13, after eye-opening, is shown in Figure 4A. We collected high resolution confocal z-series at 0.5um intervals across the entire dendritic arbor of each cell. Dendritic arbors in DWV neurons of the deep SGS are highly branched, and follow tortuous paths in the neuropil. Because of this, compression of single optical sections from confocal z-series collected through the depth of a dendritic branch in these neurons resulted in inadequate resolution of spines on most dendrites, as well as frequent inaccurate measurement of the length of dendritic segments upon which the protrusion density measurements are made. Analysis of sequential, single optical slices in three-dimensional z-series, however, permitted dendrites to be followed along any path through the neuropil, and allowed spines and filopodia to be resolved without interference from other labeled dendrites, axons of passage, or adjacent protrusions which collapse on top of one another. Our sampling resolution was sufficient to detect spines and filopodia, which appeared in sequential optical slices, but were only counted in the slice in which they were

in sharp focus (Figure 4D). We counted dendritic spines and filopodia along dendrites through coded z-series, and expressed them as a density along the measured three-dimensional length of each dendrite.

We found a strong correlation of protrusion density with dendritic caliber. Thick dendrites in general have fewer protrusions than thin dendrites (Figure 4B-C) regardless of branch order (Figure 4F).

Visual cortex controls the local growth of filopodia on Caliber3 dendrites between P11-P13

We used this method to quantify structural changes indicative of synaptogenesis on these dually-innervated neurons before (P11) and 24 hours after controlled eye-opening (P13), as well as four days after eye-opening (P16), and at least 20 days after eye-opening (Adult) (Figure 5A).

Dendrites of all calibers had few filopodia at P11, but rapidly developed a high density of filopodia by P13 that were eliminated by adulthood (Figure 5B). These changes only reached significance on the thinnest dendrites, Caliber3 and Caliber4. On Caliber4 dendrites the density of filopodia returned to baseline levels in the adult. However, on Caliber3 dendrites filopodia density had already decreased to adult levels by P16. Due to the normalization procedure spine and filopodial densities on Caliber1 dendrites were not normally distributed and so parametric analyses were not conducted on these dendrites.

Caliber3 dendrites are predominantly localized at mid-SGS levels where cortical and retinal terminals overlap, and are the most likely to be contacted by cortical axons. Therefore we tested the hypothesis that the rapidly arborizing cortico-collicular projection could be responsible for the rapid appearance of filopodia

on these dendrites by removing the visual cortical input before eye-opening and testing the effect on spine and filopodia distribution at P13.

Lesions of ipsilateral visual occipital cortex were made in eGFP transgenic mice between P9-P10 by microaspiration of the cellular layers of VC without damage to the underlying white matter (Figure 6A). One-half of each litter received a lesion, and the other half underwent an identical surgery without cortical aspiration (Sham). Confirmation of the extent of the lesion was made in para-sagittal sections at P13, illustrated in Figure 6B.

Visual cortex removal prevented the elaboration of filopodia on Caliber3 dendrites, but had no effect on Caliber4 (Figure 6C-6D). This local effect of VC removal on Caliber3 is additional evidence that visual cortical axons innervate DWV cells at Caliber3 dendrites preferentially.

Because these changes occurred over the eye-opening period, and visual cortical pyramidal cells are more responsive to pattern stimuli than retinal ganglion cells, we tested whether these structural changes were indeed driven by the onset of visual experience at P12.

Eye-opening is required for the local stabilization of spines, not the transient elaboration of filopodia

Since this visual cortex-dependent elaboration of filopodia occurred over the EO interval from P11-P13, we asked whether this was dependent on eye-opening (ie, whether preventing the eyes from opening at P12 would have the same effect as cortical removal). Eyelids of all litters were glued shut at P11 with a thin layer of transparent glue along the eyelid seam (occasional pups who had already begun to open their eyes were excluded). On P12, the strip of glue covering both eyelid seams was peeled away on one half of each litter.

Nest material and excess bedding was removed from the cage, and the entire litter including the mother was allowed to survive for 24 hours and then sacrificed for analysis at P13. Thus one half of each litter received pattern visual experience and the other half received only diffuse light stimuli through closed eyelids. Examination of dendrites in the eye-closed group revealed that visual experience did not drive the filopodial genesis observed between P11 and P13 on either Caliber3 or Caliber4 dendrites. Filopodia increased normally on both Caliber3 and Caliber4 in the eye-closed group (Figure 7A-B). Eye-closure did affect spine density, however. Animals from the eye-closed group had significantly fewer spines on Caliber3 than the control littermates (Figure 7C). This effect was confined to Caliber3 dendrites. Caliber4 dendrites were unaffected.

The three-fold increase in synaptogenesis before and after eye-opening that we observed with mEPSC frequency is correlated with an increase in filopodia on both Caliber3 and Caliber4, suggesting that some of these new contacts may be on filopodia. However, the mEPSC frequency increase is eliminated by eye-closure, and the filopodia are not, so most filopodia probably do not have synapses on them. Spine density, however, is reduced by eye-closure, suggesting that at least some of the synapses lost after eye-closure are from dendritic spines. We hypothesize that filopodia promote formation of new contacts using EO-independent mechanisms, and pattern visual experience is required to stabilize these new contacts and convert them to stable dendritic spines and/or shaft synapses.

PSD-95 and eye-opening dependent maintenance of release sites

In the sSC, PSD-95 is enriched at post-synaptic membranes within two hours after controlled eye-opening (Yoshii et al. 2003). PSD-95 is involved in glutamate receptor trafficking and synaptic plasticity (Elias et al. 2006, Migaud

et al. 1998), and thus is a good candidate for involvement in synaptogenesis in the sSC over eye-opening. Spine formation is already known to be impaired in both the striatum and hippocampus of mice expressing a truncated mutant form of the glutamate receptor scaffold PSD-95 (Vickers et al. 2006), however, not all spines are affected, suggesting that there is some heterogeneity among synaptic sites as to their need for PSD-95 at any given point in time. Because dendritic PSD-95 trafficking is tightly controlled by visual experience after eye-opening and PSD-95 mediates activity-dependent AMPA-R trafficking and synaptic plasticity, we hypothesized it could be involved in the EO-dependent spine stabilization we observed. We therefore examined mEPSCs in DWV neurons in wild-type and PSD-95 mutant mice to see whether the visual-experience dependent increase in mEPSC frequency still occurred after eye-opening (Figure 8A). mEPSC frequency was significantly reduced approximately three-fold in PSD-95 mutant mice after eye-opening compared to wild-type mice (Figure 8B). This suggests that PSD-95 is necessary for the net gain of new visual experience-dependent synaptic release sites seen in WT mice after eye-opening.

These mutant mice are targeted knock-ins of a PSD-95 gene truncated in the middle of the third PDZ domain (Migaud et al. 2000) (Figure 9A). In order to understand whether the phenotype is due to the absence of PSD-95 at sSC synapses, or a dominant-negative effect of the expressed truncated protein, we used N-terminal specific PSD-95 antibodies to test whether the Migaud et al. strain expresses truncated protein in the sSC (Figure 9B-C). The expected 40kD truncated N-terminus is not detected by either immunohistochemistry on fixed tissue, or western blotting of whole lysates (not shown) and synaptoneurosomes prepared from the sSC of WT and mutant mice. This is comparable to observations from a second strain of mice generated with a truncation at the more distal C-terminal GK domain (Yao et al. 2004), which also lacks detectable PSD-95 protein in either whole lysates or

synaptoneurosomes when detected on Western blots using N-terminal specific antibodies.

DISCUSSION

Previous work from our lab and others has shown that eye-opening drives a number of biochemical and functional changes in local circuitry at various stages in the visual pathway. In the superior colliculus eye-opening is associated with a wave of new synaptogenesis and within 12 hours a significant synaptic potentiation and refinement of inputs to single neurons studied electrophysiologically (Lu and Constantine-Paton 2004). In the current study we have used voltage-clamp recordings of mEPSCs in acute brain slices and confocal imaging of dendritic structure in anatomically identified DWV neurons of the mid-SGS to investigate morphologies associated with these functional changes induced by pattern visual experience. In these cells we observed changes in the density of filopodia (but not spines), and changes in functionally identified synaptic sites over the eye-opening interval. Eye-opening in rodents does not result in changes in pre-synaptic release probability but it does rapidly drive an increase in mEPSC frequency; an increase that is absent over the same interval in mice lacking PSD-95 (Lu and Constantine-Paton 2004, Chen and Regehr 2000).

Taken together, our results suggest a mechanism by which pattern vision, by triggering synaptic increases in PSD-95, can induce stabilization of newly formed contacts on filopodia, induced by the presence of active cortical terminals in the neuropil. On dendrites receiving input from cortical axons, a three-fold increase in release sites over eye-opening was correlated with an increase in filopodial density, rather than an increase in spine density. We suspect that the dramatic, transient sprouting of filopodia over eye-opening is critical to the formation of stable synaptic contacts by P13. In the absence of instructive sensory activity, synapses are eliminated on both filopodia and

spines. However, filopodia continue to sprout in response to cues from cortical axons which continue to seek and form tentative connections. Thus, we do not think the stability of spine density over eye-opening necessarily reflects the absence of spine synaptic rearrangements during this period. Rather, spines with synapses which cannot be stabilized may be lost, and new spines formed by filopodial conversion or outgrowth from the shaft.

That eye-opening affects spines on dendrites receiving most of their input from the visual cortex suggests that arborizing cortical inputs were probably the pre-synaptic partners of many of these spines before eye-opening. During the transient filopodia increase immediately following eye-opening, more refined cortical inputs driven by pattern vision displaced the initially profusely arborizing cortical projection. Significantly, the lack of changes in the density of spines detected in the DWV neurons does not match the increase in synaptic release sites detected in electrophysiological recordings or EM analyses indicating an increase in active sites over this period. These observations suggest that the number of release sites on anatomically identified spine structures probably increase over the eye-opening period, possibly because the cortico-collicular projection is refining to align and focus its terminal field at the same topographic collicular loci where the direct retinal input is projecting (Lund 1966).

A number of observations from other laboratories support this explanation of the present data. First – an increase in visual cortical inhibition within layer IV has been reported to occur with the advent of pattern vision in rodents(). This would serve to focus ascending input activity from a particular retinal locus within a refined area of cortex. These spatially refined patterns of activity are likely to be reflected in the output of the Layer V neurons that project to the SC. Second, several investigations using anterograde transported tritiated-proline and analyses of local position of axon arborization during the 3rd post-natal

week have described a refinement of the cortico-collicular projection that seemed likely to depend on eye-opening (Dreher et al. 1985, Inoue et al. 1992).

Visual cortical inputs are uniquely sensitive to the initial 24 hours of visual experience through open eyelids, in contrast to retinal inputs. Depriving the animals of this early experience disrupts spines post-synaptic to cortical axons, but has no effect on either spines or filopodia post-synaptic to retinal axons. One explanation for this dichotomy may involve the fact that pattern stimuli are capable of driving high "gamma" frequency synchronous oscillatory activity in the cortex of both cats and mice which temporally correlates activity across spatial locales, at a frequency which is particularly suited to inducing Hebbian synaptic potentiation (Brecht et al. 1998,1999,2001; Nase et al. 2003). Surprisingly, the superior colliculus is the only other region of the brain where these oscillations have been observed to occur (Merker 2007). PSD-95 is known to be able to modify synaptic plasticity and thus could enable potentiation of newly formed cortico-collicular synapses receiving pattern visual stimuli.

1. Spines and Filopodia as Indicators of the Locus of Synaptogenesis over Eye-opening

We have used a – to our knowledge – novel method to quantify the density of dendritic spines and filopodia based on dendrite caliber, rather than branch order. Branch caliber was more predictive of spine density in sSC neurons, because thin, spiny branches were commonly observed branching directly from thick primary dendrites and even the cell soma. This made traditional primary, secondary, and tertiary designations relatively un-predictive of spine density, and measurements using these classifications highly variable. By considering the unique structural geometry of these cells, and by using a three-dimensional approach to measure density along branches of different widths, we were able

67

to detect differential patterns of spine and filopodial development across the dendritic arbor. These patterns are surprisingly dependent on the type of axonal afferents dendrites receive.

The number of filopodia increase ~300% over eye-opening, comparable to the three-fold increase in total synaptic inputs over that time. We cannot rule out that some of the new contacts detected by electrophysiology resulted from conversion of silent synapses or formation of new synapses, on existing or new spines or even the dendritic shaft of branches other than Type3. Studies of synapse structure and function associated with protrusion geometry suggest that spines as we and others have generally classified them (Zuo et al., 2005;, Harris 1999; Ziv and Smith 1996) are more likely to contain stable synapses and mature synaptic structures (spine apparatus, smooth ER, high concentration of glutamate receptors) than filopodia (defined as length >>> width), which by P15 in CA1 were reported to be devoid of synapses anywhere along their length (Spacek and Harris 1998, Harris 1999, Harris et al. 1992). However, this clearly does not preclude synapse formation on filopodia in younger animals, or when activity levels are pharmacologically manipulated (Fiala et al. 1998, Petrak et al. 2005, Ziv and Smith 1996, Saito et al. 1992, Ramoa et al. 1987). Current data support the view that filopodia are indicative of dynamic synaptogenesis, and are immature protrusions that can be converted to spines if they successfully stabilize a mature synaptic contact (Ziv and Smith 1996, Zuo et al. 2005). As animals mature, many fewer filopodia are observed, and mature, stable, spines predominate (Harris 1999, Zuo et al. 2005).

2. PSD-95 in activity-dependent synapse formation and/or stabilization

PSD-95 is predominantly known as an important scaffold of AMPARs containing GluR1 via stargazin, however, in the sSC PSD-95 is also associated with

NMDARs, preferentially those containing the NR2A subunit (Townsend et al. 2003). The present study has shown a direct functional outcome of this pattern vision-induced trafficking of PSD-95 to dendritic membranes. After PSD-95 has been driven into dendrites, synaptic density increases of about 300% are detected in wild-type mice, and they have ~300% more synapses than PSD95KO mice after eye-opening. In this respect, PSD95KO animals resemble age-matched wild-type animals who have not experienced pattern vision. The inability to stabilize synaptic sites that is seen in WT animals with eyes closed, is correlated with a loss of dendritic spines on dendrites that receive cortical input, and not those that receive retinal input. Thus vision-driven modifications are input-specific due to differential afferent innervation, which might explain some of the synaptic heterogeneity observed in PSD-95 loss of function studies (eg Elias et al. 2007).

Also consistent with these reports, we have not found any evidence for a generalized defect in synapse formation in PSD-95 mutant mice. And, while we did not assay the effects of PSD95 deletion on spine density in DWV neurons of the sSC due to the difficulty of breeding and maintaining this strain (see Methods), it is already known that genetic deletion of PSD-95 disrupts adult spine density on Golgi-impregnated dendrites in both the striatum and hippocampus, also in a heterogeneous way (Vickers et al. 2006).

Overexpression of PSD-95 can enhance AMPAR current amplitude at individual synaptic sites, but we did not detect any significant increase in the average amplitude of the mEPSC in the mutant (El-Husseini et al. 2000, Beique and Andrade 2003, Ehrlich and Malinow 2004). Our results are more consistent with experiments using shRNA to knockdown PSD-95 in acute hippocampal slices, which detected a reduced mAMPAR frequency without a change in amplitude (Elias et al. 2006). We suspect that more severe deficits were not observed because other MAGUKs (SAP102, PSD-93), can stabilize AMPARs in

the absence of PSD-95 (Fitzjohn et al. 2006). We also suspect that the insertion of AMPARs into a new synaptic site is a rapid event, and in a sea of already formed synapses may be difficult to detect.

Does eye-opening induce a rapid LTP which recruits PSD-95 to specific synapses for stabilization? Or does the sudden onset of high intensity visual input drive PSD-95 into synapses across the entire dendritic arbor, enabling synaptic maintenance of only those sites which are responding to pattern stimuli, and are engaged in patterns of activity conducive to stabilization? Our data and that of others suggests the latter. Initial studies which assayed PSD-95 trafficking into dendrites by immunohistochemistry, did not detect differential targeting of PSD-95 to deep vs superficial layers of the neuropil, or to proximal vs distal regions of the dendritic shafts (Yoshii et al. 2003, A Yoshii personal communication), where retinal synapses predominate. In addition, PSD-95 is not differentially expressed at synapses on hipoocampal pyramidal neurons *in vitro* (Elias et al. 2006).

One potential mechanism by which PSD-95 might stabilize synapses in response to sensory activity includes preferential stabilization of NMDARs containing NR2A at central synaptic sites (Townsend et al. 2003, Zhao et al. 2007, reviewed in van Zundert et al. 2004). NMDARs containing NR2A appear to be important for the induction of LTP with tetanic stimuli in both hippocampus and sSC (Zhao et al. 2007, Ito et al. 1996, Kiyama et al. 1998, Liu et al. 2004, JP Zhao personal communication), while activation of NMDARs containing NR2B preferentially cause LTD in the sSC (Zhao et al. 2007). Alternatively, or in addition, PSD-95 might act downstream of NR2A activation to participate in the cycling of AMPARs containing GluR1 at synaptic sites via stargazin interactions. Whatever the proximal mechanism, our data strongly suggest that vision-induced trafficking of PSD-95 enables the potentiation of specific cortico-collicular synapses in response to patterned visual activity.

3. Predicted Role of PSD-95 in Experience-dependent Refinement and LTP

Our model predicts that animals deficient in PSD-95 should not be able to stabilize synapses in response to sensory experience during development or later experience-dependent remodeling. Indeed, PSD95 mutant mice fail to develop normal orientation preferences in visual cortex (Fagiolini et al. 2003) and are deficient in learning and memory tasks later in life (Migaud et al. 1998),

In the visual system, experience-dependent refinement is probably enabled by a rapid switch in the decay time of mixed 2A/B NMDARs driven by retinal activity just before the eyes open (Townsend et al. 2003), followed by a progressive increase in expression of the NR2A subunit after eye-opening. NMDARs containing NR2A may be more effective at following high frequency cortical spikes driven by pattern activation than NMDARs containing NR2B which preferentially cause LTD in the sSC (Constantine-Paton and Cline, 1998), Zhao et al. 2007). It is interesting that mice lacking NR2A mimic the PSD95 mutant phenotype in visual cortex, however are additionally deficient in ocular dominance plasticity (Fagiolini et al. 2003). Our model further predicts that precocious sensory activity should not be able to drive precocious refinement unless it also drives the simultaneous maturation of NMDA receptors and associated scaffolding and signaling machinery.

Our results show that PSD-95 is required for synapse stabilization, and thus are not consistent with the enhanced field LTP detected in the hippocampus of older PSD-95 mutant mice (Migaud et al. 1998). We doubt that this paradoxical effect is due to the remaining truncated protein reported to be present in hippocampus, because in a second strain of mice with a more conservative C-terminal truncation, truncated protein is not detectable in either whole lysates or synaptoneurosomes in both hippocampus and striatum (Yao et al. 2004).

Rather, this enhanced LTP may be explained by the upregulation or recruitment of compensatory mechanisms (eg, SAP102 upregulation, (Vickers et al. 2006, Cuthbert et al. 2007)) in older knockout animals on which field LTP studies are typically conducted. We have recently discovered that in the sSC, PSD-95 knock-down by shRNA eliminates the ability to induce whole-cell LTP with tetanic stimuli around 2-3 days after eye-opening (Y Murata and JP Zhao, personal communication). This result confirms our conclusion that PSD-95 is required in the sSC for the input-specific potentiation and stabilization of synaptic sites in response to patterned visual experience after eye-opening.

LITERATURE CITED

Bakkum BW, Benevento LA, Cohen RS. 1991. Effects of light/dark- and dark-rearing on synaptic morphology in the superior colliculus and visual cortex of the postnatal and adult rat. J Neurosci Res. Jan;28(1):65-80.

Beique JC, Andrade R. 2003. PSD-95 regulates synaptic transmission and plasticity in rat cerebral cortex. J Physiol. Feb 1;546(Pt 3):859-67.

Blakemore C, Van Sluyters RC. 1975. Innate and environmental factors in the development of the kitten's visual cortex. J Physiol 248: 663-716.

Bourne JN, Kirov SA, Sorra KE, Harris KM. 2007. Warmer preparation of hippocampal slices prevents synapse proliferation that might obscure LTP-related structural plasticity. Neuropharmacology. Jan;52(1):55-9.

Chen C, Regehr WG. 2000. Developmental remodeling of the retinogeniculate synapse. Neuron 28(3):955-66.

Colonnese MT, Constantine-Paton M. 2006. Developmental period for N-methyl-D-aspartate (NMDA) receptor-dependent synapse elimination correlated with visuotopic map refinement. J Comp Neurol. 494(5):738-51.

Colonnese MT, Zhao JP, Constantine-Paton M. 2005. NMDA receptor currents suppress synapse formation on sprouting axons in vivo. J Neurosci. 2005 Feb 2;25(5):1291-303.

Constantine-Paton M, Cline HT, Debski E. 1990. Patterned activity, synaptic convergence, and the NMDA receptor in developing visual pathways. Annu Rev Neurosci. 13:129-54.

Constantine-Paton M, Cline HT. 1998. LTP and activity-dependent synaptogenesis: the more alike they are, the more different they become. Curr Opin Neurobiol. 8(1):139-48.

Cuthbert PC, Stanford LE, Coba MP, Ainge JA, Fink AE, Opazo P, Delgado JY, Komiyama NH, O'Dell TJ, Grant SG. 2007. Synapse-associated protein 102/dlgh3 couples the NMDA receptor to specific plasticity pathways and learning strategies. J Neurosci. 27(10):2673-82.

De Simoni A, Griesinger CB, Edwards FA. 2003. Development of rat CA1 neurones in acute versus organotypic slices: role of experience in synaptic morphology and activity. J Physiol. Jul 1;550(Pt 1):135-47.

Drager UC, Hofbauer A. 1985. Depth segregation of retinal ganglion cells projecting to mouse superior colliculus. JCN 234: 465-74.

Dreher B, Shameem N, Thong IG, McCall MJ. 1985. Development of cortical afferents and cortico-tectal efferents of the mammalian (rat) primary visual cortex. Australian and New Zealand Journal of Ophtalmology 13: 251-261.

El-Husseini AE, Schnell E, Chetkovich DM, Nicoll RA, Bredt DS. 2000. PSD-95 involvement in maturation of excitatory synapses. Science 290: 1364-1368

Elias GM, Funke L, Stein V, Grant SG, Bredt DS, Nicoll RA. 2006. Synapse-specific and developmentally regulated targeting of AMPA receptors by a family of MAGUK scaffolding proteins. Neuron. Oct 19;52(2):307-20.

Engert F, Tao HW, Zhang LI, Poo MM. 2002. Moving visual stimuli rapidly induce direction sensitivity of developing tectal neurons. Nature 419:470-5. Exp Brain Res. 94:444-55.

Fagiolini M, Katagiri H, Miyamoto H, Mori H, Grant SG, Mishina M, Hensch TK. 2003. Separable features of visual cortical plasticity revealed by N-methyl-D-aspartate receptor 2A signaling. Proc Natl Acad Sci 100(5):2854-9

Feng G, Mellor RH, Bernstein M, Keller-Peck C, Nguyen QT, Wallace M, Nerbonne JM, Lichtman JW, Sanes JR. 2000. Imaging neuronal subsets in transgenic mice expressing multiple spectral variants of GFP. Neuron 28(1):41-51.

Fiala JC, Kirov SA, Feinberg MD, Petrak LJ, George P, Goddard CA, Harris KM. 2003. Timing of neuronal and glial ultrastructure disruption during brain slice preparation and recovery in vitro. J Comp Neurol. Oct 6;465(1):90-103.

Fitzjohn SM, Doherty AJ, Collingridge GL. 2006. Promiscuous interactions between AMPA-Rs and MAGUKs. Neuron. Oct 19;52(2):222-4. Review.

Gerrow K, Romorini S, Nabi SM, Colicos MA, Sala preformed complex of postsynaptic proteins is involved in excitatory synapse development. Neuron 49(4):547-62.

Harris KM, Jensen FE, Tsao B. 1992. Three-dimensional structure of dendritic spines and synapses in rat hippocampus (CA1) at postnatal day 15 and adult ages: implications for the maturation of synaptic physiology and long-term potentiation. J Neurosci. Jul;12(7):2685-705.

Harris KM. 1999. Structure, development, and plasticity of dendritic spines. Curr Opin Neurobiol. Jun;9(3):343-8.

Hollingsworth EB, McNeal ET, Burton JL, Williams RJ, Daly JW, Creveling CR. 1985 Biochemical characterization of a filtered synaptoneurosome preparation from guinea pig cerebral cortex: cyclic adenosine 3':5'-monophosphate-generating systems, receptors, and enzymes. J Neurosci. Aug;5(8):2240-53.

Hooks BM, Chen C. 2006. Distinct roles for spontaneous and visual activity in remodeling of the retinogeniculate synapse. Neuron 52:281-91.

Inoue K, Terashima T, Inoue Y. 1992. Postnatal development of the corticotectal projection from the visual cortex of the mouse. Okajimas Folia Anatomica Japonica 68: 319-332.

Ito I, Sakimura K, Mishina M, Sugiyama H. 1996. Age-dependent reduction of hippocampal LTP in mice lacking N-methyl-D-aspartate receptor epsilon 1 subunit. Neurosci Lett. 203(1):69-71.

King AJ, Carlile S. 1993. Changes induced in the representation of auditory space in the superior colliculus by rearing ferrets with binocular eyelid suture. Exp Brain Res 94(3):444-55.

Kirkwood A, Lee HK, Bear MF. 1995. Co-regulation of long-term potentiation and experience-dependent synaptic plasticity in visual cortex by age and experience. Nature 375(6529):328-31.

Kirov SA, Petrak LJ, Fiala JC, Harris KM. 2004. Dendritic spines disappear with chilling but proliferate excessively upon rewarming of mature hippocampus.

Kirov SA, Sorra KE, Harris KM. 1999. Slices have more synapses than perfusion-fixed hippocampus from both young and mature rats. J Neurosci. Apr 15;19(8):2876-86.

Kiyama Y, Manabe T, Sakimura K, Kawakami F, Mori H, Mishina M. 1998. Increased thresholds for long-term potentiation and contextual learning in mice lacking the NMDA-type glutamate receptor epsilon1 subunit. J Neurosci.18(17):6704-12.

Lambot MA, Depasse F, Noel JC, Vanderhaegen P. 2005. Mapping labels in the human developing visual system and the evolution of binocular vision. J Neurosci 3;25(31):7232-7.

Law CC, Bear MF, Cooper LN. 1994. Role of the visual environment in the formation of receptive fields according to the BCM theory. Prog Brain Res. 102:287-301.

Liu L, Wong TP, Pozza MF, Lingenhoehl K, Wang Y, Sheng M, Auberson YP, Wang YT. 2004. Role of NMDA receptor subtypes in governing the direction of hippocampal synaptic plasticity. Science. 304(5673):1021-4.

Lu W, Constantine-Paton M. 2004. Eye opening rapidly induces synaptic potentiation and refinement. Neuron 43(2):237-49.

Lund RD. 1966. The occipitotectal pathway of the rat. J Anat 100: 51-62.

Majewska A, Brown E, Ross J, Yuste R. 2000. Mechanisms of calcium decay kinetics in hippocampal spines: role of spine calcium pumps and calcium diffusion through the spine neck in biochemical compartmentalization. J Neurosci. Mar 1;20(5):1722-34.

Mataga N, Mizuguchi Y, Hensch TK. 2004. Experience-dependent pruning of dendritic spines in visual cortex by tissue plasminogen activator. Neuron. Dec 16;44(6):1031-41.

Mathers LH Jr, Mercer KL, Marshall PE. 1978. Synaptic development in the rabbit superior colliculus and visual cortex. Exp Brain Res. Nov 15;33(3-4):353-69.
McLaughlin T, Torborg CL, Feller MB, O'Leary DD. 2003. Retinotopic map refinement requires spontaneous retinal waves during a brief critical period of development. Neuron 40(6):1147-60.

McLaughlin T, O'Leary DD. 2005. Molecular gradients and development of retinotopic maps. Annu Rev Neurosci. 28:327-55.

Merker. 2007. Consciousness without a cerebral cortex. Behav Brain Sci 30:1

Migaud M, Charlesworth P, Dempster M, Webster LC, Watabe AM, Makhinson M,

He Y, Ramsay MF, Morris RG, Morrison JH, O'Dell TJ, Grant SG. 1998. Enhanced long-term potentiation and impaired learning in mice with mutant postsynaptic density-95 protein. Nature. 396(6710):433-9.

Mower GD, Berry D, Burchfiel JL, Duffy FH. 1981. Comparison of the effects of dark rearing and binocular suture on development and plasticity of cat visual cortex. Brain Res 220: 255-276.

Nase G, Singer W, Monyer H, Engel AK. 2003. Features of neuronal synchrony in mouse visual cortex. J Neurophysiol 90(2): 1115-23.

Noguchi J, Matsuzaki M, Ellis-Davies GC, Kasai H. 2005. Spine-neck geometry determines NMDA receptor-dependent $Ca2+$ signaling in dendrites. Neuron. May 19;46(4):609-22.

Nusser Z, Lujan R, Laube G, Roberts JD, Molnar E, Somogyi P. 1998. Cell type and pathway dependence of synaptic AMPA receptor number and variability in the hippocampus. Neuron. Sep;21(3):545-59.

Okabe S, Miwa A, Okado H. 2001. Spine formation and correlated assembly of presynaptic and postsynaptic molecules. J Neurosci. 21(16):6105-14.

Philpot BD, Sekhar AK, Shouval HZ, Bear MF. 2001. Visual experience and deprivation bidirectionally modify the composition and function of NMDA receptors in visual cortex. Neuron 29(1):157-69.

Philpot BD, Cho KK, Bear MF. 2007. Obligatory role of NR2A for metaplasticity in visual cortex Neuron 53(4):495-502.

Ramoa AS, Campbell G, Shatz CJ. 1987. Transient morphological features of identified ganglion cells in living fetal and neonatal retina. Science 237(4814):522-5.

Rhoades RW, Mooney RD, Fish SE. 1985. Subcortical projections of area 17 in the anopthalmic mouse. Dev Brain Res 17: 171-181.

Rocha M, Sur M. 1995. Rapid acquisition of dendritic spines by visual thalamic neurons after blockade of N-methyl-D-aspartate receptors. Proc Natl Acad Sci U S A. 92(17):8026-30.

Saito Y, Murakami F, Song WJ, Okawa K, Shimono K, Katsumaru H. 1992. Developing corticorubral axons of the cat form synapses on filopodial dendritic protrusions. Neurosci Lett. Nov 23;147(1):81-4.

Schikorski T, Stevens CF. 1999. Quantitative fine-structural analysis of olfactory cortical synapses. Proc Natl Acad Sci U S A. Mar 30;96(7):4107-12.

Schmidt KE, Galuske RAW, Singer W. 1999. Matching the modules: Cortical maps and long-range intrinsic connections in visual cortex during development. J Neurobiol 41: 10-17.

Smith SL, Trachtenberg JT. 2007. Experience-dependent binocular competition in the visual cortex begins at eye opening. Nat Neurosci. 10:370-5.

Spacek J, Harris KM. 1998. Three-dimensional organization of cell adhesion junctions at synapses and dendritic spines in area CA1 of the rat hippocampus. J Comp Neurol 393(1):58-68.

Staras K. 2007. Share and share alike: trading of presynaptic elements between central synapses. Trends Neurosci. Apr 26; [Epub ahead of print]

Thong IG, Dreher B. 1986. The development of the corticotectal pathway in the albino rat. Brain Res. Mar;390(2):227-38.

Tian N, Copenhagen DR. 2003. Visual stimulation is required for refinement of ON and OFF pathways in postnatal retina. Neuron 39(1):85-96.

Tokunaga A, Otani K. 1976. Dendritic patterns of neurons in the rat superior colliculus. Exp Neurol. Aug;52(2):189-205.

Townsend M, Yoshii A, Mishina M, Constantine-Paton M. 2003. Developmental loss of miniature N-methyl-D-aspartate receptor currents in NR2A knockout mice. Proc Natl Acad Sci U S A. Feb 4;100(3):1340-5.

van Zundert B, Yoshii A, Constantine-Paton M. 2004. Receptor compartmentalization and trafficking at glutamate synapses: a developmental proposal. Trends Neurosci. Jul;27(7):428-37

Verhage M, Maia AS, Plomp JJ, Brussaard AB, Heeroma JH, Vermeer H, Toonen RF, Hammer RE, van den Berg TK, Missler M, Geuze HJ, Sudhof TC. 2000. Synaptic assembly of the brain in the absence of neurotransmitter secretion. Science 287(5454):864-9.

Vickers CA, Stephens B, Bowen J, Arbuthnott GW, Grant SG, Ingham CA. 2006. Neurone specific regulation of dendritic spines in vivo by post synaptic density 95 protein (PSD-95). Brain Res. 1090:89-98.

Warton SS, McCart R. 1989. Synaptogenesis in the stratum griseum superficiale of the rat superior colliculus. Synapse.;3(2):136-48.

Yao WD, Gainetdinov RR, Arbuckle MI, Sotnikova TD, Cyr M, Beaulieu JM, Torres GE, Grant SG, Caron MG. 2004. Identification of PSD-95 as a regulator of dopamine-mediated synaptic and behavioral plasticity. Neuron.41(4):625-38.

Yoshii A, Sheng MH, Constantine-Paton M. 2003. Eye opening induces a rapid dendritic localization of PSD-95 in central visual neurons. Proc Natl Acad Sci 100(3):1334-9.

Yuste R, Majewska A, Holthoff K. 2000. From form to function: calcium compartmentalization in dendritic spines. Nat Neurosci. Jul;3(7):653-9.

Zhao JP et al. [Visual experience and LTP in sSC of WT and 2AKO mice] In Prep

Zhou Q, Tao HW, Poo MM. 2003. Reversal and stabilization of synaptic modifications in a developing visual system. Science. 300:1953-7.

Ziv NE, Smith SJ. 1996. Evidence for a role of dendritic filopodia in synaptogenesis and spine formation. Neuron. Jul;17(1):91-102.

Zuo Y, Lin A, Chang P, Gan WB. 2005. Development of long-term dendritic spine stability in diverse regions of cerebral cortex. Neuron. 46(2):181-9.

Zhao J, Constantine-Paton M. 2006. Roles of L-type calcium channel and the NR2A NMDAR subunit in superior colliculus and hippocampal CA1 LTP, Program No. 786.7. Neuroscience Meeting Planner. Atlanta, GA: Society for Neuroscience. Online.
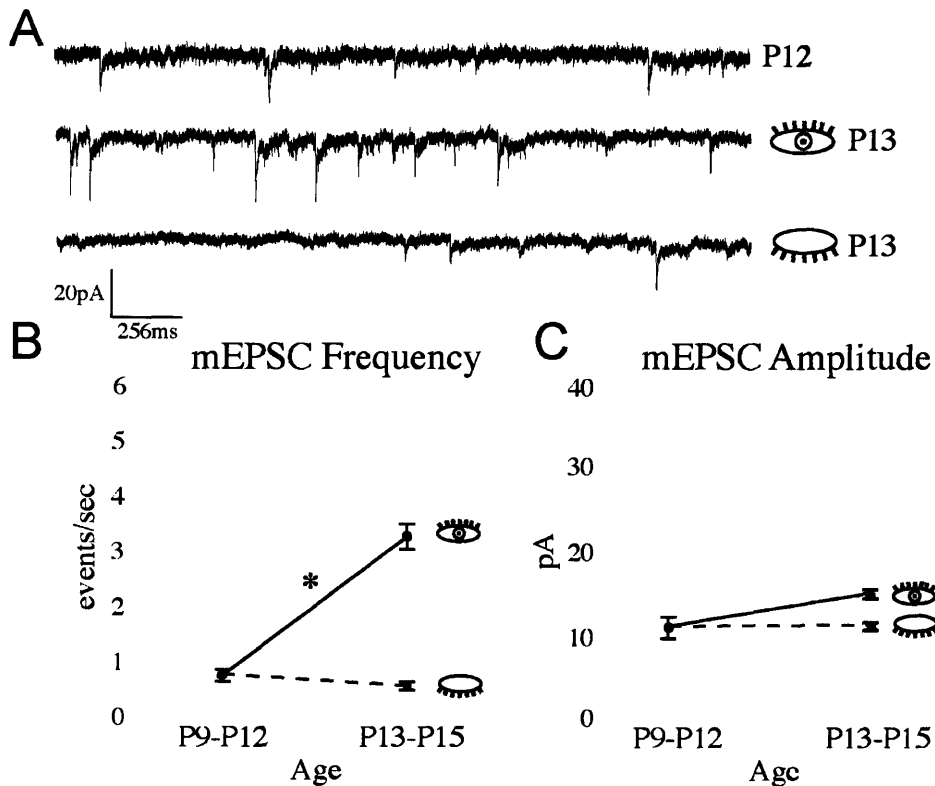
Figure 1. Eye-opening induces synapse formation on visual collicular (DWV) neurons

(A) Example traces of glutamatergic quantal events (mEPSCs) recorded from DWV cells of the deep SGS at -70mV before (BEO) and after eye-opening (AEO), and in animals whose eyes were never opened (ENO). External solution contained 0Mg++, BMI, TTX.

(B) mEPSC frequency increases ~ three-fold after eye-opening (*p < 0.05 Student's t test with correction for multiple comparison to before eye-opening group). No increase in mEPSC frequency occurs when the eyes are kept closed over the same period (p > 0.05). (n=5 P9-P12; n=6 P13-P15 EO; n=4 P13-P14 eyes closed). No significant change in mEPSC amplitude was detected. (p > 0.05)

A

B

C

V1
V2

D

sSGS
dSGS

SO

E

RETINA
CORTEX

F Overlap

G

H

Original

Rotated

I

Original

Rotated

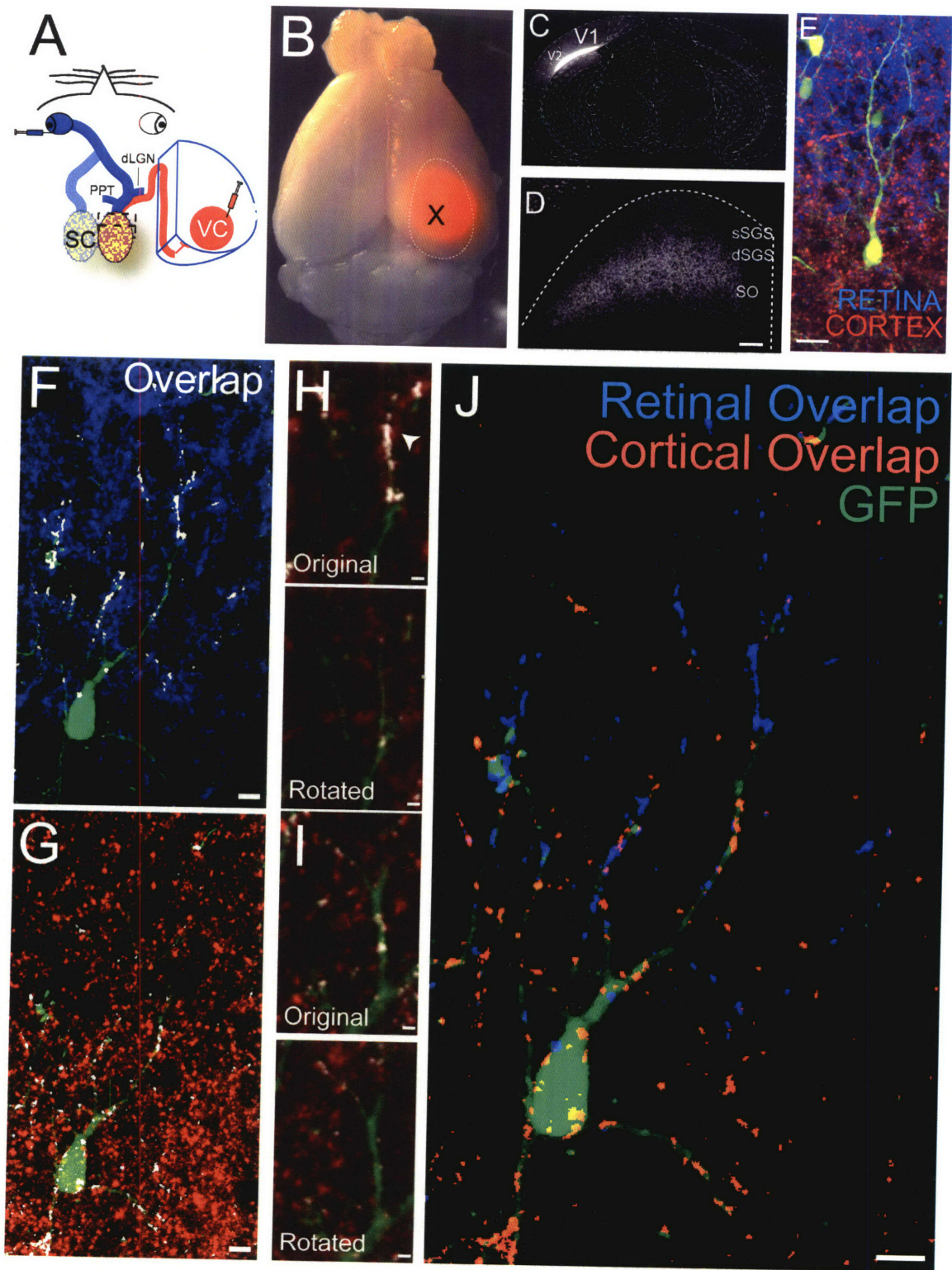J Retinal Overlap
Cortical Overlap
GFP

Figure 2. Visual collicular (DWV) neurons are contacted by axons from the retina and visual cortex.

(A) Diagram of dual anterograde tract tracing in eGFP-S transgenic mice. Intravitreal injection of Alexa633-CTB into the contralateral eye is coupled with intracortical microinjection of Alexa546-CTB into the ipsilateral visual cortex. VC = visual cortex, SC = superior colliculus, dLGN = dorsolateral geniculate nucleus, PTN = pre-tectal nucleii

(B-D) Extent of cortical label, visualized in wholemount (B) and coronal section (C). Cortical axon distribution in the SC is shown in coronal section (D). Scale, 50um

(E) Representative eGFP-expressing DWV neuron after dual labeling of axons from retina and visual cortex. DWV cells are located in the deep stratum griseum superficiale (dSGS) at the interface of retinal and cortical afferents. Scale, 20um

(F-G) Two-dimensional projection of a representative confocal z-series showing overlapped pixels between retinal axons (RED) or cortical axons (BLUE) and eGFP (GREEN). Overlapped pixels are in WHITE. Scale, 10um

(H-I) Comparison of original images and rotated controls to detect non-specific overlap of retinal (H) or cortical (I) axons. In original images, large contiguous clusters of overlapped pixels may arise from axons which course along the dendritic shaft (eg, retinal axon in (H), arrowhead indicates CTB-labeled axon running alongside eGFP-labeled dendrite). Overlap is also detected in images in which the axon label has been rotated with respect to the eGFP-labeled neuron. However, overlapped clusters in rotated images are significantly smaller and consist of fewer contiguous pixels (Mann-Whitney for cluster sizes in original vs rotated images CTP and RTP < 0.02). Scale, 2um

(J) Distribution of overlapped pixels from either the retinal (blue) or cortical (red) projection on the eGFP-labeled dendritic arbor. Scale, 10um
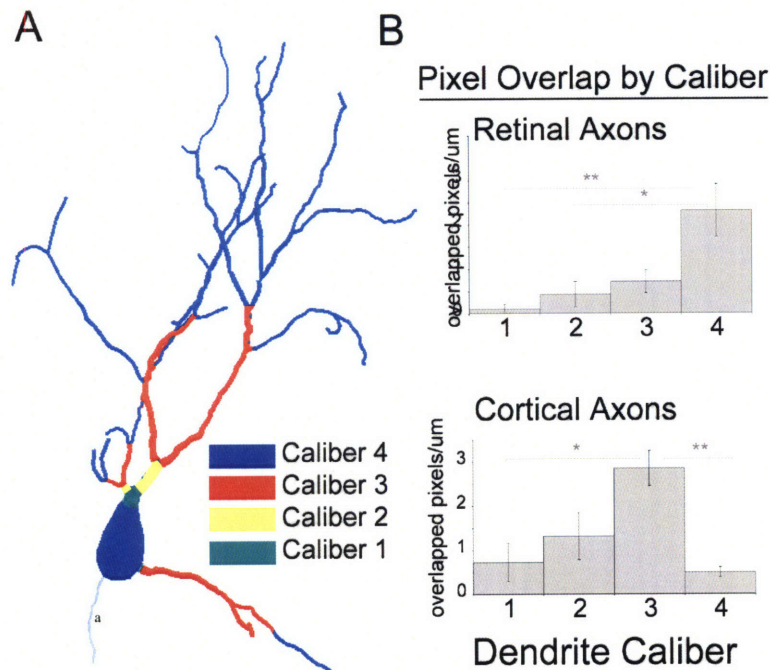
A

B

Pixel Overlap by Caliber

Retinal Axons

overlapped pixels/um

** *

1 2 3 4

Caliber 4
Caliber 3
Caliber 2
Caliber 1

Cortical Axons

overlapped pixels/um

3
2
1
0

* **

1 2 3 4

Dendrite Caliber

Figure 3. Retinal and visual cortical axons are differentially distributed on dendrites of different Calibers.
(A) Neurolucida reconstruction of dendrites of different widths across the dendritic arbor. Dendritic segments are categorized according to their average thickness between branch points. "Caliber 1" represents segments that are 81–100% as thick as the widest primary trunk originating from the soma, "Caliber 2" are 61–80% as thick as the primary trunk, "Caliber 3" are 41–60% as thick as the primary trunk and "Caliber 4" segments that are 20–40% as thick as the primary trunk.
 (B) Quantification of overlapped pixels per um of dendritic length in three-dimensional confocal z-series

There is a significant effect of caliber on overlapped pixel density for both the retinal and cortical projection (from three reconstructed cells from two independent dual labeling experiments).Retinal (F=11.58, n=43, p < 0.05)
Cortical (F=3.57, n=37, p < 0.0001) .

When branches are analyzed by caliber categories, individual differences among thin and thick calibers can be observed. * p < 0.05, ** p<0.01 Games-Howell post-hoc.
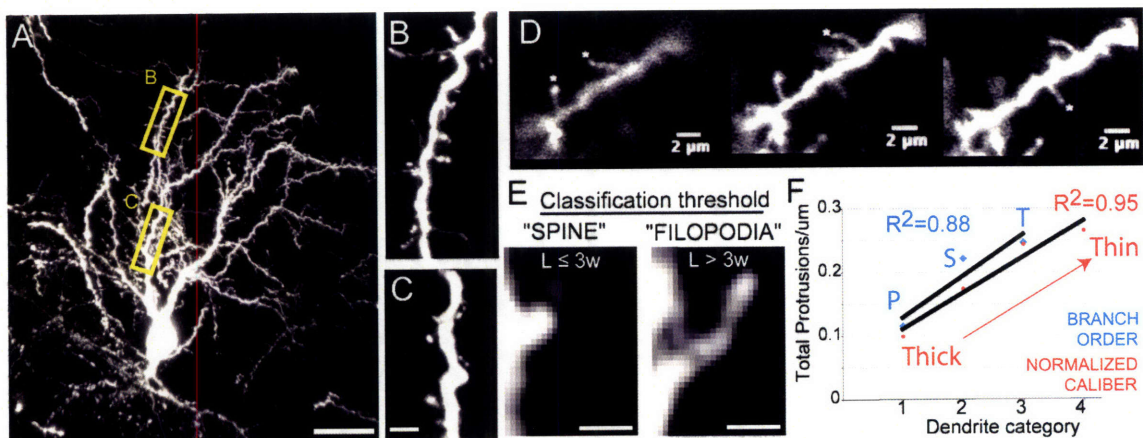
82

Figure 4. Protrusion density on DWV neurons is correlated with dendritic caliber
(A) Z-series projection of an eGFP labeled neuron at P13. Scale, 20um. Boxed regions
are magnified in (B-C).
(B-C). Thin dendrites (B) have more protrusions than thick dendrites (C).
(D) Single, sequential optical slices of a confocal z-series used for quantification of
dendritic protrusions along three-dimensional dendritic segments. Protrusions (white
asterisk), were counted only in the section in which they were in sharp focus. The
number of protrusions on a given dendritic branch was expressed as a density by
measuring the three-dimensional length of each dendritic segment through the z-series.
(E) All dendritic protrusions were classified as "Spine" or "Filopodia" structures according
to the length vs maximal width threshold shown. L = three-dimensional length from
base to tip. w = width at widest point (neck or head). Protrusions were not counted if
shorter than 0.6um, or longer than 6w. Scale, 2um.
(F) Protrusion density is correlated with branch caliber. Linear correlation coefficients
(R^2) are indicated. Total spine+filopodial density is plotted against normalized caliber (1
= 81-100% as thick as primary trunk [1.2-3.0um] ----> 4 = 21-40% as thick as primary
trunk [0.2-0.4um]). Density is better correlated with caliber than the canonical branch
order classification: 1 = Primary, 2 = Secondary, 3 = Tertiary).
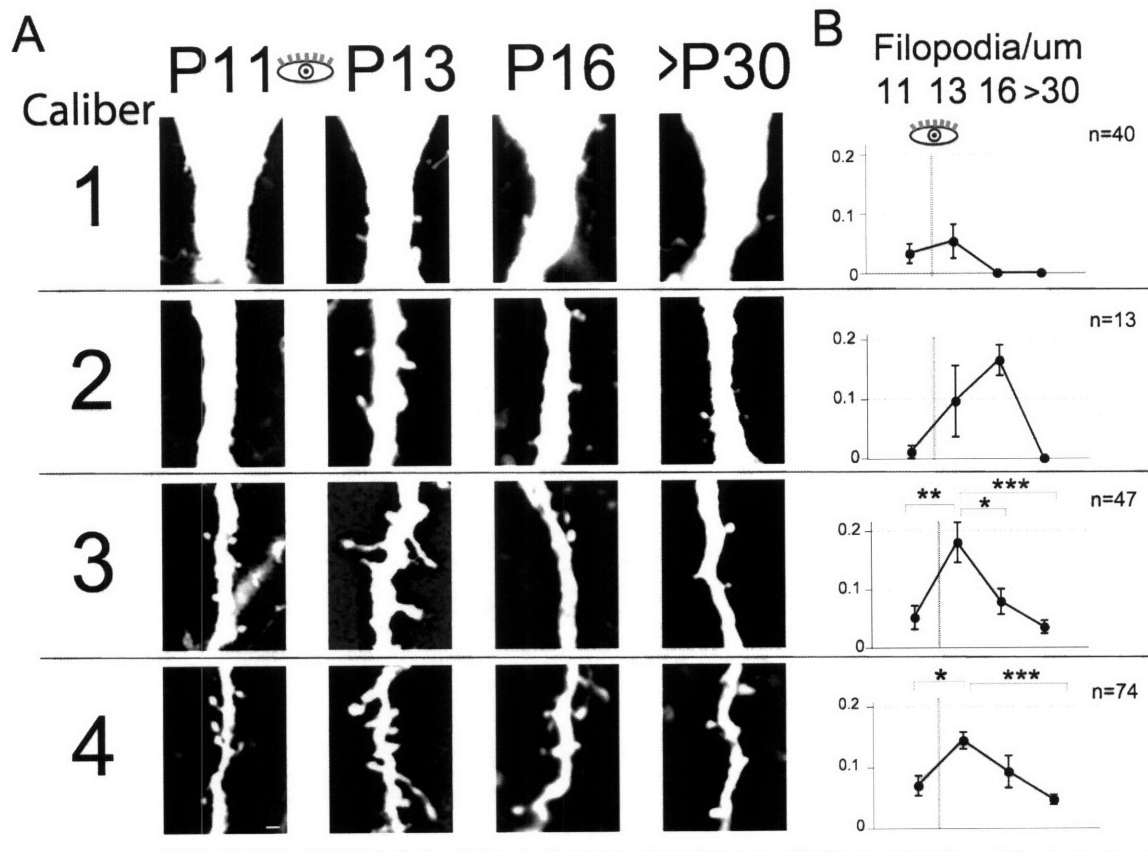
Figure 5. A transient burst of new filopodia formation occurs after 24h of visual experience

(A) Representative dendritic segments, organized by normalized branch caliber and age. Note that images shown are two-dimensional projections of three-dimensional z-series upon which actual analysis was conducted. Spine/filopodia visibility and resolution is reduced by stack projection, and thus example images have been contrast enhanced for visibility, resulting in pixel saturation. Scale, 2um

(B) Quantification of spine and filopodia density reveals a transient increase in filopodia over eye-opening on Caliber3 (n=47 from 6-13 cells at each age, **$p<0.01$, Tukey HSD post-hoc) and Caliber4 (n=74, *$p<0.05$) that returns to baseline levels as early as P16 on Caliber3 dendrites (*$p<0.05$), and by adulthood on Caliber4 (***$p<0.001$).

No significant differences in spine density were observed at any age, on any caliber (One-way ANOVA, $p>0.05$ Calibers 2, 3, 4)
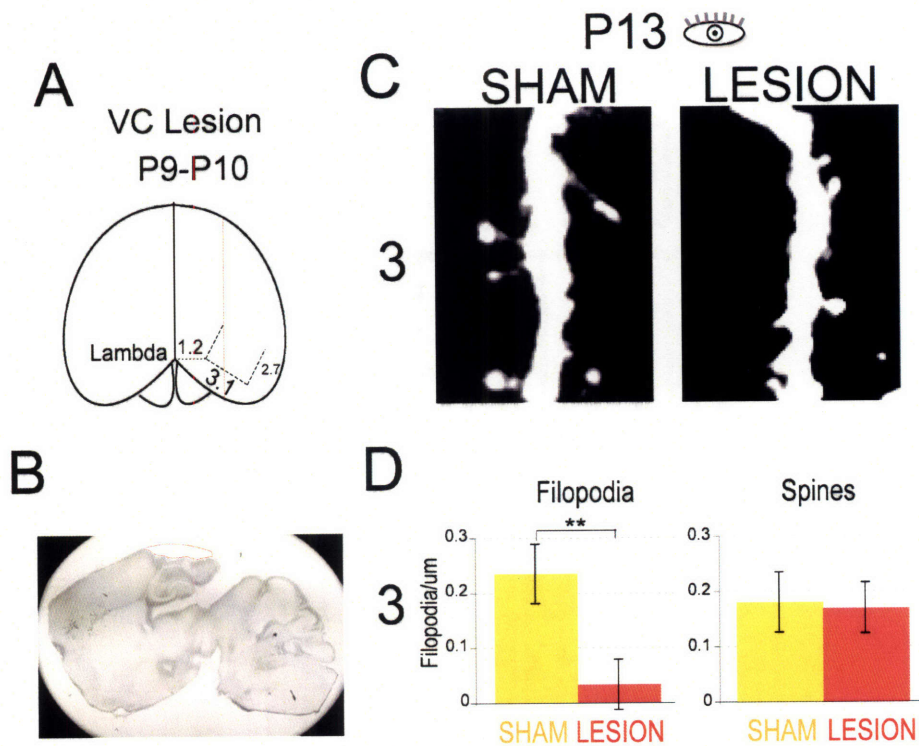
Figure 6. New filopodia sprout locally over P11–P13 in response to visual cortical axons

(A) Diagram of the cortical area removed just before eye-opening

(B) Para-sagittal section confirming extent of lesion at P13

(C) Representative 2D projection of confocal z-series through Caliber3 dendrites after VC lesion or sham surgery at P9–P10.

(D) Visual cortex removal before eye-opening reduces filopodia density by P13 (n=15, *p<0.05, Student's t test) on Caliber3 dendrites. No significant effect on spine density (p>0.90).

No significant changes were observed on Caliber4 dendrites on filopodia or spine density (n=47, p>0.70).

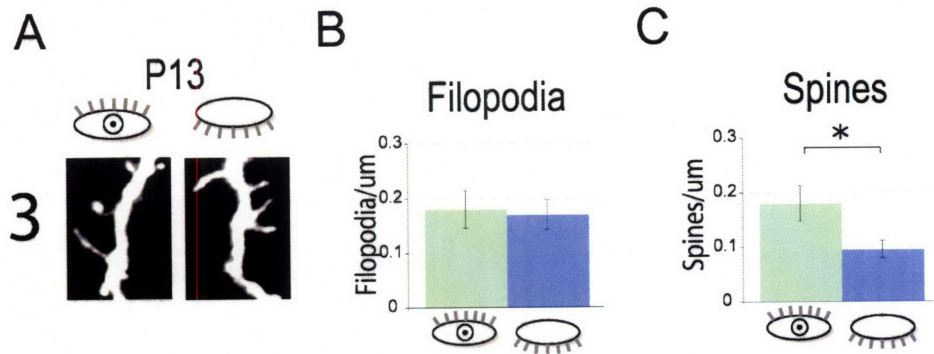A   B   C

P13

Figure 7. Visual experience is required for local stabilization of spines, not sprouting of filopodia
(A) Representative 2D projection of confocal z-series through Caliber3 dendrites at P13 24 hours after eye-opening or with eyes kept closed.
(B) Filopodia density at P13 is unaffected by eye-closure between P12-P13 (n = 18, p>0.30, Student's t test).
(C) Spine density at P13 is reduced by eye-closure between P12-P13 (p < 0.05 Student's t test corrected for multiple comparisons). Spine and filopodia density on Caliber4 are unaffected by eye closure (n = 25, p > 0.50)
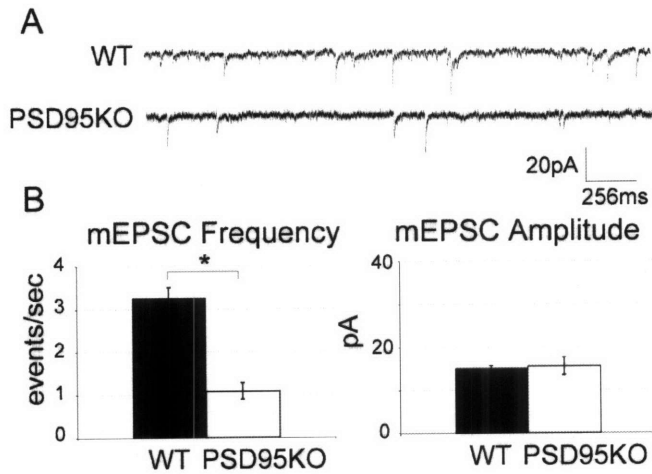
Figure 8. PSD-95 is required for eye-opening dependent gain of new release sites after eye-opening

(A) Sample traces of mEPSCs recorded blind to genotype at -70mV from deep SGS neurons of wild-type and PSD-95 mutant mice at P13–P15, after eye-opening. ACSF contained 0Mg++, BMI, and TTX.

(B) Eye-opening induced increases in mEPSC frequency do not occur in PSD95 mutant mice. mEPSC frequency is reduced three-fold compared to WT mice (n = 6 WT, n = 3 mutant, *p < 0.05, Student's t test corrected for multiple comparisons). No change in mEPSC amplitude, rise, or decay time was detected (p > 0.05). 99% confidence intervals were [1.8–4.7 Hz] for WT and [0.28–1.8 Hz] for PSD95 mutant.

Figure 9. PSD95 mutant mice lack PSD-95 protein in the sSC

(A) tPSD-95+/+ mutant mice have a truncated form of the PSD-95 gene at the PSD-95 locus (Migaud et al. 1998). (circles = PDZ domain, hexagon = SH3, oval = GK).

(B) PSD-95 is abundantly expressed in the dendrites of deep SGS vertical neurons of wild-type mice, in both vibrotome and cryostat sections. The same N-terminal antibody does not label cells in the sSC of homozygous mutant mice processed in parallel (low-magnification samples from two separate animals are shown).

(C) Neither full-length nor truncated protein (expect ~40kD) is detected in synaptoneurosomes of sSC using an N-terminal antibody.

CHAPTER THREE

Laminar organization of the superficial visual layers of the superior colliculus of the mouse

----

ABSTRACT

The superficial layers of the mouse superior colliculus (sSC) are an important model system for the study of molecular and activity-dependent guidance cues in the development of visual pathways. The availability of genetically modified mouse strains is enabling new approaches to understanding the mechanisms of circuit formation and function in visual pathways. These studies could be aided by knowledge of the anatomical organization of the mouse sSC. We have used a transgenic mouse strain that expresses eGFP in subsets of neurons (eGFP-S), to define a laminar organization of cell classes in the mouse sSC that is consistent with patterns observed by Golgi studies in the rat. We found that this laminar organization is also reflected in the distribution of GABAergic neurons in transgenic mice which express GFP under control of the GAD-67 promoter. Using anterograde tract tracing in eGFP-S transgenic mice we have simultaneously labeled the two major visual projections to the sSC from retinal ganglion cells and Layer V pyramids in visual cortex and have observed their termination pattern relative to the sSC laminae. Our data suggest there are distinct but overlapping patterns of visual afferents in the sSC, and distinct but overlapping patterns of excitatory and inhibitory cell classes that align with the laminar organization of cell classes as we and others have defined them. We provide evidence for at least four distinct laminae in the mouse sSC (the SZ, sSGS, dSGS, and zWFV) defined by cellular morphology, expression of excitatory and inhibitory neurotransmitters, and the pattern of afferent innervation. We

have additionally used this strain to monitor postnatal dendritic growth in a morphologically-defined cell class, and detected dendritic growth on the order of 20% between P11 and adulthood. This is much less than previously estimated using Golgi studies which label a random assortment of cell types at different ages.

INTRODUCTION

The superior colliculus (SC) is critical to normal visual behavior in both primates (Schiller et al. 1979, 1980) and rodents (Goodale and Murison 1975, Goodale et al. 1978, Milner et al. 1984, Carman and Schneider 1992). The superficial layers of the SC (sSC) in the mouse receive direct visual input via the retina (Drager and Hofbauer 1985) and Layer V pyramids in visual cortex (Rhoades et al. 1985, Inoue et al. 1992), and cells in the upper layers of the sSC (the stratum griseum superficiale, SGS) can be driven by visual stimuli (Siminoff et al. 1966, Stein 1984, Kao et al. 1994). The function of the descending projection to the sSC from layer V pyramidal neurons in visual cortex is not yet clear. Simple response properties to flashes of light and direction selectivity for moving stimuli have been reported for cells of the SGS (Stein et al. 1973a, b), and the projection from visual cortex may be involved in the development of responsiveness and/or tuning of SGS neurons. Lesion of visual cortex in neonates prevents the development of direction selectivity (Flandrin et al. 1977, Mize and Murphy 1976, Stein and Magalhaes-Castro 1975) and decortication in adults similarly abolishes direction selectivity of SC cells (Berman and Cynader 1976, Wickelgren and Sterling 1969). Acute cortical inactivation by cooling can reversibly change the number of discharges from SC neurons evoked by presentation of a visual stimulus. (Stein and Gallagher 1981). Recent data also shows that cells of the superficial SGS actually have much more complex receptive field properties than previously expected (Girman and Lund 2007).

The rodent sSC is one of the few regions of the brain where both the chemotrophic and activity-dependent cues necessary for development of its afferent projections have been well characterized (McLaughlin and O'Leary 2005, Flanagan and Vanderhaeghen 1998). Genetic manipulations in mice have been crucial to these studies, and have revealed many of the signaling mechanisms underlying these processes. Further understanding of these processes, as well as the functional circuitry of the SC underlying visually mediated behavior, requires detailed knowledge of the relative organization of cell types and afferent axons within the SC. In this respect, a number of excellent studies have separately described the general organization of cells, afferents, and synapses in the mammalian sSC of various species (Langer and Lund 1974, Lund 1966, Warton and Jones 1985, Takunaga and Otani 1976, Mathers 1977, Labriola and Laemle 1977, Mize 1983, Dreher et al. 1985, Inoue et al. 1992, Rhoades et al. 1985, Mooney et al. 1988, Albers et al. 1990, Saito and Isa 2004, Sachs and Schneider 1984, Graham and Casagrande 1980). These descriptions have not typically been performed in the same animal, and thus precise relative relationships of afferents, cell types, and synapses, have been difficult to ascertain. We have therefore used a dual tract tracing approach in eGFP transgenic mice combined with an analysis of inhibitory and excitatory synaptic markers to relate the organization of the major cell classes of the sSC to the retinal and cortical afferent pathways to the SC.

MATERIALS AND METHODS

Animals All procedures followed MIT IACUC-approved protocols. Wild-type C57BL/6 mice were purchased (Jackson Laboratories, ME). Heterozygous C57BL/6 transgenic mice expressing eGFP under control of the Thy-1 promoter (Feng et al. 2000) were genotyped by epifluorescent detection of GFP-fluorescence in ear punches at weaning, and bred to homozygosity as confirmed by test matings to wild-type mice that resulted in 100% inheritance rates of the eGFP allele. The day of birth was labeled "P0". Surgeries at all ages

were performed under vaporized oxygen/isofluorane with depth of anesthesia assessed by foot pinch. Loss of young pups due to cannibalism by these mothers after surgery was improved by handling pups with gloves and cross-fostering to Balb/c or Swiss-Webster mothers. However, these mothers are excellent groomers and frequently open wounds by removal of sutures. The fostering procedure was as follows: 1) Removal of the foster mother from the cage and culling of the Balb/c litter to 3-5 pups. 2) Introduction of post-op pups into nest with existing litter, and burying under nest and waste material. 3) Reintroduction of the mother after 15-20 minutes.

Anterograde afferent labeling. Retinal and cortical afferents to the SGS were labeled by direct injection of a 0.5% solution of Alexa 488, 555, or 647-conjugated Cholera Toxin B subunits (Invitrogen) dissolved in 2% DMSO/sterile PBS pH 7.4. Intravitreal: Under vaporized isofluorane anesthesia, the eye was prolapsed out of the socket, and a small slit was made at the ciliary margin under stereoscopic guidance (Bausch&Lomb scope) with the point of a #12 scalpel blade to relieve ocular pressure and allow leakage of some ocular media. Dye solution was injected through this small hole, using a blunt custom Hamilton syringe (5ul volume, 32G tip) to completely fill the vitreous with dye solution (total volume varied with age). Complete fill was confirmed by observation of the dye through the cornea. After successful fills the dye in the filled vitreous could still be observed after needle retraction. For pups labeled before eye-opening, the eyelids were prematurely opened along the presumptive eyelid seam, the eyes prolapsed, and sutured closed after injection with #6 Silk sutures (Amicon).

Cortical: Microinjection tips were prepared from glass capillaries (Drummond #1-000-0300) and broken using a sterile forceps to the following tip dimensions: 0.8 cm L x 36 um ID, 45 degree bevel. 1-3ul of dye solution was injected through a small burr hole in medio-posterior cortex (Using Paxinos'

coordinates from Lambda: 3mm in adult mice, scaled for other ages) using a positive displacement injection system (CellTram Vario, Eppendorf). Successful labeling only occurred when injections were performed slowly (over ~30-40 minutes), and wound did not leak during injection or after needle retraction. Skin was sutured with #6 Silk sutures and sealed with Vetbond (3M). After 1-3 days animals were perfused, and confirmation of complete fills and localization and extent of cortical injection confirmed under stereoscopic examination of optic nerves, cortices, and collicular lobes with combination brightfield and epifluorescence microscopy using the appropriate filters.

Histology. Animals were anesthetized with vaporized isofluorane (Samuel Perkins, MA), given a heparin flush through the left ventricle, and rapidly gravity perfused with 0.2um filtered PBS pH 7.4 until the underside of the liver just cleared, followed by 4% paraformaldehyde/PBS pH 7.4 prepared fresh (EMS, 1ml per gram animal). The rate of flow was adjusted for age. Brains were dissected, trimmed if necessary to fully expose the midbrain, and post-fixed at 4C for 4-12 hours. Coronal or para-sagittal 60-200um vibratome sections were collected floating into PBS, and mounted in aqueous antifade media (Fluoromount G, EMS).

Cell Classification. Cells were classified by the following morphological criteria: Marginal: All visible dendrites originate and are located ventral to soma. Stellate: Dendritic shafts of approximately equal width originating from the soma at multiple locations other than dorsal and ventral positions. Horizontal: Horizontally oriented soma with proximal dendrites extending approximately lateral to pial surface. Granule: Brightly labeled, round soma but no identifiable dendrites. Vertical-Pear: Vertical pear-shaped soma, with vertically oriented proximal dendrites. Vertical-Fusiform: Vertically elongated fusiform soma, with vertically oriented proximal dendrites. Vertical neurons with pear somas in the upper dSGS had dorsally-weighted dendrites (DWV cells). Vertical neurons with

fusiform somas in the mid-upper dSGS also had dorsally-weighted dendrites (DWV cells). Vertical neurons with fusiform somas that had non-biased dendrites (equal ventral and dorsal) were restricted to the lower portion of the dSGS. Wide-field Vertical: Elongated V-shaped soma with exactly two dorsal apical dendrites of equal thickness each leaving the soma at ~45 degree angle. No ventral originating dendrites present.

Cell depth analysis. Cell depth was assayed in sequential coronal and para-sagittal sections through the SC of adult eGFP-S mice. Low-magnification z-series were collected with confocal microscopy across the entire extent of each section, projected in three-dimensions, printed, and used as a guide for cell identification. Each section was systematically scanned for the presence of cells with the majority of their dendritic arbor intact. Once such a cell was found, it was more closely investigated under high magnification (20-60X) epifluorescence, classified according to the rules above, and tagged on the projected image. Many smaller, granule type cells were observed throughout the depth of the sSC, however, typically few or no dendrites were apparent and so these cells were not classified. Z-series were then imported into ImageJ and the depth of each identified soma measured as the distance between the pia and the dorso-ventral midpoint of the soma. Due to the curvature of the SC and the compression of layers at the edges, each cell depth was expressed as a percentage of the total depth of the sSC. The somata of wide-field vertical cells were used to set the deepest extent, and individual cell depth's were expressed as a percentage of a WFV depth that was at a similar rostro-caudal latero-medial position as the cell in question. The depth of WFV cells was observed to be highly reproducible and restricted to a small lamina at the most dorsal region of the SO.

Afferent depth analysis. Confocal z-series of coronal or para-sagittal sections were collected with 10x or 20x objective. Aquisition gain was set to be below

94

the level which saturated any pixels in the image. Z-series containing eGFP-labeled neurons were imported into ImageJ (NIH), and the levels of each dye channel adjusted if necessary to normalize the maximum intensity values. This was necessary because the pixel intensity distributions collected using Alexa633 were typically shifted to the left (lower intensity) than those using other dyes. A region surrounding an eGFP-labeled neuron of interest was identified, and a line drawn from the pia to the deepest extent of the sSC through the soma of the eGFP labeled neuron in a single optical slice. The intensity profile for each channel (eGFP, retinal axons, and cortical axons) along that line was then obtained, and the raw value plotted (Figure 5C), or the average of multiple measurements through several cells plotted (Figure 5D). Images in figures have been contrast enhanced, in some cases saturating pixels to improve visibility, especially of images collected in the blue channel or of the ipsilateral retinal projection which is sparse and therefore not strongly labeled.

Immunohistochemistry. 60um vibrotome sections were prepared from 4%para/PBS, perfused and post-fixed. All sections were processed floating, blocked with 10% goat serum, permeabilized with 0.3% TX100, followed by incubation with polyclonal antibody against alpha-CamKII or GABA (Sigma), in 1% goat serum/0.1% TX100 solution overnight at 4C, followed by goat or donkey secondary antibodies conjugated to Alexa dyes (1-2 hours at room temp, 1% goat serum/0.1% TX100) (Invitrogen, 1:700). Single image planes from the mid rostro-caudal SGS were collected by confocal microscopy from mounted sections from eGFP-S transgenic or wild-type mice with a 20x/0.75NA objective.

Confocal Microscopy. Serial sections from every animal were scanned under low magnification epifluorescence (20X/xxNA) on a Nikon Fxxx microscope for the presence of well-labeled cylindrical narrow field vertical neurons. Once a

well-labeled neuron of this type was identified, it was first confirmed that the majority (>80-90%) of its dendritic arbor was well labeled and present in a single slice. Every cell that fulfilled these criteria was selected for further analysis. Confocal z-series of the dendritic arbor were then collected at high magnification with a 60X/1.4 NA oil-immersion objective at 2um intervals on a Nikon PCM2000 (MVI) with SimplePCI acquisiton software (Compix), for a final pixel resolution of x y z. The acquisition gain was determined independently for each cell to be below the maximum threshold which caused saturation of pixels in spines. The acquisition gain was determined independently for each cell to be below the maximum threshold which caused saturation of pixels in dendrites.

Structural Analyses. Confocal z-series covering the entire dendritic arbor from P11, P13, and Adult mice were randomly intercalated, coded by an independent investigator, and imported to Neurolucida. Dendritic arbors were investigated for completeness, and only those arbors without obvious truncations were accepted for final analysis. The cell soma and dendrites were traced in three-dimensions with the investigator blind to group identity, and measures of TDBL and dendritic branching patterns generated within Neurolucida.

RESULTS
Retinal and cortical afferent distribution in the mouse sSC

The two major visual afferents to the mouse SC, from retina and Layer V visual cortex, can be anterogradely labeled in a single mouse by injection of the Cholera toxin B subunit (CTB) conjugated to Alexa fluorophores (Figure 1A-1D). CTB-Alexa is transported rostrally from visual cortex in axons in the internal capsule, which turn caudally to approach the SC (Figure 1D). Retinal axons arborize profusely in the pretectal nucleii before entering the brachium of the

SC and forming a dense arborization there (Figure 2A-2B). Cortical axonal fibers or terminals are not as dense and are difficult to detect in wholemounts.

Retinal axons enter the brachium of the SC slightly dorsal to cortical axons (Figure 2D-2F). Retinal axon labeling gains a punctate appearance upon turning dorsally into the superficial layers of the SC (Figure 2G). Smooth cortical axons can also be detected in the brachium to the SC (Figure 2E-2F), and intermixed with retinal axons in the SO (Figure 2G). However, punctate cortical axon labeling has a could be observed throughout depth of the sSC. The bright punctate accumulation of CTB in axons usually occurs at arbors which support pre-synaptic release sites (Colonnese et al, 2005; Colonnese and Constantine-Paton, 2006).

The dominant retinal projection is from the contralateral retina, and the ipsilateral retinal projection is minimal by comparison (Figure 3A). Axons from contralateral retina form a dense band in the superficial layers of the sSC, and diminish ventrally, towards the SO. Ipsilateral retinal axons form small, symmetric patches ventral to the contralateral retinal projection, visible in coronal section. Axons from contralateral retina are largely excluded from these patches (Figure 3A). Occasional individual axons from ipsilateral retina are visible in more superficial layers within the zone of the contralateral retina, and are intertwined with contralateral retinal axons (in pink or red on the right SC, Figure 3A). Vertically oriented neurons visible in the SGS of the eGFP-S transgenic mouse (Feng et al., 2000) are situated in the ventral margin of the contralateral retinal projection.

The dominant cortical projection is from the ipsilateral visual cortex. Labeled fibers form a dense band in the deepest layers of the sSC (presumptive SO), and diminish towards the pial surface (Figure 3B). Labeled cortical axons were not detected in the contralateral SC (not shown).

Distribution of cell types in eGFP-S and GAD67-GFP transgenic mice

eGFP is strongly expressed by cells in the SC of (Thy-1)eGFP-S transgenic mice (Feng et al. 2000). Scattered labeling enables visualization of dendritic arbors throughout the depth of the SC (Figure 4A). The somas of the major cell types labeled in the eGFP-S mouse are located at different depths (Figure 4B). Marginal cells are the most superficial (within the top 5% of the sSC), followed by stellates (~20-35%), and then Vertical-Pear (Vertical pear-shaped soma, with vertically oriented proximal dendrites) or Vertical-Fusiform (Vertically elongated fusiform soma, with vertically oriented proximal dendrites)-shaped cell bodies (~40-80%). Vertical neurons with pear somas in the upper dSGS had dorsally-weighted dendrites (DWV cells). Vertical neurons with fusiform somas in the mid-upper dSGS also had dorsally-weighted dendrites (DWV cells). Vertical neurons with fusiform somas that had non-biased dendrites (equal ventral and dorsal) were restricted to the lower portion of the dSGS. Wide-field vertical neurons occupy the most ventral position (>80%). Laminar boundaries drawn in Figure 4A reflect these depth profile distinctions. Marginal cells do not strongly express eGFP and labeled horizontal neurons were not detected in this study. The somas of wide-field vertical neurons are highly restricted to a narrow stratum and are used to mark the ventral boundary of the sSC. The stratum opticum laminar designation is not used here – it spreads across laminae defined by particular cell classes and is not visible at all ages due to lack of myelination in young animals.

Although not well labeled in the eGFP-S transgenic mouse SC, GABAergic neurons can be observed in transgenic mice which express GFP under control of the GAD67 promoter (Chattopadhyaya et al. 2004). These cells form a dense plexus in the SZ and superficial SGS (Figure 4C). Marginal cells express high levels of GFP driven by the GAD67 promoter in the SZ (Figure 4C-4D). Labeling

in the sSGS is largely due to a large number of horizontal neurons (Figure 4C and 4E), and smaller granule type neurons without identifiable dendritic arbors (Figure 4C). These smaller granule type neurons are seen throughout the depth of the sSC.

Immunoreactivity for alpha-CaMKII, which is highly enriched in the somas of excitatory neurons in hippocampus and cortex (Jones et al. 1994, Longson et al. 1997) is particularly enriched in the somas of neurons located in the deeper portion of the sSC, however, diffuse punctate immunoreactivity is visible at all depths.

Dual afferent labeling in eGFP-S transgenic mice

Vertically oriented neurons in eGFP-S transgenic mice reside in the dSGS at the interface of retinal and cortical afferents to the sSC (Figure 5A-5B). An intensity profile along the dotted line marked in (A) reveals opposing dorso-ventral gradients of retinal and cortical axonal labeling in the SC (Figure 5C). Averaged intensity profiles along sample lines collected at the mid rostro-caudal and medio-lateral position in the SC show the mean intensity (+/- SE) of labeled cortical axons by depth in an adult eGFP-S mouse, and the range of positions of vertical neuronal somata along those lines (Figure 5D).

Excitatory synapse markers on dendrites of vertical neurons in deep SGS

Anti-CamKII-alpha antibody immunolabels bright surface puncta around the soma and proximal dendrites of eGFP-labeled vertical neurons (Figure 6A). In eGFP-labeled neurons whose dendrites run close enough to the surface to be accessible to the antibody (Figure 6B), numerous CaMKII-alpha puncta are also detected along the dendritic shaft and in spine heads (Figure 6C). The AMPA-R subtype of glutamate receptor subunit GluR1 is also detected in numerous

puncta along the ascending dorsal dendrite of a vertically oriented neuron in dSGS (Figure 6D).

Postnatal dendritic growth of vertical neurons of the deep SGS

Vertical neurons of the deep SGS express eGFP as early as P11 in eGFP-S transgenic mice (Figure 7A). As in adult animals, dendritic arbors are complex and highly branched, and well filled with eGFP at this age (Figure 7B-7C). Total dendritic branch length was measured in three-dimensional reconstructions of dendritic structure. Total dendritic branch length is somewhat variable in these neurons, but moderate dendritic growth of about 20% can be detected between P11 and adulthood with sufficient sampling (Figure 7D).

DISCUSSION

We have combined anterograde tract tracing of visual afferents, analysis of cellular morphology, and immunohistochemistry in C57BL/6 wild-type and the eGFP-S transgenic C57BL/6 strain (Feng et el., 2000) to describe the laminar organization of the mouse sSC. Our results provide evidence for at least four laminae defined by 1) The dorso-ventral position of the major sSC cell classes, 2) The dorso-ventral distribution of retinal and visual cortical afferents, 3) The dorso-ventral distribution of GAD67-GFP positive GABAergic neurons, and 4) The dorso-ventral distribution of CamKII-alpha enriched neuronal somata. These results are consistent with a laminar organization previously described in the adult rat sSC from Golgi stained material (Langer and Lund 1974). We have extended these findings using dual tract tracing in eGFP-transgenic mice, and show that axons from the contralateral retina, the ipsilateral retina, and ipsilateral visual cortex occupy distinct, but overlapping, zones within the sSC. Furthermore, there appears to be a distinct, but overlapping, laminar organization of inhibitory and excitatory cell types within the sSC. Finally, because the eGFP-transgenic mouse line labels reproducible neuronal classes,

100

we have been able to assay the development of an individual cell class over postnatal development. Our identification of neuron classes from early postnatal development should be useful for future assays of neuronal structure and function as the sSC matures in wild-type or mutant mice.

Laminar organization of the mouse sSC

We have named sSC laminae consistent with the conventions used for the rat (Warton and Jones 1985), but with a few modifications we have here described. In the mouse sSC we describe four layers, from the pial surface as follows:

1. The stratum zonale (**SZ**) contains the cell bodies of GABAergic marginal neurons.

2. The superficial stratum griseum superficiale (**sSGS**), contains the cell bodies of GABAergic horizontal neurons and stellate neurons.

3. The deep stratum griseum superficiale (**dSGS**), contains the cell bodies of vertical neurons.

4. The zone of wide-field vertical neurons (**zWFV**) contains the cell bodies of wide-field vertical neurons.

Small (6-12um) diameter GABAergic granule-type neurons without identifiable dendrites in the eGFP-S strain are distributed throughout the depth of the sSC (sSGS, dSGS, zWFV).

This classification is entirely derived the eGFP-S and GAD67-GFP mice. Therefore, it is possible our analysis missed some cell classes of the mouse that are not labeled in either of strain. Indeed, some vertically oriented neurons were detected in the zWFV by anti-CamKIIa immunohistochemistry that were not labeled in the eGFP-S strain (see Figure 4F). Thus, there are likely additional members of these classes that exist within these laminae as well. However, our classification does include all of the six major cell classes that

have been previously described in the rat using the Golgi technique (Langer and Lund 1974).

The current classification differs from the earlier rodent work mainly in our treatment of vertically oriented neurons. We label these cells according to the shape of their somata. The distribution of these types overlaps within the deep SGS. Previous classifications have relied on the shape and depth of the soma, accompanied by the abundance of dorsal and/or ventral dendrites to classify the vertical types (Langer and Lund 1974, Takunaga and Otani 1976). However, we found that vertically oriented neurons in the mouse were most distinguishable by the shape of the soma (pear or fusiform) the shape of the proximal dendritic shaft, and the distribution of the dendritic arbor towards the pial surface, or toward the pia and deeper SC layers.

Nevertheless, we observed that cells that had dorsally oriented dendrites could have either pear or fusiform-shaped somata. Even within these categories, there was further heterogeneity in the number and thickness of dendrites originating from the soma, as well as the branching patterns distal to the soma. This is not an unusual observation and molecular expression profiles used as a more "functional" classification of cell types in the retina have revealed extensive heterogeneity within neuronal classes defined by morphological criteria of dendritic arbors and axonal destinations (Yamagata et al. 2006). We therefore refrain from suggesting that these morphological criteria necessarily reflect functional neuronal "types", and suggest instead that they are more useful for defining the potential location of a cell within the neural circuit. For example, somatic and/or dendritic location relative to afferent innervation patterns may provide informative cues about the identity of inputs to a cell, and/or the relative impact those inputs might have on a cell's functional output. Vertically oriented neurons with a preponderance of dorsal dendrites compared to ventral dendrites ("Dorsally-weighted vertical neurons"), might be expected

to receive a higher proportion of their synaptic inputs from retinal axons, compared to vertical neurons with dendrites equally distributed dorsal and ventral to their soma, for example.

A segregation of cell classes in the sSC relative to afferent input may be related to the laminar segregation of functional characteristics of neuronal response properties. A recent study in the rat has provided some evidence for a differential laminar localization of responses to orientation vs movement and direction selectivity (Girman and Lund 2007).

Laminar organization of visual afferents to the mouse SC

Retinal and visual cortical afferents to the sSC form opposing dorso-ventral gradients in an intriguing pattern that suggests competitive or repulsive interactions among ingrowing afferents. However, neither retinal nor cortical axons are absolutely excluded from either the dorsal or ventral extent of the sSC. The relatively deep localization of the cortical projection in this study is consistent with some observations in the mouse (Rhoades et al. 1985, Inoue et al. 1992) and clarifies some additional ambiguities. HRP injected into the visual cortex of C57BL mice labeled deep axons in the sSC, and retrograde analysis confirmed that these axons originate exclusively from pyramidal neurons in LayerV (Rhoades et al. 1985). However, qualitative anterograde DiI labeling studies of groups of corticotectal axons to the sSC concluded that visual cortical axons, while present in the SO, made an "L-shaped" turn and arborized dorsally in the superficial SGS (Inoue et al. 1992). Much of the apparent discrepancy may stem from the lack of dual or triple labeling of complete afferent projections in single animals in which the location of the termination zone of each afferent and each cell type can be determined in relation to one another. This, confusion as well as the paucity of information about the organization of cell types and afferents in the mouse sSC, in part motivated the

current study.

Assays of collicular function which use slices to stimulate visual afferents and record post-synaptic response properties are critical to an understanding of collicular function and connectivity. Our results suggest that retinal and cortical axons could synapse on entirely different cell classes, and differentially modify the output of the sSC. Even though we assayed axon, and not synapse, distributions, retinal axonal labeling was punctate only within superficial laminae, whereas cortical axonal labeling was punctate throughout the depth of the sSC. This suggests either 1) That CTB-filled retinal axons begin to form branches and arborize only within the superficial layers and/or 2) That the punctate appearance of these axons in the superficial layers reflects the more superficial location of retinal release sites because CTB-Alexa accumulates in pre-synaptic sites (Colonnese ref). This suggests that not only are the retinal and cortical axons differentially distributed, but the synapses they make are differentially distributed as well.

We also show that stimulation of the afferents in the "SO" as defined by the presence of shiny, myelinated axons with brightfield microscopy probably activates both retinal and cortical axons. We have not defined the "SO" in our sections, because we found both retinal and cortical axons entering the SC in para-sagittal sections to be widely dispersed and intermixed along the dorso-ventral axis, and it was difficult to assign a dorsal or ventral margin to the traveling axons. Furthermore, in the absence of myelination in the young animals typically used for whole cell electrophysiology recordings, axons within the SO are not easily detectable with brightfield microscopy (Warton and McCart 1985). We were not able to define a slice angle which would allow complete separation of retinal and cortical axons in the same slice. However, we did observe cortical axons at the brachium of the SC located at a slightly (~50um) ventral position to retinal axons. With a minimal stimulation of axons at the

surface of the brachium, it could be possible to preferentially isolate retinal axons here.

Implications for collicular function

Neurons of the SGS were originally reported to respond to light "ON" and light "OFF" signals, and to develop motion and direction selectivity for moving stimuli post-natally (Stein et al. 1973a, b). The removal of visual cortex can disrupt the normal development of direction selective tuning (Berman and Cynader 1976, Wickelgren and Sterling 1969) in the sSC, and cooling of visual cortex acutely depresses spiking rates in the SGS (Stein and Gallagher 1981). The elaboration and refinement of visual cortical axons in the SC is delayed relative to the early refinement of retinal axons (Dreher et al. 1985), and thus it is reasonable to assume that the acquisition of these more complex properties may be mediated by the ingrowth of cortical afferents, as opposed to retinal axons, which are thought to encode simpler spatial information about light "ON" and "OFF".

The current data also suggest some segregation of afferent inputs to inhibitory and excitatory cell types in the SGS. Both retinal and cortical axons are glutamatergic, and consistent with this, excitatory synapses are located throughout the depth of the sSC. Retinal axons are in a position to form excitatory synapses onto all of the cell classes of the superficial SGS, as well as the dendrites of deeper cells in the dSGS and zWFV (and potentially even the dendrites of deeper SGI neurons which extend into the sSC). Axons from visual cortex, in contrast, are more likely to form excitatory synapses on the soma and proximal dendrites of neurons in the dSGS and zWFV, and the dendrites of cells in the deeper layers. This would mean that retinal axons are in a somewhat exclusive position to provide input to the lateral inhibitory circuit formed by horizontal neurons in the sSGS, as well as the GABAergic marginal

105

and granule type neurons, whose function remains unknown. The function of the visual cortical input to the dSGS and zWFV also remains unclear, however, future attempts to independently drive retinal and cortical afferents to the sSC should be revealing.

LITERATURE CITED

Albers FJ, Meek J, Hafmans TG. 1990. Synaptic morphometry and synapse-to-neuron ratios in the superior colliculus of albino rats. J Comp Neurol. 291(2):220-30.

Berman N, Cynader M. 1976. Early versus late visual cortex lesions: Effects on receptive fields in cat superior colliculus. Exp Brain Res 25: 131-37.

Carman LS, Schneider GE. 1992. Orienting behavior in hamsters with lesions of superior colliculus, pretectum, and visual cortex. Exp Brain Res. 90(1):79-91.

Chattopadhyaya B, Di Cristo G, Higashiyama H, Knott GW, Kuhlman SJ, Welker E, Huang ZJ. 2004. Experience and activity-dependent maturation of perisomatic GABAergic innervation in primary visual cortex during a postnatal critical period. J Neurosci 24: 9598-9611

Drager UC, Hofbauer A. 1985. Depth segregation of retinal ganglion cells projecting to mouse superior colliculus. JCN 234: 465-74.

Dreher B, Shameem N, Thong IG, McCall MJ. 1985. Development of cortical afferents and cortico-tectal efferents of the mammalian (rat) primary visual cortex. Australian and New Zealand Journal of Ophtalmology 13: 251-261.

Feng G, Mellor RH, Bernstein M, Keller-Peck C, Nguyen QT, Wallace M, Nerbonne JM, Lichtman JW, Sanes JR. 2000. Imaging neuronal subsets in transgenic mice expressing multiple spectral variants of GFP. Neuron 28(1):41-51.

Flanagan JG, Vanderhaeghen P. 1998. The ephrins and Eph receptors in neural development. Annu Rev Neurosci. 1998;21:309-45.

Flandrin JM, Jeannerod M. 1977. Lack of recovery in collicular neurons from the effects of early deprivation or neonatal cortical lesion in the kitten. Brain Res 120: 362-66.

Girman SV, Lund RD. 2007. The most superficial sublamina of rat superior colliculus: neuronal response properties and correlates with perceptual figure-ground segregation. J Neurophysiol. May 2; [Epub ahead of print]

Goodale MA, Foreman NP, Milner AD. 1978. Visual orientation in the rat: a dissociation of deficits following cortical and collicular lesions. Exp Brain Res. 31(3):445-57.

Goodale MA, Murison RC. 1975. The effects of lesions of the superior colliculus on locomotor orientation and the orienting reflex in the rat. Brain Res. 88(2):243-61.

Graham J, Casagrande VA. 1980. A light microscopic and electron microscopic study of the superficial layers of the superior colliculus of the tree shrew (Tupaia glis). J Comp Neurol. 191(1):133-51.

Inoue K, Terashima T, Inoue Y. 1992. Postnatal development of the corticotectal projection from the visual cortex of the mouse. Okajimas Folia Anatomica Japonica 68: 319-332.

Jones EG, Huntley GW, Benson DL. 1994. Alpha calcium/calmodulin-dependent protein kinase II selectively expressed in a subpopulation of excitatory neurons in monkey sensory-motor cortex: comparison with GAD-67 expression. . J Neurosci. 14(2):611-29.

Kao CQ, McHaffie JG, Meredith MA, Stein BE. 1994. Functional development of a central visual map in cat. J Neurophysiol. Jul;72(1):266-72.

Labriola AR, Laemle LK. 1977. Cellular morphology in the visual layer of the developing rat superior colliculus. Exp Neurol. 55(1):247-68.

Langer TP and Lund RD. 1974. The upper layers of the superior colliculus of the rat: A golgi study. J Comp Neurol 158: 405-436.

Longson D, Longson CM, Jones EG. 1997. Localization of CAM II kinase-alpha, GAD, GluR2 and GABA(A) receptor subunit mRNAs in the human entorhinal cortex. Eur J Neurosci. 9(4):662-75.

Lund RD. 1966. The occipitotectal pathway of the rat. J Anat. 100(Pt 1):51-62.

Mathers LH Jr. 1977. Retinal and visual cortical projection to the superior colliculus of the rabbit. Exp Neurol. 57(3):698-712.

McLaughlin T, O'Leary DD. 2005. Molecular gradients and development of retinotopic maps. Annu Rev Neurosci. 2005;28:327-55.

Milner AD, Lines CR, Migdal B. 1984. Visual orientation and detection following lesions of the superior colliculus in rats. Exp Brain Res.56(1):106-14.

Mize RR, Murphy EH. 1976. Alterations in receptive field properties of superior colliculus cells produced by visual cortex ablation in infant and adult cats. J Comp Neurol. Aug 1;168(3):393-424.

Mize RR. 1983. Patterns of convergence and divergence of retinal and cortical synaptic terminals in the cat superior colliculus. Exp Brain Res. 51(1):88-96.

Mooney RD, Nikoletseas MM, Hess PR, Allen Z, Lewin AC, Rhoades RW. 1988. The projection from the superficial to the deep layers of the superior colliculus: An intracellular horseradish peroxidase injection study in the hamster. J Neurosci 8: 1384-1399.

Rhoades RW, Mooney RD, Fish SE. 1985. Subcortical projections of area 17 in the anopthalmic mouse. Dev Brain Res 17: 171-181.

Sachs GM, Schneider GE. 1984. The morphology of optic tract axons arborizing in the superior colliculus of the hamster. J Comp Neurol. 230(2):155-67.

Saito Y, Isa T. 2004. Laminar specific distribution of lateral excitatory connections in the rat superior colliculus. J Neurophysiol. 92(6):3500-10.

Schiller PH, True SD, Conway JL. 1980. Deficits in eye movements following frontal eye-field and superior colliculus ablations. J Neurophysiol. 44(6):1175-89.

Schiller PH, True SD, Conway JL. 1979. Effects of frontal eye field and superior colliculus ablations on eye movements. Science 206(4418):590-2.

Siminoff R, Schwassmann HO, Kruger L. 1966. An electrophysiological study of the visual projection to the superior colliculus of the rat. J Comp Neurol. Aug;127(4):435-44.

Stein BE, Gallagher H. 1981. Maturation of cortical control over superior colliculus cells in cat. Brain Res 223: 429-35.

Stein BE, Labos E, Kruger L. 1973b. Determinants of response latency in neurons of superior colliculus in kittens. J Neurophysiol 36: 680-89.

Stein BE, Labos E, Kruger L. 1973a. Sequence of changes in properties of neurons of superior colliculus of the kitten during maturation. J Neurophysiol 36: 667-79.

Stein BE, Magalhaes-Castro B. 1975. Effects of neonatal cortical lesions upon the cat superior colliculus. Brain Res 83: 480-85.

Stein BE. 1984. Development of the superior colliculus. Ann Rev Neurosci 7: 95-125.

Tokunaga A, Otani K. 1976. Dendritic patterns of neurons in the rat superior colliculus. Exp Neurol. 52(2):189-205.

Warton SS, Jones DG. 1985. Postnatal development of the superficial layers in the rat superior colliculus: a study with Golgi-Cox and Kluver-Barrera techniques. Exp Brain Res. 58(3):490-502.

Wickelgren BG, Sterling P. 1969. Influence of visual cortex on receptive fields in the superior colliculus of the cat. J Neurophysiol 32: 16-23.

Yamagata M, Weiner JA, Dulac C, Roth KA, Sanes JR. 2006. Labeled lines in the retinotectal system: markers for retinorecipient sublaminae and the retinal ganglion cell subsets that innervate them. Mol Cell Neurosci. 33(3):296-310.
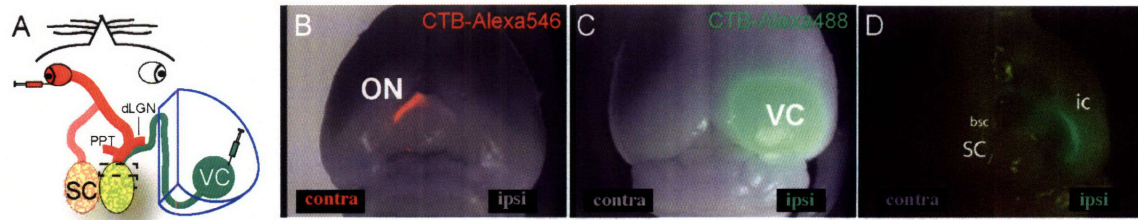
Figure 1. Anterograde labeling of retinal and visual cortical afferents with CTB-Alexa.

(A) Diagram of dual anterograde tract tracing approach. Intravitreal injection of Alexa-CTB (Alexa-546 is shown) into the contralateral eye is coupled with intracortical microinjection of Alexa-CTB (Alexa-488 is shown) into the ipsilateral visual cortex. VC = visual cortex, SC = superior colliculus

(B-C) Fill of the contralateral optic nerve (B, ventral view) and ipsilateral occipital cortex (C, dorsal view) was confirmed in wholemounts before sectioning with combination brightfield and epifluorescent filters appropriate for the Alexa dye used. ON = optic nerve

(D) Partial removal of the right cortical hemisphere confirms anterograde transport of CTB-Alexa in cortical axons traveling in the internal capsule (ic). Labeled fibers are visible on the dorsal surface of the thalamus and slightly laterally to the brachium of the superior colliculus (bsc).
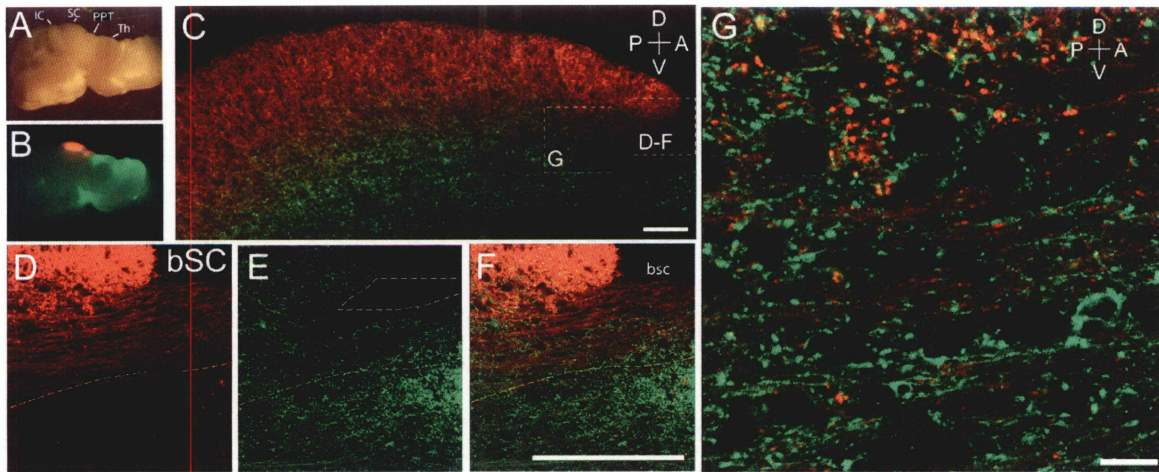
Figure 2. Dissection of retinal and cortical afferent pathways to the mouse SC
(A) Brightfield image of para-sagittal hemisection through the mouse brain shown in Figure 1. IC = inferior colliculus, PPT = pre-tectal nuclei, Th = thalamus
(B) Fluorescent image of hemisection in (A) of Alexa546-labeled retinal axons (red) and Alexa488-labeled cortical axons (green). Retinal arborizations in the PPT and SC are easily visible.
(C) Single confocal image through a para-sagittal vibrotome section of the brain labeled in (B). Square marks area enlarged in D-F.
(D) Retinal axons entering the rostral edge of SC through the brachium of the SC. Note unbranched axons traveling in the bSC which form dense arbors immediately upon entering the sSC. Dotted line marks ventral extent of the majority of retinal axons.
(E) Cortical axons in the SC in the same labeled section. Dotted line marks border of a region in the bSC from which cortical axons appear to be excluded.
(F) Overlay of images in D-E.
(G) Magnification of mixed retinal and cortical axons at the rostral edge of the sSC. Retinal and cortical axons run together as parallel fibers. Note punctate appearance of retinal axons dorsally, and punctate appearance of cortical axons both ventrally and dorsally.
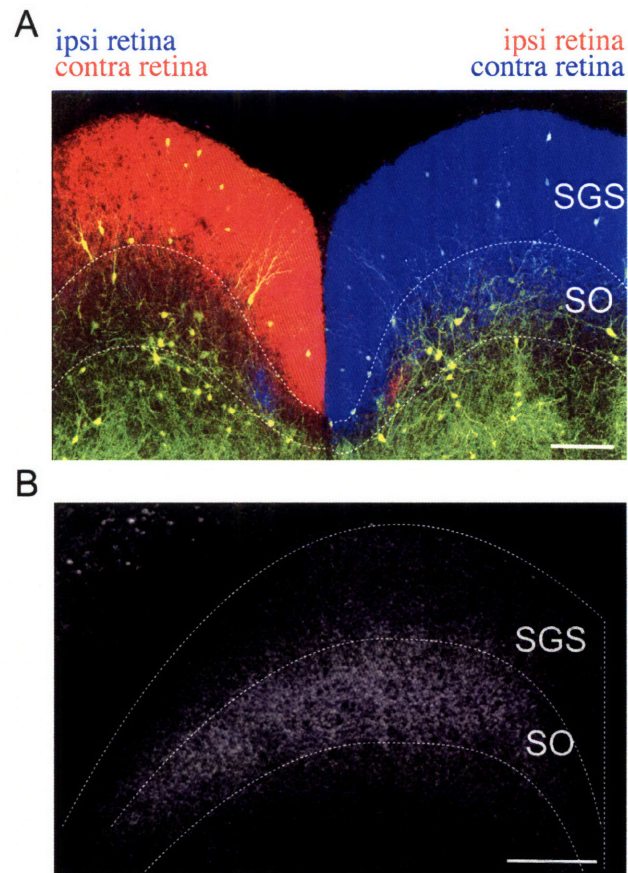
Figure 3. Distribution of retinal and cortical afferents in the mouse sSC
(A) Dual retinal labeling in an adult eGFP-S mouse. Shown is a projection of
confocal z-series through a coronal section of the mid rostro-caudal SC. Left
eye was labeled with CTB-Alexa633 and right eye labeled with CTB-Alexa546.
Ipsilateral axons form small patches ventral to the contralateral projection.
However, sparse, individual ipsilateral axons can also be detected more
superficially. Note eGFP-labeled vertically oriented neurons which are visible
at the ventral border of the contralateral retinal projection.
(B) Cortical axon distribution in an adult C57BL/6 mouse. Shown is a
projection of a confocal z-series through a coronal section of the mid rostro-
caudal SC. Right occipital cortex was labeled as in Figure 1C–D. Labeling is
dense in the stratum opticum (SO) and decreases towards the pial surface.
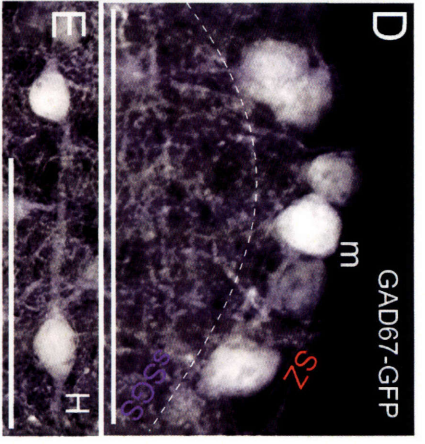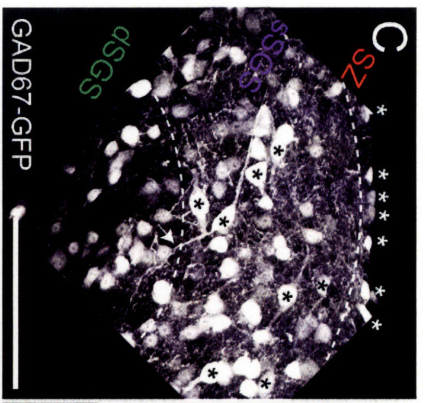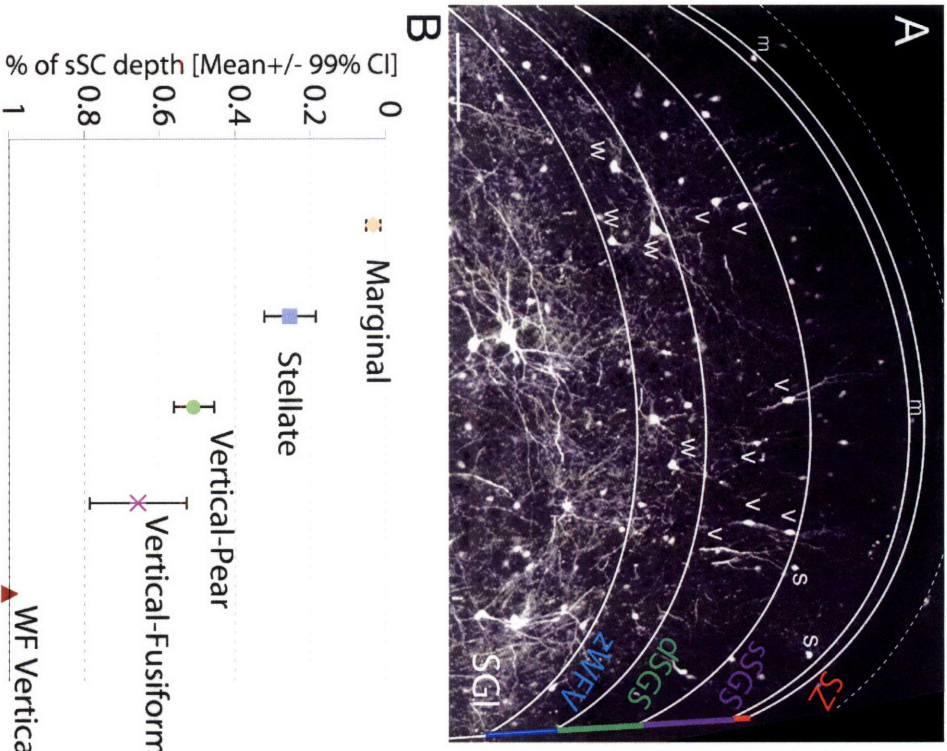SGS = stratum griseum superficiale. Scale, 100um
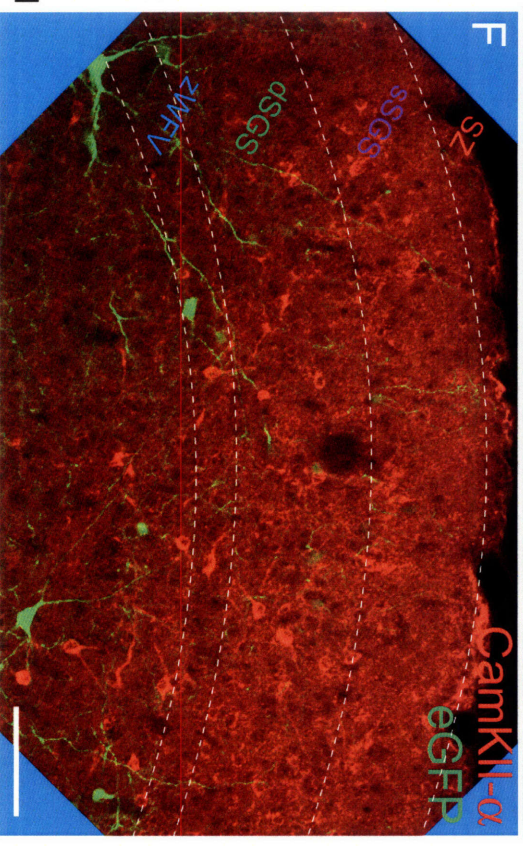
Figure 4. Laminar organization of cell types in the mouse sSC

(A) eGFP expressing neurons in the SC of an adult eGFP-S mouse. Low magnification confocal micrograph of a coronal section through the mid rostro-caudal SC. Laminar borders (solid lines) drawn according to cell type distributions in (4B). Dotted line denotes artefactual extension of pial surface due to z-projection of a 200um confocal z-series and the curved surface of the SC. SZ = stratum zonale, sSGS = superficial stratum griseum superficiale, dSGS = deep stratum griseum superficiale, zWFV = zone of wide field vertical cells, SGI = stratum griseum intermediale. m = marginal, v = vertical, s = stellate. Scale, 100um

(B) Distribution of major eGFP-labeled cell types in the sSC analysed by depth. Means+/- 99% confidence intervals (CI) are shown. Depth is expressed as percent of total SGS depth at that position. Only cells with identifiable dendritic arbors are represented. See methods for cell classification details. Note that Vertical-Pear are vertical neurons with pear-shaped soma in upper layer of dSGS, Vertical-Fusiform are vertical neurons with fusiform soma, with vertically oriented proximal dendrites. Vertical neurons with pear somas in the upper dSGS had dorsally-weighted dendrites (DWV cells, unmarked). Some vertical neurons with fusiform somas in the mid-upper dSGS also had dorsally-weighted dendrites (DWV cells, unmarked). Vertical neurons with fusiform somas that had non-biased dendrites (equal ventral and dorsal) were restricted to the lower portion of the dSGS (non-DWV cells, unmarked).

(C) Distribution of GFP-positive inhibitory neurons in the GAD67-GFP mouse. A dense lamina of neurons are labeled superficial to the dSGS. Marginal neurons (white asterisk) and horizontal neurons (black asterisk) are the major cell populations labeled in the sSGS, along with a multitude of small (~6-12um diameter), granule-type neurons without identifiable dendritic arbors that are visible throughout the depth of the SC. Horizontal dendrites are not exactly parallel to SC surface, somas and dendrites are often off-axis (white arrow), and can give the appearance of a vertically oriented dendrite. Image shown is a projection of a confocal z-series through a coronal vibratome section. Scale, 100um

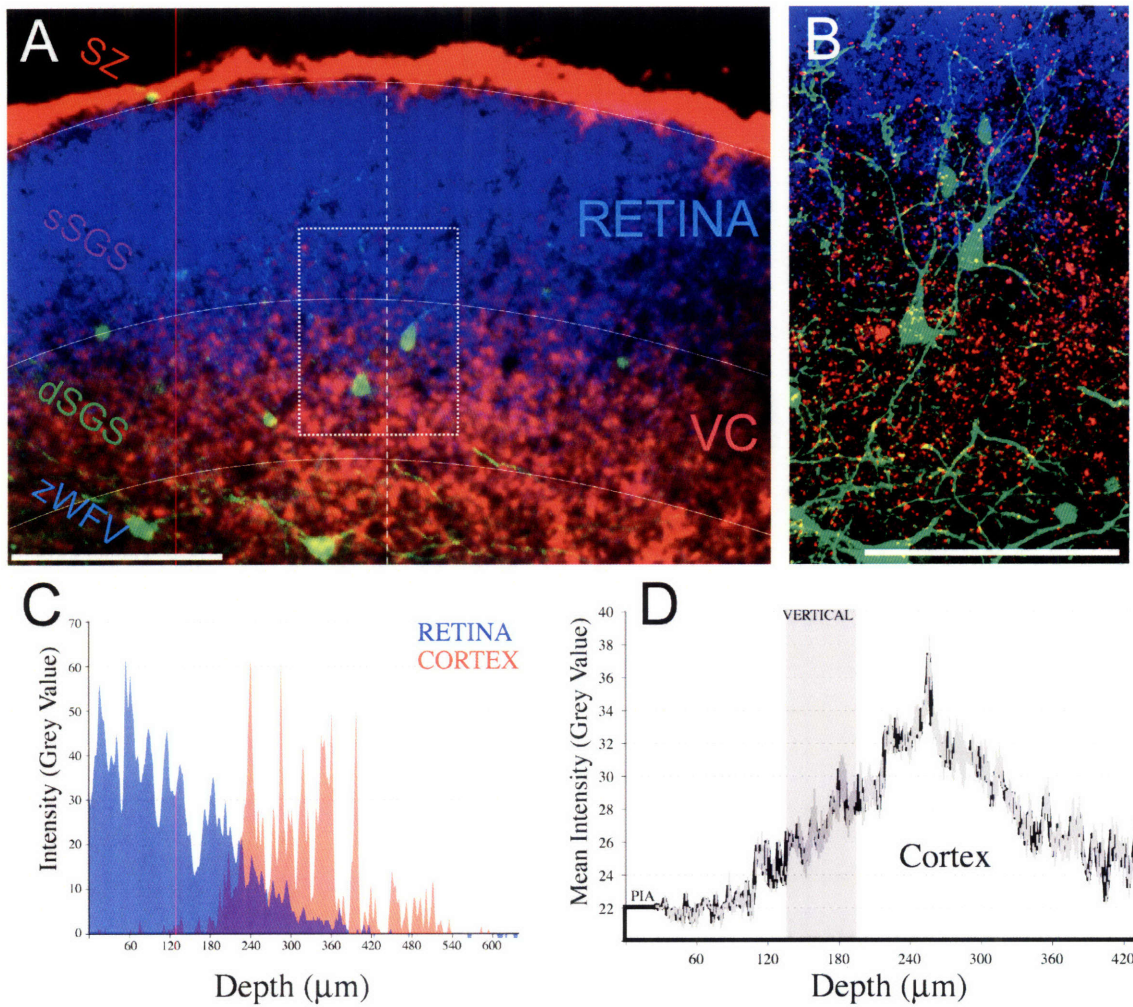(D) High-magnification of labeled marginal cells in the SZ. Scale, 50um

Figure 5. Vertical neurons of the deep SGS are located at the interface of visual afferents to the mouse sSC

(A) Retinal and visual cortical afferents in a coronal slice through the SC of an eGFP-S mouse. Retinal axons are labeled with CTB-Alexa633 (BLUE) and cortical axons with CTB-Alexa546 (RED). Image is a projection of a confocal z-series through a 200um vibratome section. Scale, 100um.
(B) Higher resolution image collected for the two vertical neurons circled in (A) and the retinal and cortical axons surrounding them. Scale, 100um.
(C) Intensity profiles of the retinal and cortical dye channels along the dotted line indicated in (A), by depth from pial surface. Cortical axons are relatively excluded from the most superficial layers, and retinal axons are nearly excluded from the deepest layers, with a large interface region in the mid dorso-ventral position.
(D). Quantification of the mean intensity of the cortical projection as measured in (C) along multiple lines through the somata of vertical neurons in multiple sections. Range of vertical somata position is indicated in GREY. Superimposed grey line represents mean+/-SE.
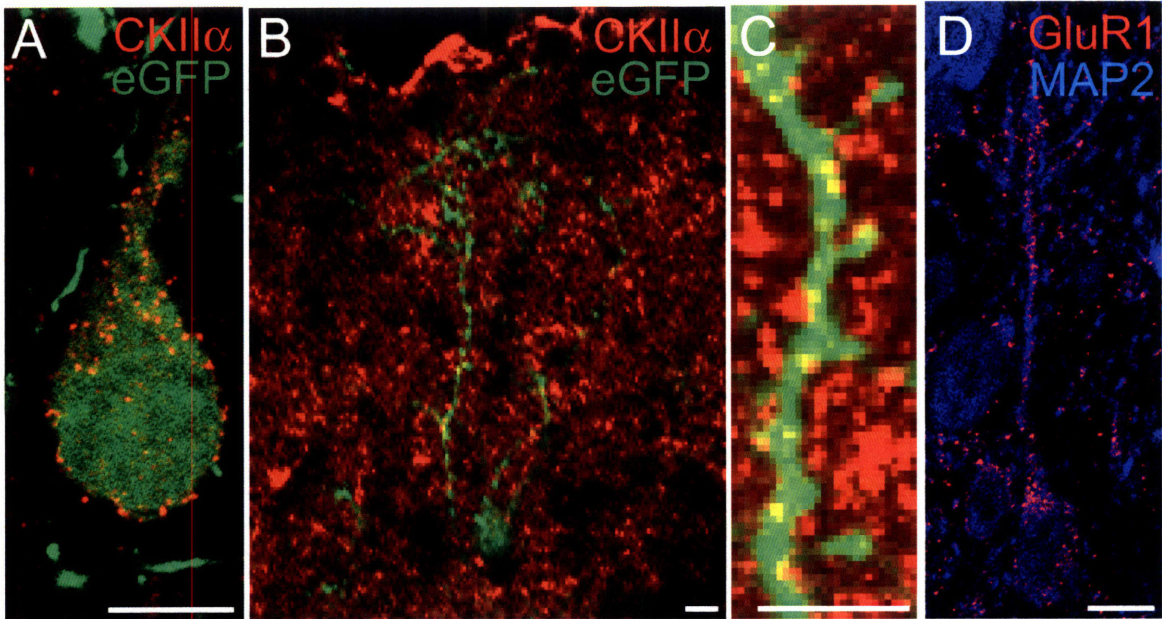
Figure 6. Vertical neurons in the deep SGS express dendritic CamKII-alpha and GluR1

(A) Immunohistochemistry with anti-CamKIIalpha antibody in the SC of an eGFP-S mouse. Staining is present in puncta on the surface of the soma and proximal dendrite. The rest of the dendrites plunged too deep in the slice to be accessed by the antibody. Scale, 10um

(B) A second eGFP-labeled vertical neuron in the dSGS has a portion of its distal dendrite on the surface of the slice, accessible to the immunostain. Scale, 10um

(C) Higher resolution image of a portion of the dendrite in (B) shows CamKII-a puncta along the dendritic shaft and in spine heads. Scale 10um

(D) GluR1 punctate immunostain along the dorsal dendrite of a vertical neuron in dSGS labeled with MAP2. Scale, 10um
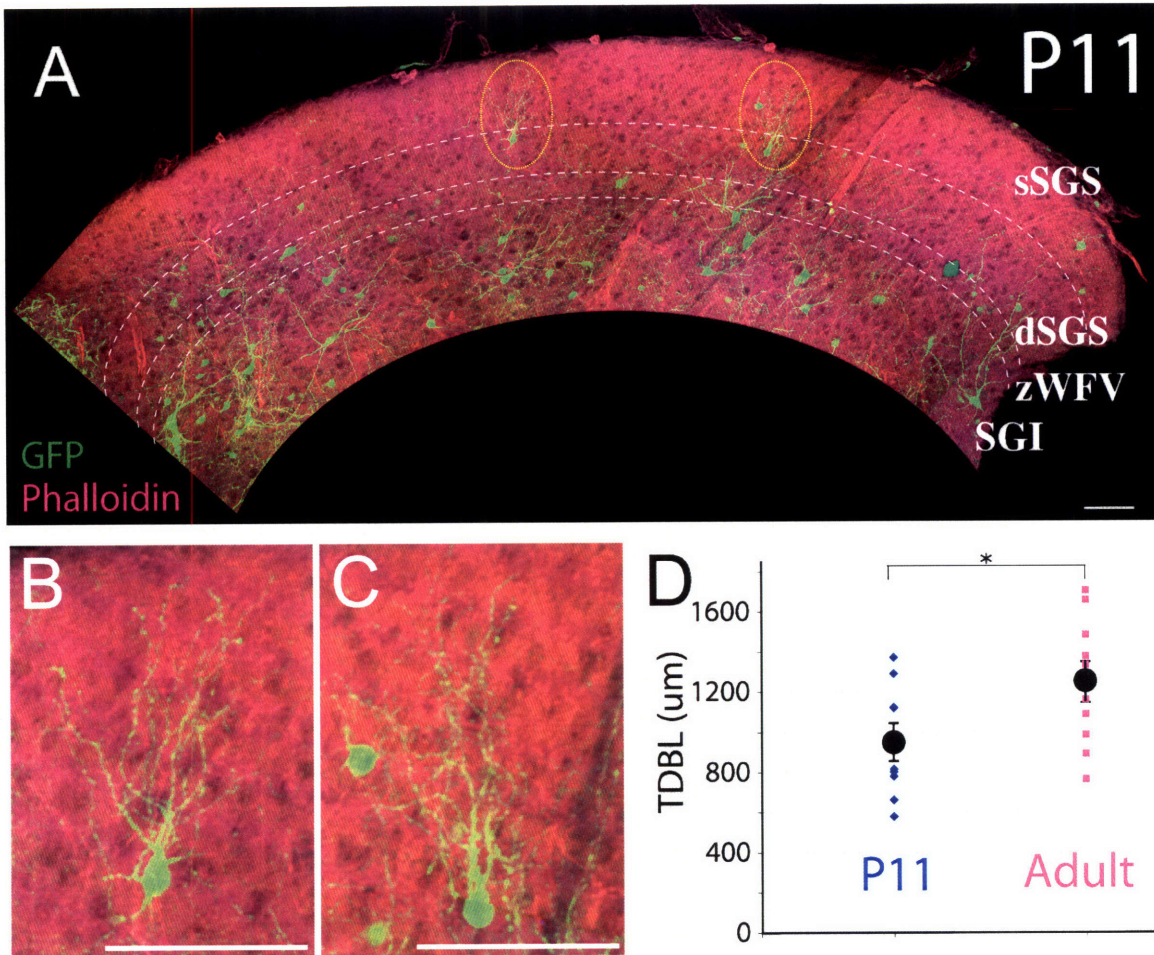
116

Figure 7. Dendritic growth of eGFP-labeled vertical neurons in the deep SGS between P11 and adulthood

(A) Montage of a series of z-projections of confocal z-series through a para-sagittal section of a P11 eGFP-S mouse. Actin is counterstained with Phalloidin-Alexa555 to enable visualization of labeling density. sSGS = superficial stratum griseum superficiale, dSGS = deep stratum griseum superficiale, zWFV = zone of wide-field vertical neurons, SGI = stratum griseum intermediale.

(B-C) Vertical neurons of the deep SGS are well filled with eGFP at this age, enabling three-dimensional measurement of dendrites in Neurolucida.

(D) Total dendritic branch length of vertical neurons in the deep SGS at P11 and Adult in eGFP-S transgenic mice. Mean +/- SE. * p<0.05

117

CHAPTER FOUR

Organization and development of synaptic connectivity in the mouse sSC

The present work has focused on the organization and development of the visual layers of the mouse superior colliculus over the eye-opening period. The mouse SC is a useful model for investigations of activity-dependent development for three reasons. 1) Input activity can be directly manipulated by closing or opening the eyelids, dark rearing, or silencing the retina, 2) Like many other regions of the brain, high fidelity maps form by competition among inputs, 3) Genetically modified mice enable testing of the biochemical mechanisms underlying this development. I have chosen the mouse SC for all of these reasons, and have used it to assay the mechanisms of pattern vision-dependent development after eye-opening. However, fundamental knowledge about the organization of the visual layers of the mouse SC is relatively lacking. I thus described the organization of neurons and visual inputs from retina and visual cortex in the sSC of wild-type, GAD67-GFP, and eGFP-transgenic C57BL/6 mice.

A model for the organization of the mouse sSC
I have provided evidence for a vertical laminar organization of the mouse sSC that is generally consistent with the organization of the rat sSC as described by Golgi and qualitative tract tracing approaches. A dual labeling approach has allowed me to extend these findings in the mouse and clarify the spatial relationships among laminae, excitatory and inhibitory cell classes, and visual afferents.

A general model for cellular and afferent organization in the mouse sSC is thus proposed (Figure 1).
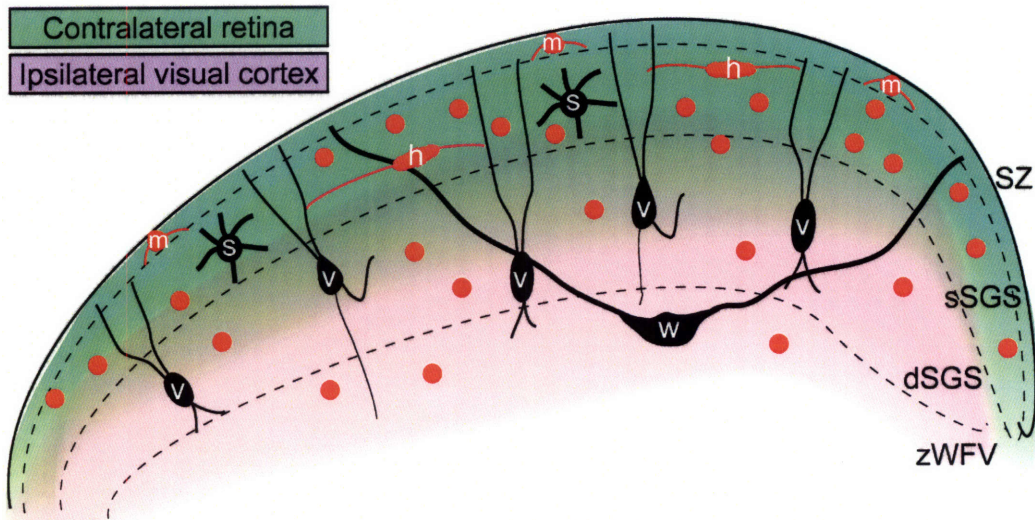
Figure 1. Schematic of superficial superior colliculus in the mouse.
An idealized view of a unilateral coronal section through the visual layers of the
mouse SC. Dotted lines show the divisions based on neuron class designation
as described in the present manuscript. Major cell types with representative
processes are drawn in black (from the eGFP mouse) and red (from the GAD67
mouse, and therefore inhibitory). The approximate position of retinal (green)
and cortical (pink) axon arbors are shown by the color gradients. Darkening at
the borders represents region of high overlap. Note the vertical neurons are
the primary cell type at the junction of the two projections. m = marginal, v =
vertical, s = stellate, h = horizontal, w = wide-field vertical, SZ = stratum
zonale, sSGS = superficial stratum griseum superficiale, dSGS = deep SGS,
zWFW = zone of wide-field vertical neurons. ● Granule-type neuron without
identifiable dendrites

The stratum zonale (**SZ**) just below the pial surface contains inhibitory marginal neurons. The superficial stratum griseum superficiale (**sSGS**), is especially enriched in inhibitory horizontal neurons, as well as multipolar stellate cells. The deep stratum griseum superficiale (**dSGS**) is enriched in vertically oriented neurons and contains cells which accumulate CamKII-a in their somas. The zone of wide-field vertical cells (**zWFV**) contains the somas of wide-field vertical neurons, and cells which accumulate CamKII-a in their somas. Small, inhibitory granule-type neurons are plentiful, and distributed throughout all layers.

I have extended studies in the rat sSC by dual labeling retinal and cortical afferents in the same animal, and assaying their distribution in relation to the cell classes and laminae described above. Axons from the contralateral retina and the ipsilateral visual cortex grow into the rostral edge of the SC largely intermixed at the ventral border of the sSC, but retinal axons ascend to arborize profusely in the upper layers, the SZ and sSGS. In contrast, cortical axons are most dense in the deeper layers, dSGS and zWFV. These two afferent projections do not have a sharp border between them, but rather form opposing dorso-ventral gradients. Thus cortical axons are present, although at lower densities, in the upper layers, and retinal axons are present at lower densities in the deeper layers. However, in sagittal sections, retinal axons show synaptic-like puncta predominantly in the upper layers, whereas cortical axons show puncta throughout the depth of the sSC, suggesting that retinal and cortical synapses are mixed in the upper layers (SZ and sSGS), but only cortical axons form synapses in the deeper layers (dSGS and zWFV). The ipsilateral retinal projection is minor, and forms small patches deep in the zWFV where the contralateral retinal projection is weakest.

This organization is not entirely consistent with that described for other mammals with higher visual sensitivities (eg, cat). In particular, the projection

from visual cortex has been reported to occupy a more superficial position in the sSGS, although still somewhat ventral to the retinal projection. After lesion of the visual cortex a large number of degenerating terminals were found superficially in the sSC, at presumptive horizontal neuronal profiles that accumulate GABA (Mize et al. 1982). Thus, although both mouse and cat have a high density of inhibitory horizontal neurons superficially, the more superficial location of visual cortical axons in the cat may allow synapses on horizontal neurons. However, cortical synapses on horizontal neurons are unlikely to make up a significant portion of cortico-collicular synapses in the mouse. The local circuitry of the SC could therefore be quite different among different species, making it important to have detailed anatomical data in the species of interest.

A mechanism for eye-opening induced refinement of synaptic connectivity

The results of the anatomical and electrophysiological analyses conducted in this study are summarized in Table 1 and Figure 2.

Table 1. Effects of perturbation on development of spine and filopodial density and on miniature event frequency.

	EYE OPEN	EYE CLOSED	VC-LESION	PSD-95 KO
CALIBER 3				
FILIPODIA	↑↑↑	↑↑↑	↔	
SPINES	↔	↓	↔	
SYNAPSES				
MINI-Hz	↑↑↑	↔		↔

Arrows show the change in each parameter relative to P11 as measured on P13. Boxes are color coded to draw attention to important details. The green boxes show increases in animals in which the eyes were allowed to open. The red box shows a regressive event, in which spine density is lower than observed at P11. Blue boxes show the failure of the normal developmental event to occur, showing that it requires eye opening, an intact cortex or PSD-95.
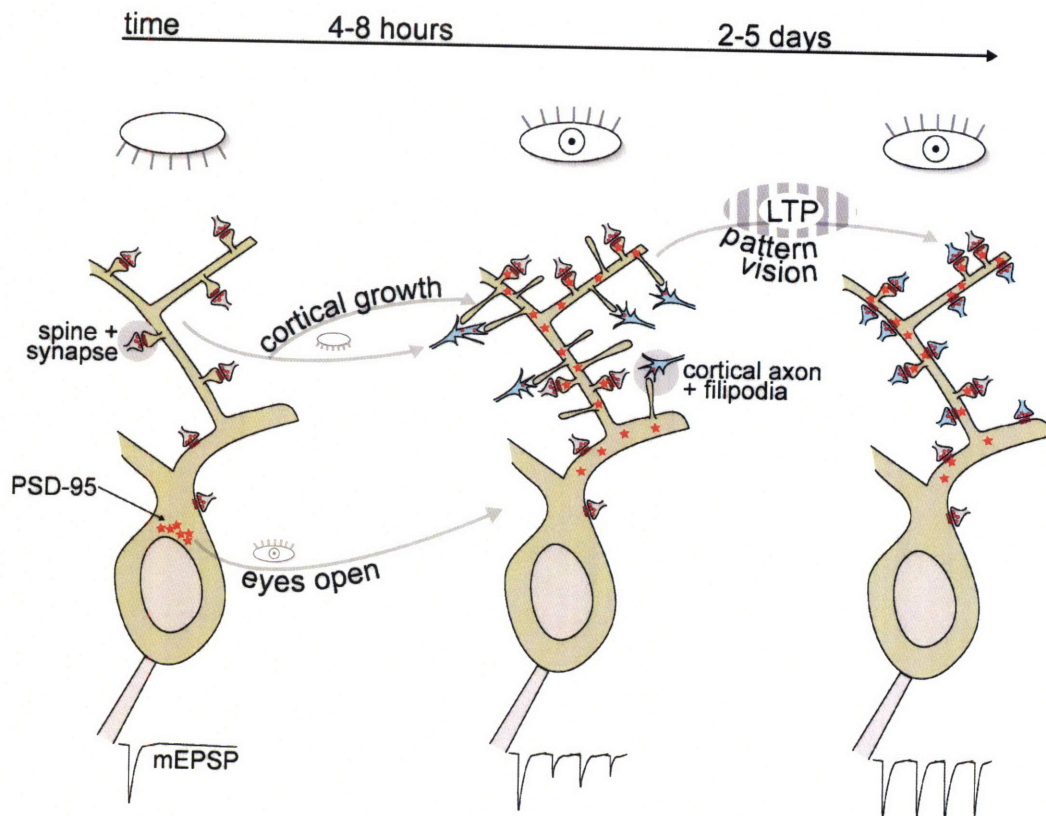
Figure 2. Synaptic development driven by eye opening.
Synthesis of present and past analyses of synaptogenesis around eye opening reveal a series of events leading to an increase in synaptic contacts on visual collicular neurons in which filopodia and elaborating visual cortical axons may play a central role. Over the period of eye opening cortical axons drive an increase in filopodial growth on the dendrite. This occurs irregardless of whether the eyes open or not between `p12 and `p13. Eye opening drives PSD–95 into the dendrites where it orchestrates a series of events at the synapse making it easier for nascent cortico–collicular synapses to be stabilized by pattern vision. These synapses may originate on or be converted to mature spine and shaft synapses (as reflected in the miniature EPSP frequency (bottom traces)).

These results suggest four novel conclusions.

1) Cortical inputs from Layer V pyramidal axons in visual cortex are sensitive to pattern vision deprivation between P12 and P13. Retinal inputs are not.

2) There is a maintenance of "Spine" structures over development, that can be acutely disrupted by pattern vision deprivation between P12 and P13.

3) There is a transient sprouting of filopodia between P11 and P13 that is resistant to pattern vision deprivation. The sprouting on Caliber3 does require the presence of cortical axons which would normally form synapses on those dendrites.

4) Vision-induced PSD-95 trafficking to dendrites enables stabilization of cortical inputs on spines by pattern vision after eye-opening.

The striking dissociation between the effects of visual deprivation and visual cortex removal on Caliber3 vs Caliber4 dendrites suggests that vision deprivation between P12 and P13 specifically disrupts cortico-collicular synapses, while retinal synapses are spared. This is somewhat paradoxical because presumably both inputs are responding to the same stimuli after eye-opening. Is there some intrinsic difference between the retina and visual cortex that might explain the sensitivity of cortical synapses to eye-opening while retinal synapses are unaffected? I suggest that the difference lies in the activity patterns in RGCs vs Layer V pyramids over the eye-opening interval, and the way in which they respond to visual stimuli.

Patterned visual stimuli presented to cats (and mice; Nase et al. 2003) drives high frequency oscillations in visual cortex that are synchronized across spatial locales. Outside of cortex, the SC is the only structure in which these fast

124

"gamma frequency" oscillations occur, and they are similar in many respects to those in cortex (Merker 2007, Brecht et al. 1998, 2001). In contrast, retinal ganglion cells at the first stage in visual processing have relatively simple receptive fields that generate responses to light increment and decrement (Kuffler 1953). Some sensitivity to motion and direction has also been detected in RGCs, but in general complex receptive fields are not observed until basic visual inputs have undergone transformation in the visual cortex. Increased intensity of visual stimuli after eye-opening might be expected to be encoded by both the retinal and visual cortical afferent pathways. However, I observed effects of eye closure only on dendrites opposite cortical axons. Visual cortical neurons have the additional ability to respond to pattern, color, and orientation. In contrast to the diffuse quality of light through closed eyelids, visual stimuli have the ability to locally correlate activity and induce high frequency spiking in cortical neurons). These activity patterns may be especially conducive to the induction of synaptic potentiation and stabilization.

Retinal inputs are perfectly capable of forming and maintaining synaptic contacts in the sSC after eye-opening. If the previous hypothesis is correct, how do they achieve this in the absence of highly correlated activity patterns due to pattern vision required to generate LTP? In contrast to the visual cortex, the retina has a high level of spontaneous activity. Spontaneous activity persists until the end of the third postnatal week in mouse, and is unaffected by dark rearing (Demas et al. 2003). In the absence of patterned visual experience, this activity is probably sufficient to refine retinal terminals. Indeed, this may explain why dark rearing has no effect on refinement at retinal synapses in the LGN (Hooks and Chen 2007), in contrast to the sSC, where refinement, presumably at cortical synapses, is eliminated when animals are deprived of pattern vision after EO (Lu and Constantine-Paton 2004). Refinement in the LGN _is_ affected by retinal silencing however, further

evidence that retinal afferents use spontaneous, rather than EO-driven pattern activity to refine.

It is especially interesting that cortical axons, which invade the sSC after retinal terminals have already refined, are able to compete with an established input. By Hebb's postulate, and evidence from the NMJ, it should be exceedingly difficult for a new input to compete with an established input that occupies the same synaptic space. This suggests that cortical inputs would have to be extremely effective to compete with retinal axons. How does such a late-developing input establish a foothold? The high-frequency gamma oscillations induced in cortex by pattern visual stimuli may be one mechanism that enables cortical axons to compete for synaptic space with retinal terminals.

One paradoxical finding from this study was that visual cortex removal before eye-opening was less destructive to spines than keeping the eyes closed over the normal eye-opening interval. Why should this be? In visual cortex pattern vision deprivations (eg monocular deprivation by lid suture), but not retinal silencing, are actively destructive to the ability of the non-deprived eye to maintain dominance (Rittenhouse et al. 1999, Frenkel and Bear 2004). In the presence of un-correlated activity, but not neuronal silencing, synapses are actively eliminated (Zhou et al. 2003). Furthermore, the vision-induced trafficking of PSD-95 in the sSC is far less sensitive to dark rearing than it is to pattern vision deprivation (Yoshii et al. 2003). I therefore hypothesize that eliminating the visual cortical afferents effectively silenced those inputs, and probably enabled retinal afferents to rapidly re-innervate the denervated Caliber3 dendrites. In the absence of pattern vision during eye-closure, spines opposite non-correlated cortical afferents were actively disrupted and could not be maintained. PSD-95 is not required for retinal synapse formation or stabilization over eye-opening, and thus the observed spine density in lesioned animals was at normal levels by P13 on Caliber3.

These data also suggest that filopodia play a crucial role in synaptogenesis over the eye-opening interval. Many investigations have observed filopodia to be more numerous during early development than in mature animals. However, our findings show that although post-synaptic to visual inputs, they are not induced to sprout by pattern visual experience per se. Consistent with early theories that long, dynamic filopodia help dendrites navigate immature neuropil to seek potential synaptic partners, our data suggest filopodia sprout in response to the presence of growing cortical axons in the neuropil. New synapses formed on filopodia after eye-opening may be converted to dendritic spines, or even withdrawn to form shaft synapses. Cortical axons may make some new contacts on these filopodia in the absence of visual experience, but cannot maintain them. The cell, however, still senses the growing axons in the neuropil, and continues to sprout filopodia even in the absence of pattern visual experience. The mechanism by which cortical axons induce filopodia to sprout is unknown, but could involve activity-independent and/or dependent cues. Clearly filopodia are indicators of a dynamic period of synaptogenesis, and given their dramatic elaboration over a period when the number of functional synapses in the cell more than triples, it's reasonable to assume they play a functional role in this new synapse formation.

LITERATURE CITED

Brecht M, Singer W, Engel AK. 1998. Correlation analysis of corticotectal interactions in the cat visual system. J Neurophysiol. 79(5):2394-407.

Brecht M, Goebel R, Singer W, Engel AK. 2001. Synchronization of visual responses in the superior colliculus of awake cats. Neuroreport. 12(1):43-7.

Demas J, Eglen SJ, Wong RO. 2003. Developmental loss of synchronous spontaneous activity in the mouse retina is independent of visual experience. J Neurosci. 23(7):2851-60.

Frenkel MY, Bear MF. 2004. How monocular deprivation shifts ocular

dominance in visual cortex of young mice. Neuron 44(6):917-23.

Hooks BM, Chen C. 2006. Distinct roles for spontaneous and visual activity in remodeling of the retinogeniculate synapse. Neuron. 52(2):281-91.

Kuffler SW. Discharge patterns and functional organization of mammalian retina. J Neurophysiol 16: 37-68, 1953.
Lu W, Constantine-Paton M. Eye opening rapidly induces synaptic potentiation and refinement. Neuron. 2004 Jul 22;43(2):237-49.

Merker B. 2007. Grounding consciousness: The mesodiencephalon as thalamocortical base. Behav Brain Sci. 30(1):110-20.

Nase G, Singer W, Monyer H, Engel AK. 2003. Features of neuronal synchrony in mouse visual cortex. J Neurophysiol. 2003 90(2):1115-23.

Rittenhouse CD, Shouval HZ, Paradiso MA, Bear MF. 1999. Monocular deprivation induces homosynaptic long-term depression in visual cortex. Nature 397:347-50.

Yoshii A, Sheng MH, Constantine-Paton M. Eye opening induces a rapid dendritic localization of PSD-95 in central visual neurons. Proc Natl Acad Sci U S A. 2003 Feb 4;100(3):1334-9. Epub 2003 Jan 27.

Zhou Q, Tao HW, Poo MM. 2003. Reversal and stabilization of synaptic modifications in a developing visual system. Science 300:1953-7.